POLITECNICO DI TORINO

Master's degree in construction engineering

Master’s Degree Thesis

SEISMIC RETROFIT OF AN EXISTING CRITICAL FACILITY WITH IRREGULAR DESIGN AND DIFFERENT FOUNDATION LEVELS

Supervisors
Prof. Gian Paolo CIMELLARO
Dr. Alessandro FERAUDI

Candidate
Francesca PALMIERI

October 2025

Abstract

This study investigates a retrofitting methodology for a critical facility in Sant'Agapito, Italy, characterized by irregular foundations on two distinct elevations that amplify dynamic asymmetries, torsional effects, and soil-structure interactions (SSI) during seismic events. The research integrates accelerometer-derived dynamic assessments with a retrofitting strategy based on elastomeric base isolators. Accelerometer data from ambient and forced vibration tests informed the calibration of numerical models, revealing torsional coupling and differential displacements under simulated ground motions. The proposed intervention employs low-damping elastomeric isolators, strategically installed at the interface between the multi-level foundations and superstructure, to decouple the building from seismic inputs while preserving its architectural integrity. Finite element analyses demonstrate a reduction in transmitted accelerations and a decrease in torsional rotations, validating the system's efficacy under heterogeneous SSI conditions. This minimally invasive approach aligns with performance-based engineering principles, offering a scalable framework for retrofitting irregular structures in high-seismicity regions. The methodology emphasizes cost-efficiency, safety, and compliance with modern seismic codes, particularly for historically sensitive contexts.

Summary

1. Introduction

In recent decades, the increasing frequency and intensity of natural disasters has highlighted the global vulnerability of urban systems. Today, the challenges of ensuring the safety of people and infrastructure are becoming increasingly complex, and cities feel an urgent need to improve their resilience to cope with sudden events and prolonged stress.

In Italy, this issue is particularly relevant as an immense architectural and historical heritage is located in one of the regions of the world most exposed to seismic risk. The situation is further aggravated by the obsolescence of much of the existing building heritage and the high number of structures built before the introduction of adequate anti-seismic standards. The intrinsic fragility of the territory, combined with high exposure to seismic risk, defines an extremely vulnerable urban texture, which has been indelibly marked in past centuries by the earthquakes of Irpinia (1980), L'Aquila (2009), and Amatrice (2016), events that caused thousands of victims [1].

In this context, the concept of urban resilience takes on a central and contemporary role in the field of urban planning and risk reduction. It can be defined as a city's ability to respond, adapt, and recover from unexpected and destructive events, restoring the functioning of the urban fabric and minimizing their effects [2]. Urban resilience thus becomes a strategic planning tool that not only concerns the robustness of the built environment, but also extends to the adaptability and responsiveness of social, institutional, and infrastructural systems. This principle represents a multidimensional construct that integrates different analytical areas: natural, economic, social, physical, and institutional [3].

A crucial aspect of urban resilience is seismic risk mitigation, as it reduces the physical vulnerability of buildings and infrastructure through targeted interventions. In practice, this is implemented through structural retrofitting projects, seismic risk assessment and zoning, as well as technical regulations and adequate training of professionals in the sector.

This thesis proposes an in-depth study of the different seismic retrofitting strategies applied to an irregular public building located in the municipality of Sant'Agapito, Italy. The analysis of this case study is of particular interest because the building is characterized by complex geometry, vertical discontinuities, and two different foundation levels. These characteristics exacerbate dynamic asymmetries and torsional effects, amplifying soil-structure interaction (SSI) and thus increasing the vulnerability of the system.

1.1 Research Objectives

The purpose of this work is to define a methodological framework for the seismic retrofitting of the building under study, evaluating the effectiveness of the structural response before and after the intervention in terms of stresses and displacements. From a multi-objective perspective, the analysis goes beyond structural performance only, integrating economic and environmental considerations, such as the impact in terms of CO_2 emissions, with the aim of providing a comparative tool for the optimal selection between different retrofitting strategies.

1.2 Methodology

The approach adopted for the present study consists of three main phases.

PHASE 1 – KNOWLEDGE

This initial phase focuses on characterizing the existing building using the tools and data available. These preliminary operations form the basis for the digital model.

- Scan-to-BIM: high-precision geometric survey using drone photogrammetry and terrestrial laser scanning; generation of a three-dimensional point cloud.
- Creation of the digital twin: parametric BIM modeling of the existing building, aimed at developing a consistent and updatable digital twin.

PHASE 2 – MODELING

This phase involves the development and calibration of the FEM numerical model, both for the pre-intervention conditions and for the proposed seismic retrofitting solutions.

- Development and calibration of the numerical model: implementation of the FEM model and its calibration based on experimental data.
- Design of retrofitting with reinforced concrete shear walls: definition of a traditional retrofitting strategy through the insertion of stiffening elements.
- Design of the seismic isolation system: alternative solution based on low-damping elastomeric isolators installed between the heterogeneous foundations and the superstructure.

PHASE 3 – INTEGRATED PERFORMANCE ASSESSMENT

Structural, economic, and environmental performance assessments converge in an integrated comparison.

- Pre- and post-intervention comparative analysis: numerical assessment of the seismic performance of each structural configuration (original, with shear walls, with isolators).
- Economic assessment: estimation of the direct and indirect costs associated with each intervention, including materials, construction work, and execution times.
- Environmental impact assessment (carbon footprint): quantification of CO_2 equivalent emissions through a simplified LCA.

2. Sant'Agapito Municipal Building

2.1 Territorial Context and Seismic Hazard

The case study discussed in this thesis concerns a strategic public building located in the municipality of Sant'Agapito, in the province of Isernia, Molise (Italy). The structure, the town hall, hosts essential community functions and is classified as a strategic building under current seismic regulations (Ministerial Decree of January 17, 2018). This designation makes its ability to remain fully operational following natural disasters and dangerous events a priority.

Sant'Agapito is located in the central sector of the southern Apennines, about 5 km from the provincial capital, Isernia. The municipal territory is characterized by a high morphological complexity, typical of the inland Apennine regions, with steep slopes and a secondary infrastructure network connecting it to the main regional centers.

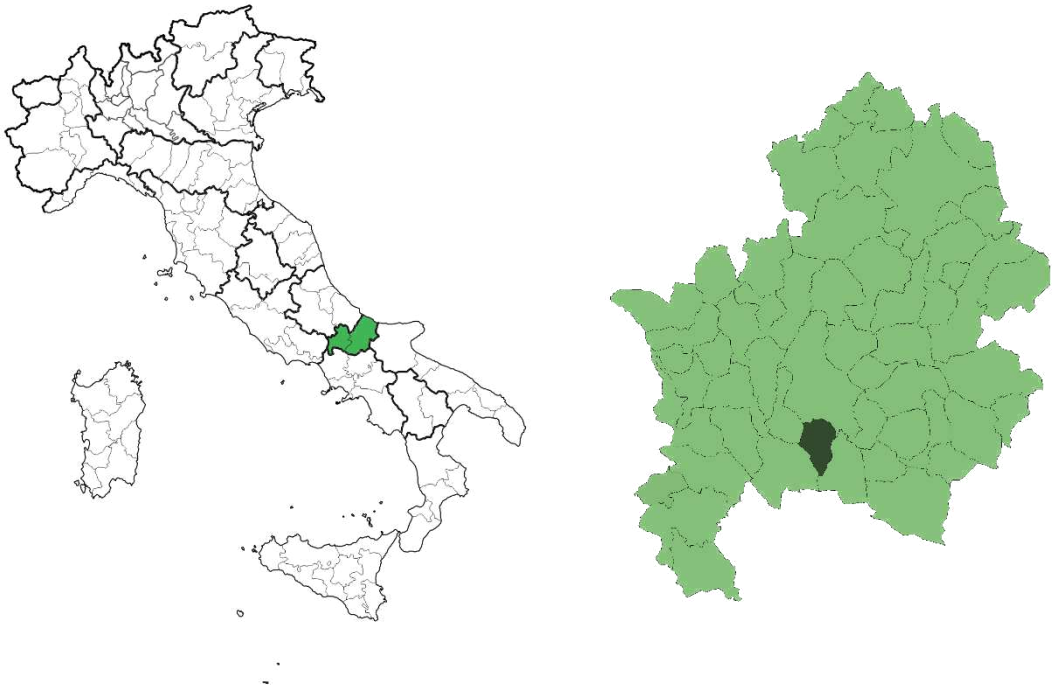

Figure 1 - Geographical location of Sant'Agapito. National location and focus on the province of Isernia

A distinctive feature of the central and southern Apennine regions is their significant seismic risk, determined by the intense tectonic activity affecting the entire mountain range. As a result, Molise is among the Italian regions exposed to a medium-high seismic risk, as demonstrated by the historically destructive events that have profoundly shaped the territory. In particular, the 1980 Irpinia earthquake and the 2002 San Giuliano di Puglia earthquake had such an impact that they influenced the evolution

of seismic classification standards at the national (Irpinia) and regional (San Giuliano di Puglia) levels.

In April 2006, following O.P.C.M. No. 3519, which established the general criteria for national seismic zoning, the Molise Region approved a new classification scheme. Based on this scheme, the municipality of Sant'Agapito was assigned to Seismic Zone 1. This zone corresponds to a high seismic risk, with maximum ground acceleration (PGA) values expected to be between 0.25 g and 0.35 g, which impose strict design requirements in terms of the seismic resistance of structures.

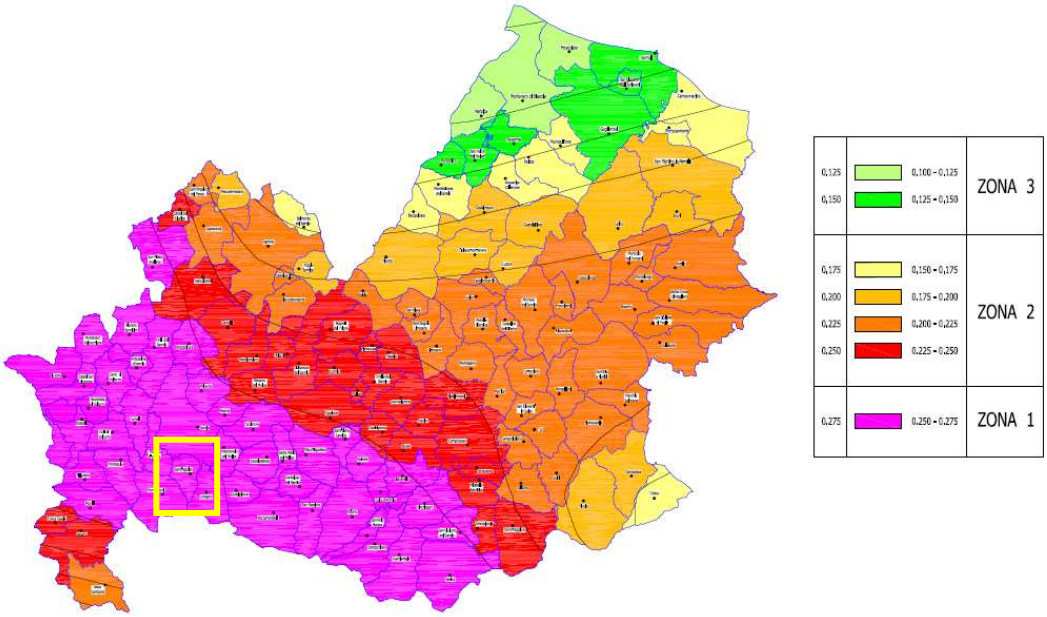

Figure 2 - Seismic hazard map of the regional territory

At the national level, the seismic classification currently in force divides Italian territory into four zones, defined according to PGA values and the frequency/intensity of seismic events:

Zone 1 – High seismicity (PGA > 0.25 g) – 708 municipalities
Zone 2 – Medium-to-high seismicity (0.15 g < PGA ≤ 0.25 g) – 2,345 municipalities
Zone 3 – Medium-to-low seismicity (0.05 g < PGA ≤ 0.15 g) – 1,560 municipalities
Zone 4 – Low seismicity (PGA ≤ 0.05 g) – 3,488 municipalities

This classification is periodically updated on the basis of advances in seismological research, new geological surveys, and local-scale microzonation studies. The overarching goal is to refine risk assessment and support effective mitigation strategies, in line with a broader framework of disaster prevention and civil protection.

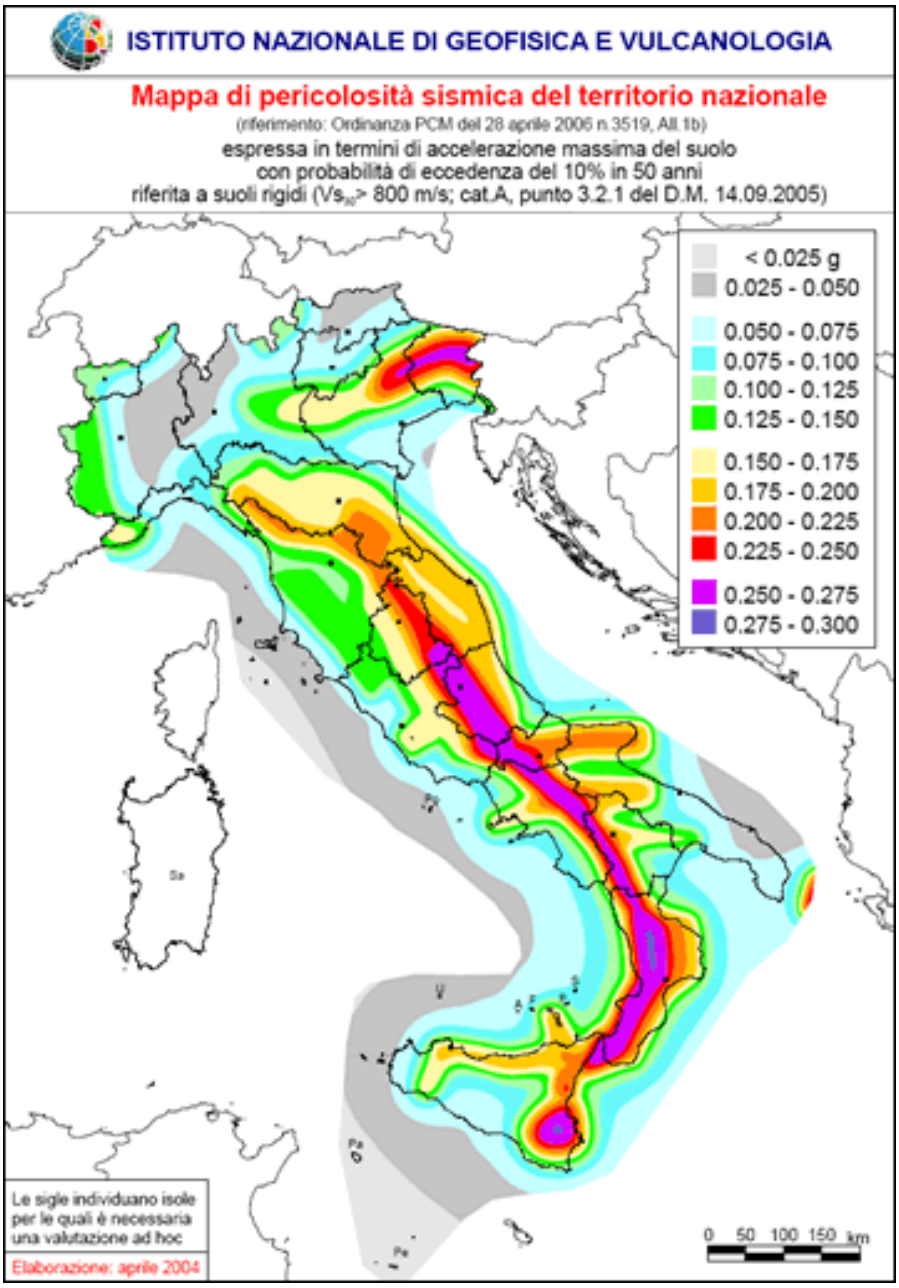

Figure 3 - Seismic hazard map of the national territory

2.1 Architectural and Structural Configuration of the Building

The building under study is the town hall of Sant'Agapito, built between the late 1970s and early 1980s. This structure is characterized by both planimetric and vertical irregularities which, combined with the significant seismic exposure of the area, make it a particularly relevant case study.

Figure 4 - Front view of Sant'Agapito Town Hall

The complex develops over three above-ground levels—ground floor, first floor, and second floor—as well as a partially underground basement, with two access points located at different elevations: a main entrance and a service entrance. The basement, on the north-west side towards Via Roma, is accessible and used as a garage/storage area, with a staircase connecting it directly to the ground floor. Currently, the building is used by both the municipality and some private offices. The discontinuity in elevation originates from the need to adapt the foundation system to the steep slope of the natural terrain. The resulting fragmentation of vertical structural continuity has significant implications for seismic performance, including torsional effects, differential displacements, and non-uniform soil–structure interactions.

From a planimetric perspective, irregularity is evident across all levels of the building. The basement, for instance, has a reduced footprint and different geometry compared to the upper floors, owing to the staggered foundation system. Moving upward, as illustrated in Figures 1 and 2 (ground and first floor plans, respectively), the spatial distribution of the rooms becomes apparent. The layout is organized around a central lightwell, partially covered at the top by a glazed roof, designed to provide

natural illumination to the otherwise dark central areas of the structure. At each level, the functional spaces are arranged into offices, meeting rooms, archives, and service areas.

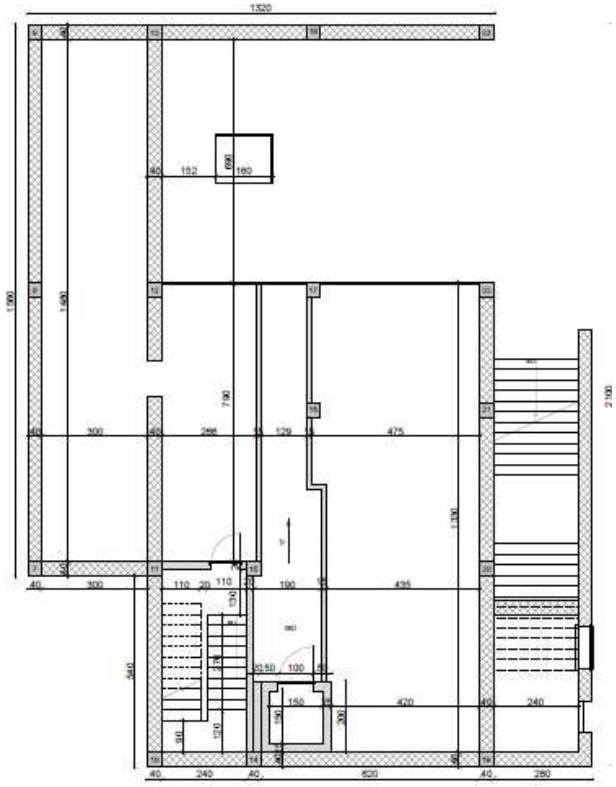

Figure 5 - Basement floor plan

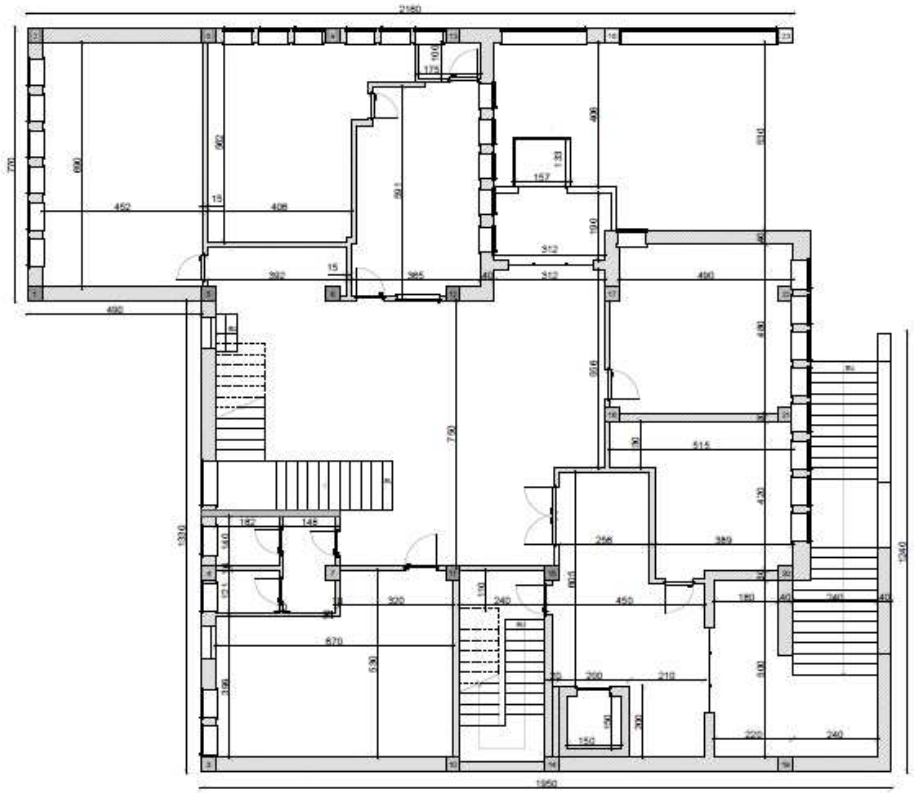

Figure 6 - Ground floor plan

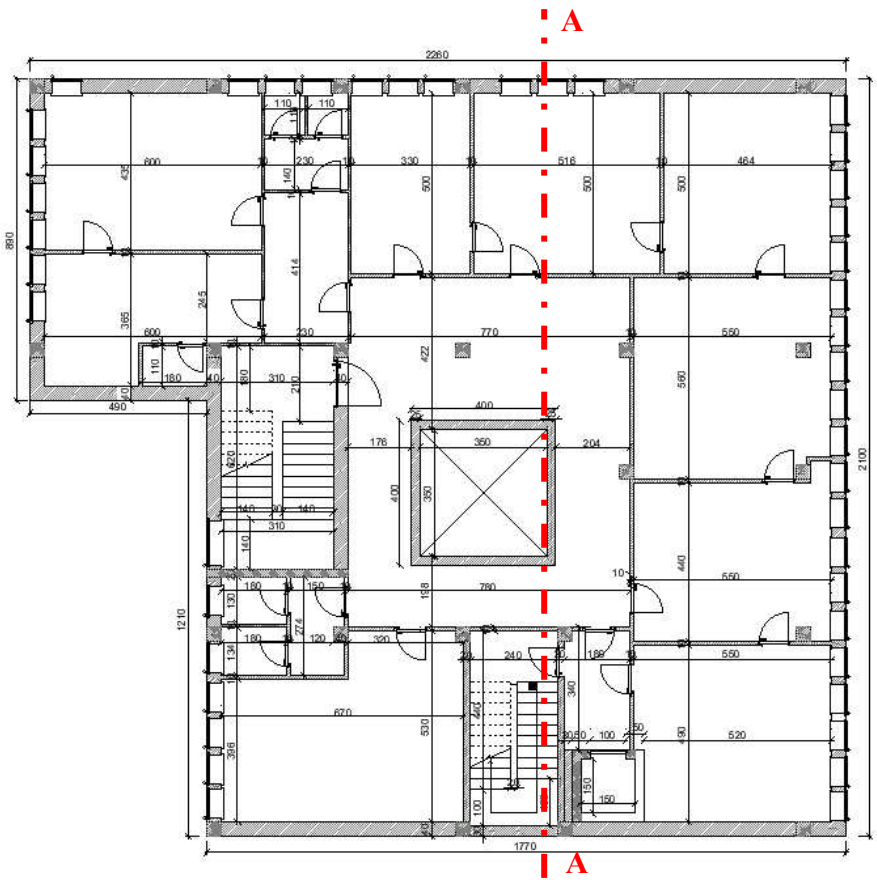

Figure 7 - First floor plan

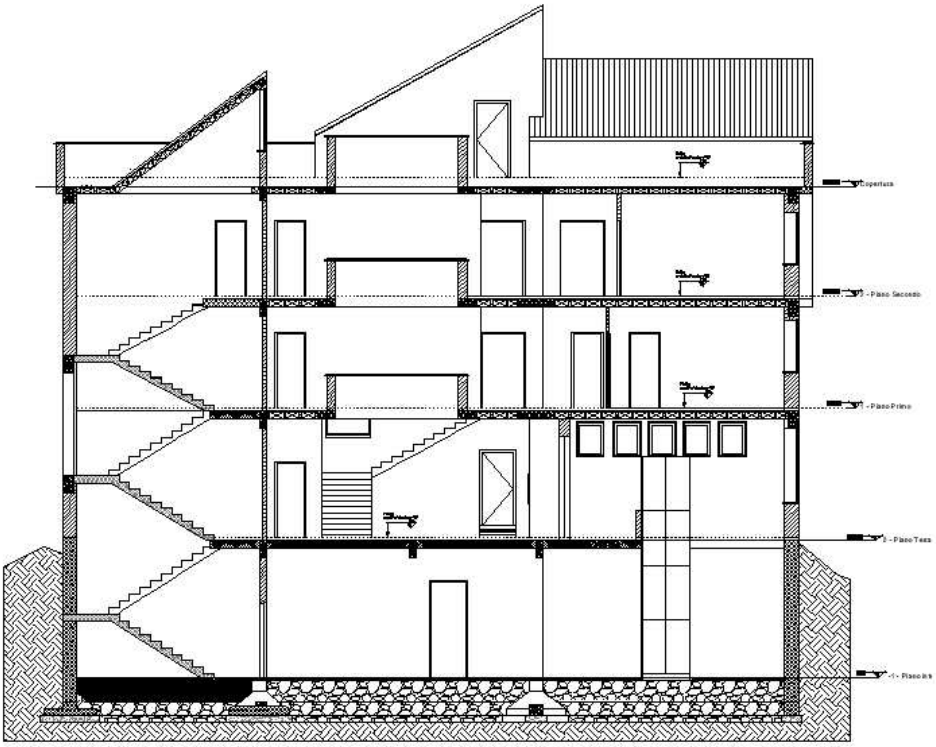

Figure 8 - Section A-A'

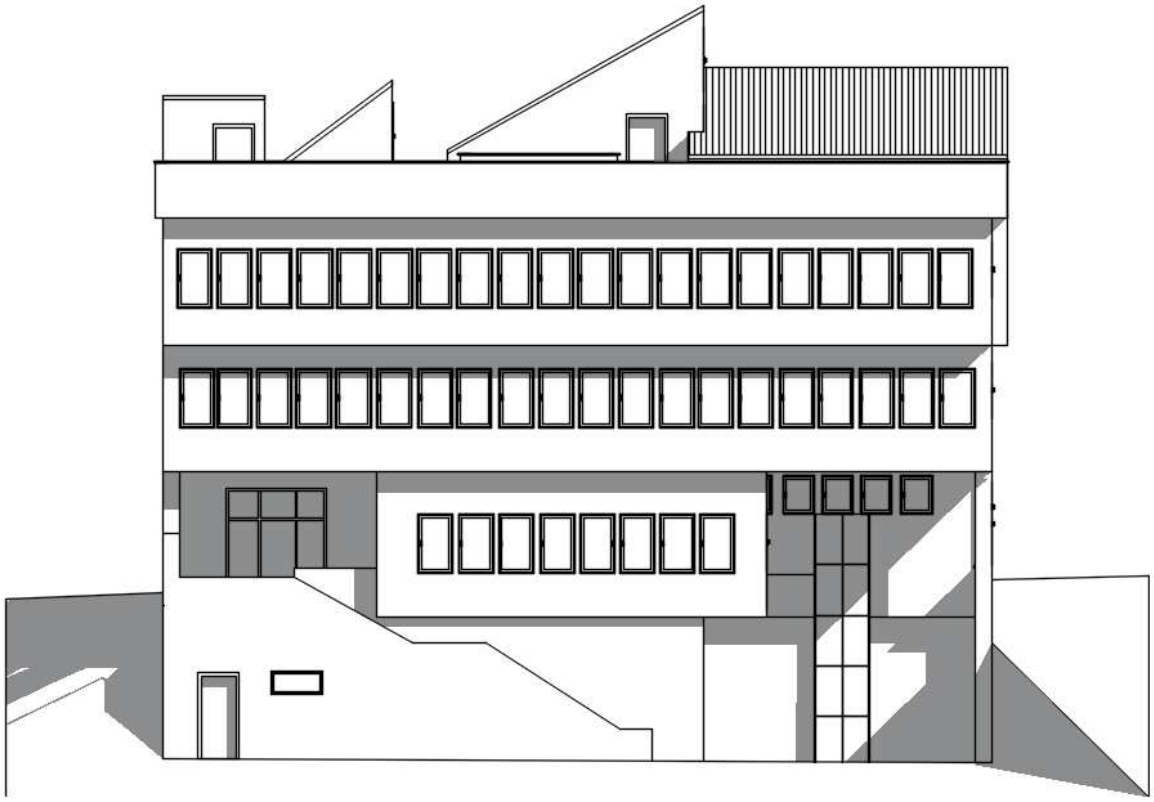

Figure 9 - West elevation . Extracted from BIM model.

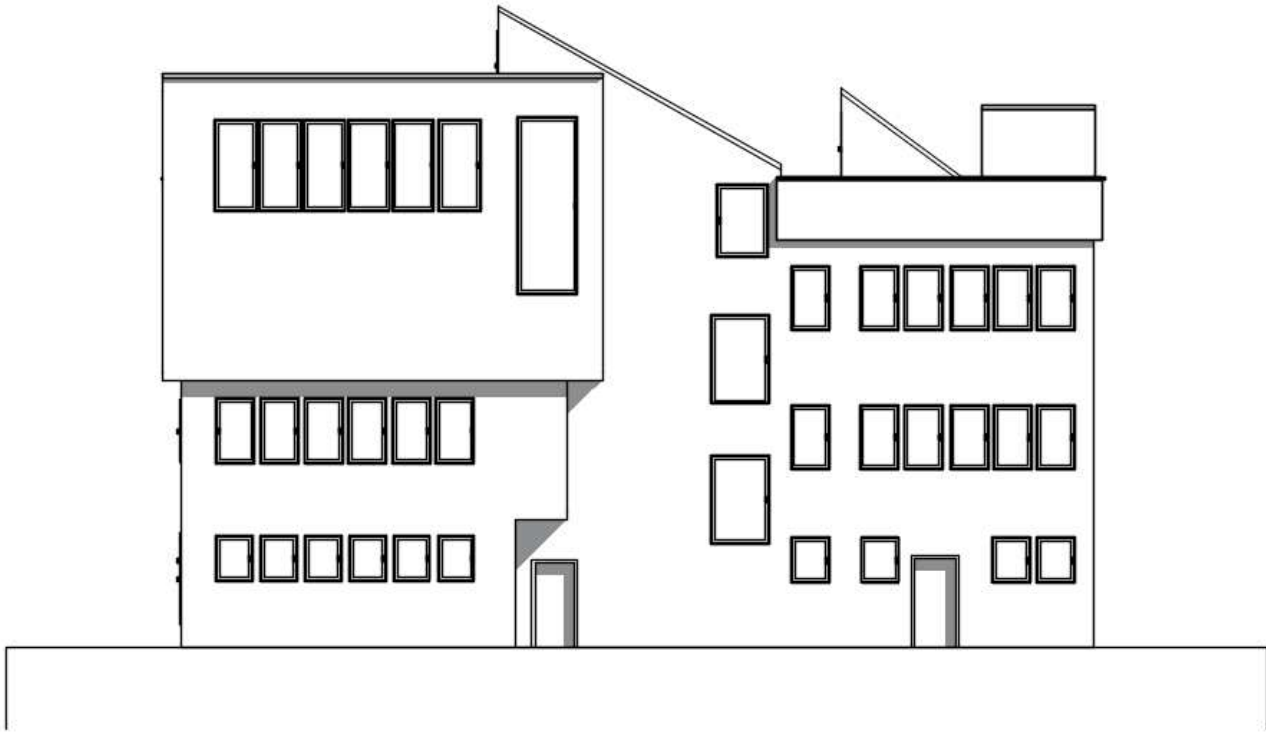

Figure 10 - Est elevation . Extracted from BIM model.

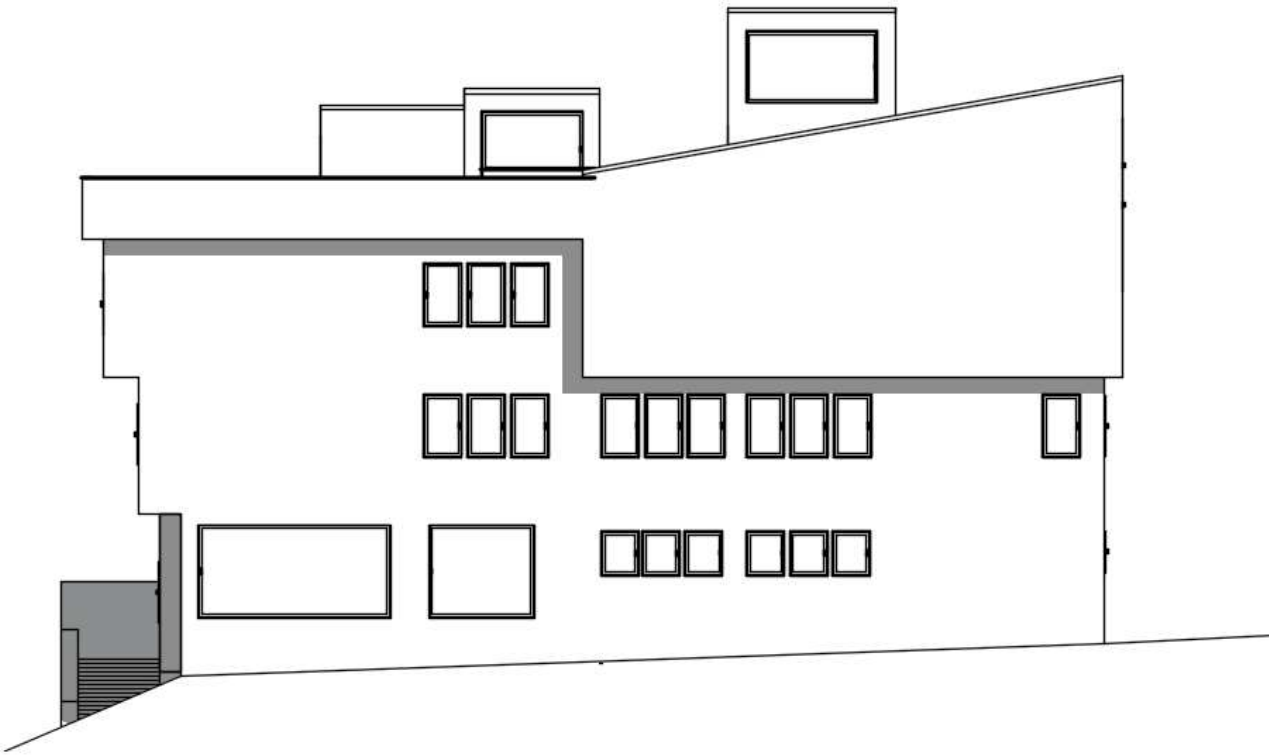

Figure 11 - South elevation . Extracted from BIM model.

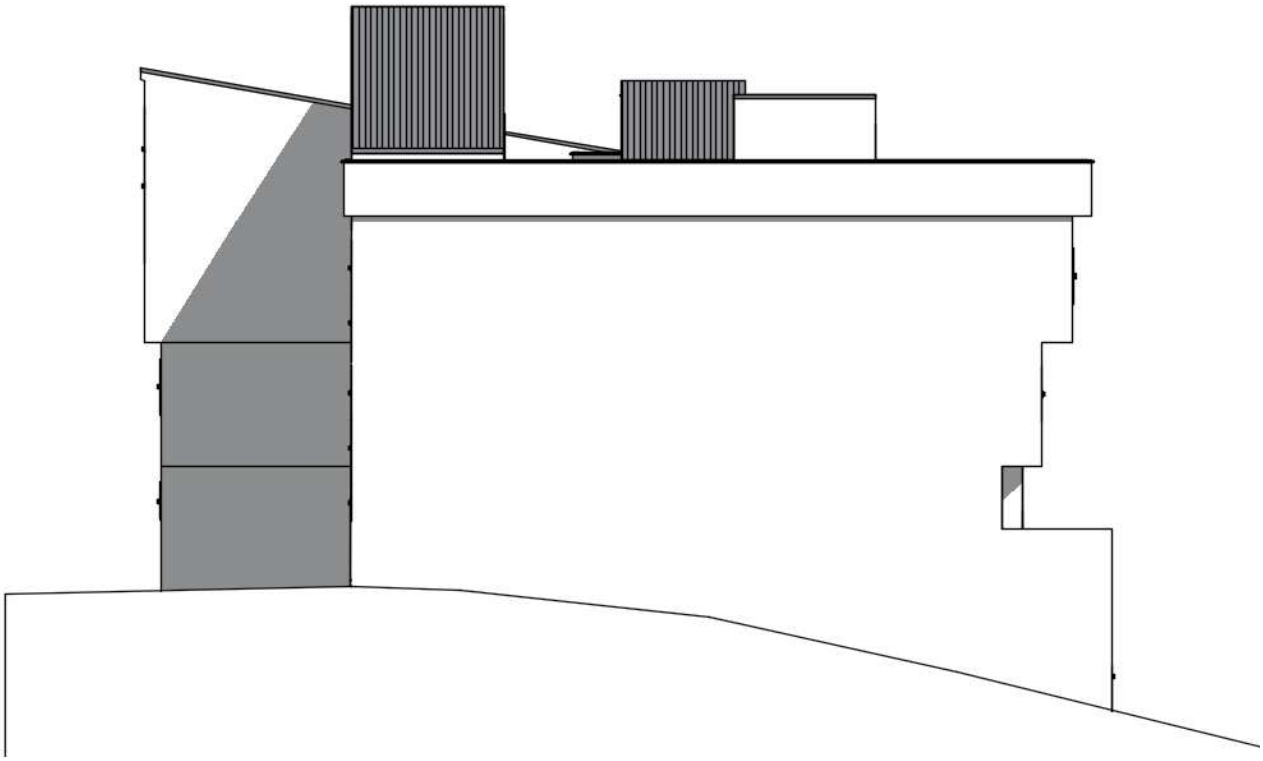

Figure 12 - North elevation . Extracted from BIM model.

The structural irregularity is also a distinctive feature of the elevation, mainly caused by the discontinuity of the foundation system. The building stands on a shallow foundation system consisting of inverted beams with reinforced concrete bases arranged on two distinct levels. Specifically, columns 1 to 9 are positioned at a height of +4.00 m, while the remaining part of the foundation is at the design height of +0.00 m. This configuration exacerbates dynamic irregularities and can lead to local rotations or loss of support in the event of strong seismic events.

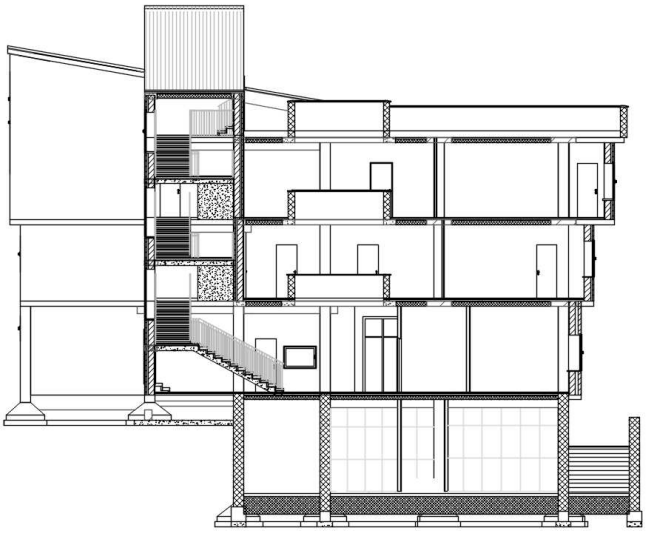

Figure 13 – Section B-B'

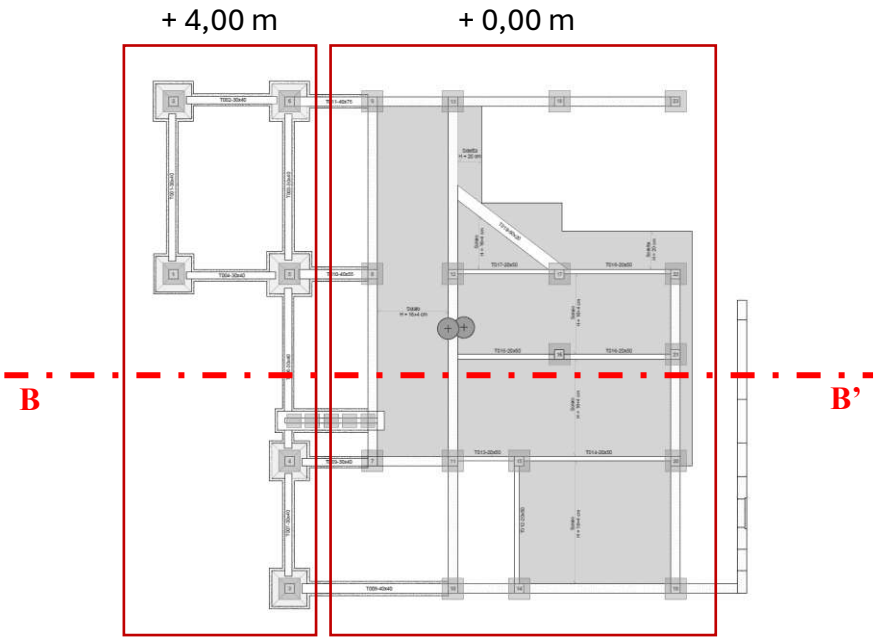

Figure 14 - Different foundation depths. Section and plan view

The load-bearing system consists entirely of cast-in-place reinforced concrete, arranged in beam-column frames according to an irregular grid, which is not always continuous between floors. The main beams have highly variable cross-sections (100 × 20 cm, 30 × 50 cm, 50 × 30 cm), while the

pillars, all measuring 40 × 40 cm, are distributed irregularly. The floors, with an average thickness of 20 cm, are mostly made of ribbed reinforced concrete with brick blocks (brick and concrete). In the basement, all the vertical partition walls are made of reinforced concrete shear walls, which end at the first floor (ground floor) ceiling, with the exception of a single 20 cm thick wall that extends the entire height of the building up to the roof ceiling. The remaining partition walls are made of masonry.

3. Survey

The survey of the building is an essential preliminary step in the development of any structural analysis and in the design of seismic retrofitting measures. Knowledge of the geometric characteristics, materials, and performance of the building allows for the creation of a numerical model consistent with reality. In the case of the Sant'Agapito town hall, surveying took on a particularly important role given the morphological complexity of the site, the irregular height of the foundations, and the irregular distribution of the load-bearing elements.

3.1 Scan-to-BIM

A Scan-to-BIM approach was adopted for the as-built restoration.

This method, which is becoming increasingly popular in the construction industry, involves surveying a building or area and converting it into a BIM model. The enormous potential of this approach lies in the combined use of advanced surveying techniques and the parametric modeling characteristic of BIM. This process is the basis of “reverse engineering,” i.e., the high-level digital reconstruction of the building.

The survey of the building in question was conducted using an integrated methodology that involved the use of aerial photogrammetry techniques with drones and ground surveying with laser scanners. Drone photogrammetry provided an overview of the building complex and the surrounding urban context, including zenithal and oblique views of the external facades and roof. Ground scanning, on the other hand, allowed for detailed surveying of the building envelope and interior spaces, which were not accessible by drone flight.

Figure 15 - Drone and terrestrial laser scanner

Figure 16 - Drone flying in front of the town hall

Figure 17 - Urban landscape viewed from a drone

The various detection techniques made it possible to acquire the georeferenced points of the scanned space, generating two high-density point clouds as output. Subsequently, once the clouds had been cleaned, it was possible to combine them to obtain a detailed and accurate three-dimensional representation of the building, which forms the skeleton of the three-dimensional model of the building.

3.2 Building Information Model

The georeferenced point cloud was then imported into Autodesk Revit®, where a three-dimensional parametric model of the building was created. Through a process of accurate modeling of the actual state, a faithful representation of the existing architecture and structure was obtained, which served as a useful information base for subsequent FEM modeling and structural analysis.

Parametric modeling made it possible to assign meaningful properties to each element, both from a geometric and informational point of view, making the model interoperable with structural calculation environments. This interoperability made it possible to develop an integrated workflow that, starting from the survey, leads to parametric modeling and then to FEM modeling, without loss of information and with a progressive enrichment of the available data.

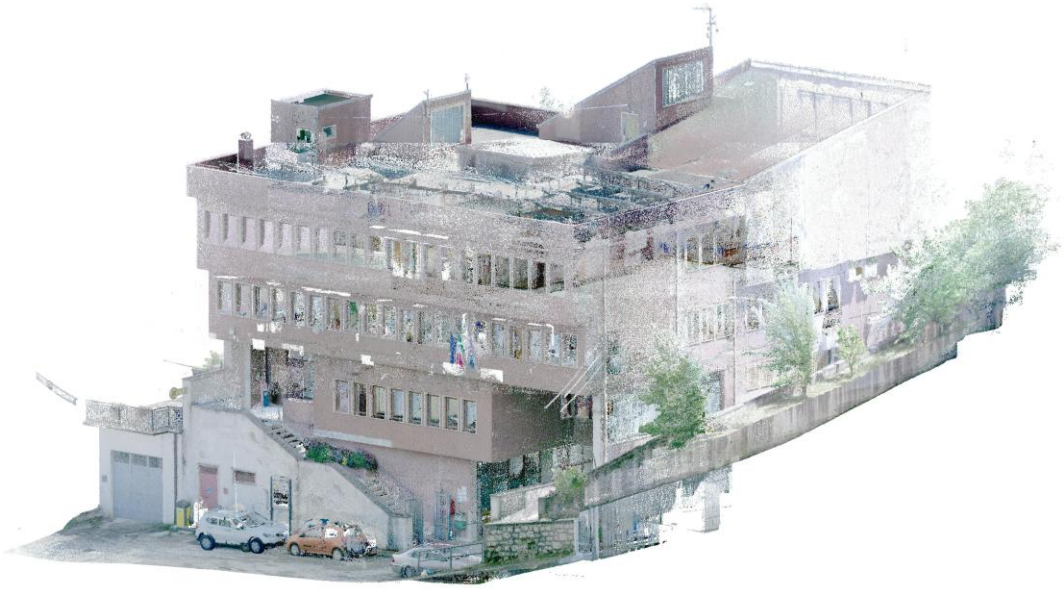

Figure 18 - Georeferencedand merged point cluod

Figure 19 - Georeferencedand merged point cluod and BIM model

The BIM interoperability process adopted in this study is part of an advanced approach to building management, where the digital model acts as a single information repository. In this way, the information collected from the survey is transferred directly to the parametric model and, from there, to the structural calculation software. This ensures consistency between the data collected, geometric modeling, and numerical analysis, reducing the risk of transcription errors and ensuring the traceability of the assumptions made.

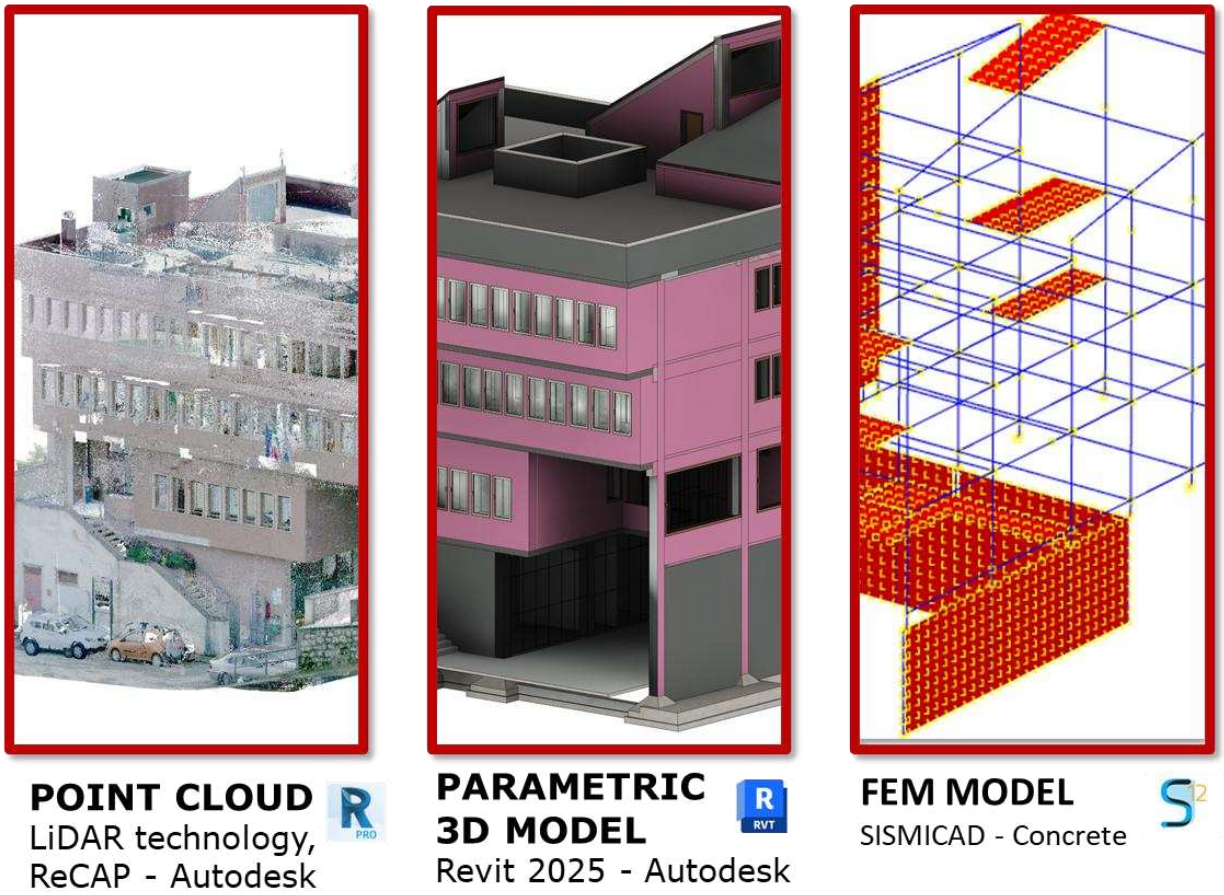

Figure 20 - Interoperability process

BIM DIMENSIONS

This study considered the main dimensions of BIM: 1D, 2D, 3D, 5D, and 6D. In addition to three-dimensional geometric representation, the model was enriched with information relating to time (4D), costs (5D), and environmental sustainability (6D). This allowed the model to be used as a multidimensional analysis and decision-making tool, as well as a simple basis for structural modeling.

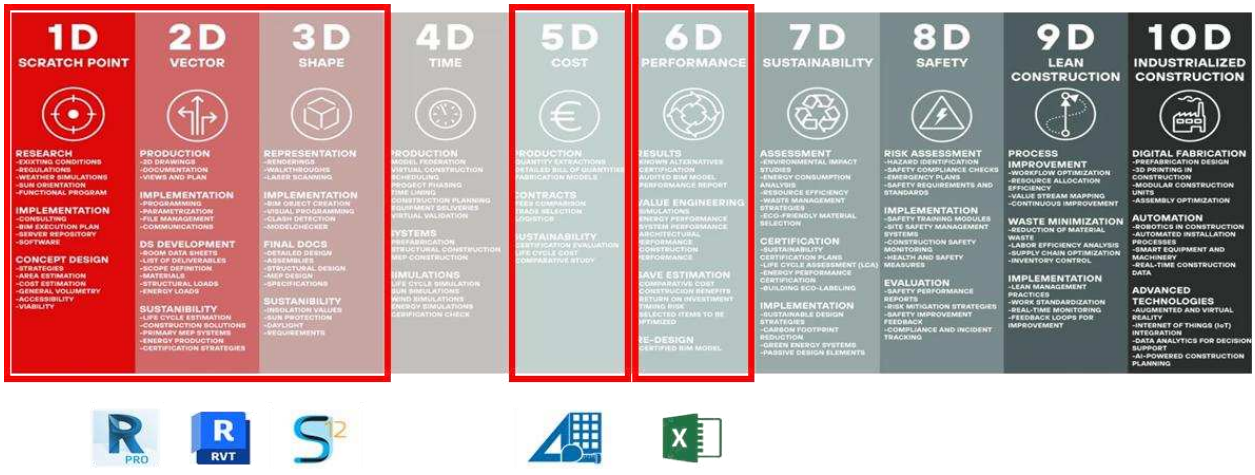

Figure 21 - BIM dimensions. [11]

3.3 Knowledge of the existing building

In order to correctly assess seismic safety and therefore design the necessary adaptation measures, it was necessary to acquire as complete and reliable knowledge as possible of the existing building. This process included both geometric and morphological surveys and an investigation of the materials and construction technologies used.

HISTORICAL DOCUMENTATION

The first phase involved collecting existing documentation from the municipal technical office, including original drawings (floor plans, sections, and elevations), calculation reports, and administrative documentation. However, these documents proved to be incomplete and out of date, making it necessary to carry out direct surveys and on-site investigations to fill in the gaps in the information.

VISUAL SURVEYS

The visual inspection made it possible to verify, where possible, the geometric characteristics of the main structural elements (dimensions of beams, pillars, partitions, floors) and the methods of connection between horizontal and vertical elements. It was possible to confirm the reinforced concrete load-bearing structure, the absence of special anti-seismic measures, and the use of brick and concrete floors. Furthermore, it emerged that the beams marked on the project drawings in the basement, identified as floor beams in the survey, were found to have a thickness of 30x50 cm².

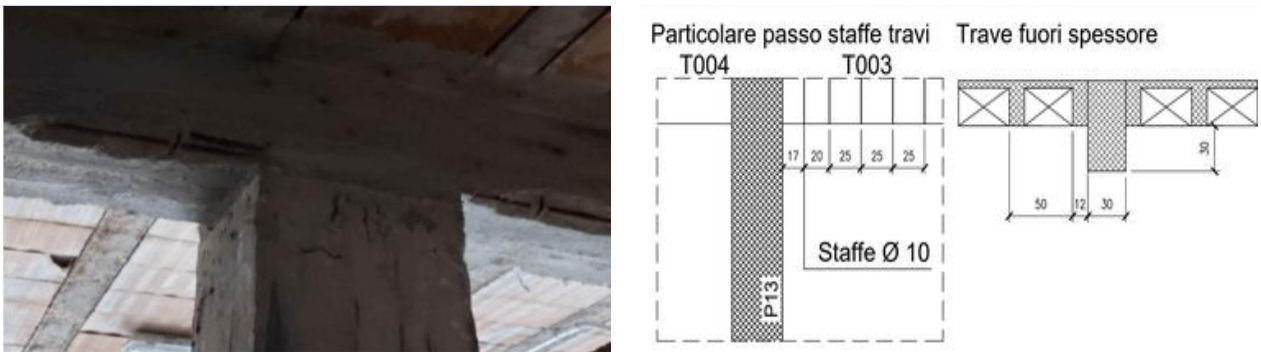

Figure 22 - Picture of beam out of thickness in the basement and extract of carpentry boards

IN SITU TESTS

With regard to the preliminary mechanical characterization of the materials, non-destructive and semi-destructive tests were carried out exclusively on the basement elements:

- Sclerometric tests on beams and pillars to estimate the compressive strength of the concrete in situ;

- Pacometric tests to identify the position, concrete cover, and diameter of the reinforcement;
- Direct visual inspections on sections made accessible by localized removal of plaster, to confirm the arrangement of longitudinal and transverse reinforcement.

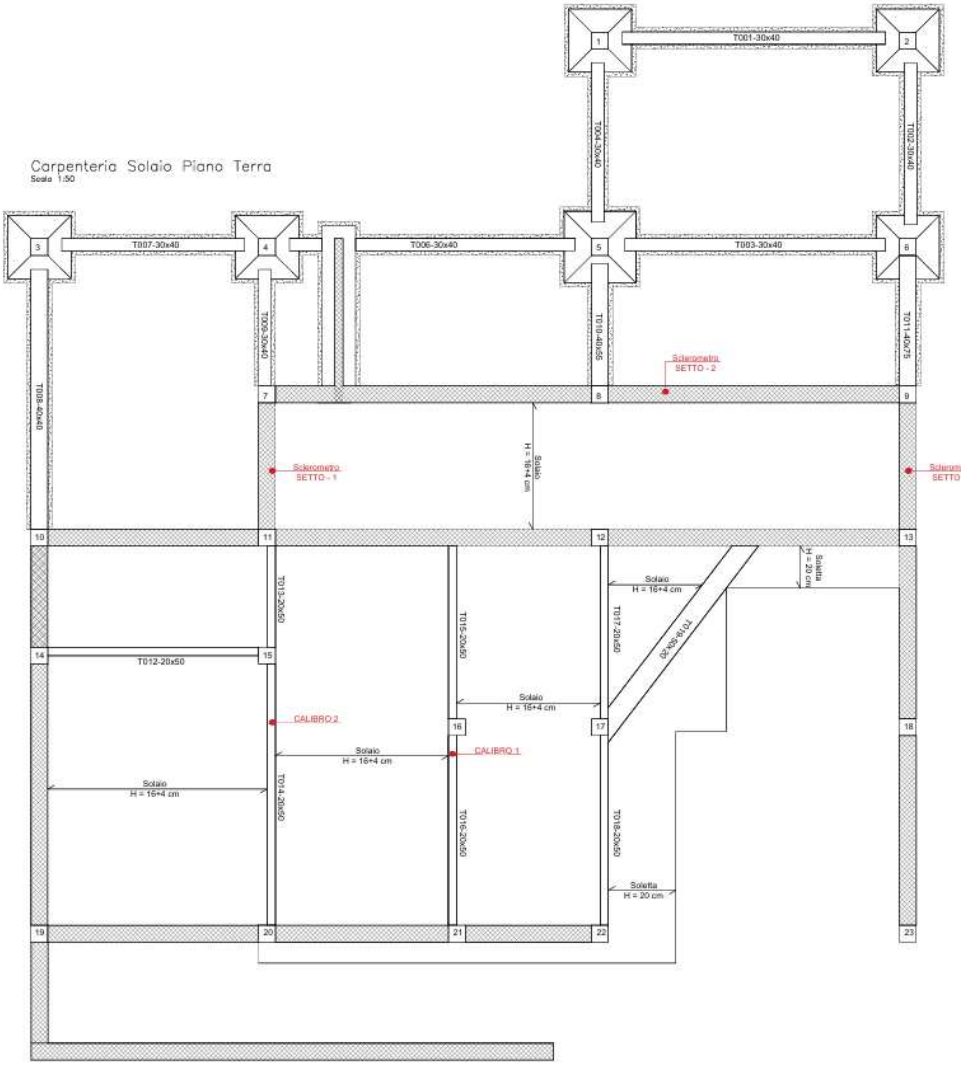

Figure 23 - Location of material investigations carried out in the basement.

PACOMETRIC TESTS

Pacometric surveys are based on measuring the magnetic field generated by reinforcing bars close to the concrete surface in structural elements such as beams, columns, and walls. These surveys make it possible to identify the position of the reinforcing bars, estimate their diameter, the distance between them, the thickness of the concrete cover for longitudinal reinforcement, and the diameter and distance of the stirrups. The tests are performed in accordance with BS 1881:204. The results were used to reconstruct the internal layout of the reinforcement and entered into the FEM model.

The position of the metal bars on the sides of the structural elements can be determined by drawing a straight line on the surface of the element that passes through the points detected on different sections. This method allows the reinforcement pattern inside the analyzed element to be mapped. The same elements subjected to sclerometric tests were examined. The information obtained will be used to define the reinforcement of the structural elements in the FEM model.

Figure 24 - Pacometric survey carried out on beams and pillars in the basement

SCLEROMETRIC TESTS

Sclerometric tests showed that the concrete had a higher strength than that indicated in the original design documents. This phenomenon is consistent with the literature, which recognizes that the estimation of in situ strength may differ from historical values due to degradation, particularly carbonation. This process, caused by the reaction between carbon dioxide and calcium hydroxide in the cement matrix, reduces the pH of the concrete and compromises the protection of the reinforcement. The presence of corrosion and loss of concrete cover observed on some elements confirmed this pattern of degradation.

In this context, sclerometric tests are useful for assessing the homogeneity of the concrete and providing an indication of the building's exposure to degradation phenomena such as carbonation. These tests make it possible to identify areas that may require restoration or consolidation, contributing to a more accurate assessment of the structural vulnerability and durability of the building.

Figure 25 - Positioning of sclerometer marks

4. Project parameters

4.1 Material characterization

When assessing existing structures, one of the fundamental aspects concerns the degree of knowledge of the materials that make up the structure itself. This knowledge is based on a series of data collected through surveys, experimental tests, and historical documentation. To classify the level of reliability of this information, technical standards establish different Levels of Knowledge (LC), which directly affect the safety coefficients used in structural checks.

In particular, the levels of knowledge are structured as follows:

- LC1: Low level of knowledge, characterized by limited or partial information on materials, without direct evidence.
- LC2: Medium level of knowledge, which involves the integration of historical data and indirect evidence on materials.
- LC3: High level of knowledge, obtainable through detailed investigations and direct evidence, including destructive testing.

The level of knowledge used to assess a structure determines the values of the confidence factors to be applied in safety checks, thus influencing the final result of the structural analyses.

In the specific case of the structure under study, it was possible to access a vast amount of information thanks to the availability of the original drawings dating back to the time of construction. These documents provide precise details on the geometric characteristics and nominal properties of the materials used, allowing for the reconstruction of a sufficiently accurate overall picture of the current state of the structure.

However, no destructive tests have yet been carried out on the materials. Tests such as breaking tests on samples taken on site are essential for accurately determining the actual mechanical properties of the materials, which is particularly important for structures with a long operational life. The absence of these investigations inevitably introduces a degree of uncertainty with regard to the data reported in the historical documentation.

In light of the availability of detailed historical data, the high accuracy of the survey, and the lack of destructive testing in the preliminary phase, a level of knowledge of LC3 has been attributed to strctur. Such level, considered high, is adequate for a feasibility study.

Tabella C8.5.IV – *Livelli di conoscenza in funzione dell'informazione disponibile e conseguenti metodi di analisi ammessi e valori dei fattori di confidenza, per edifici in calcestruzzo armato o in acciaio*

Livello di conoscenza	Geometrie (carpenterie)	Dettagli strutturali	Proprietà dei materiali	Metodi di analisi	FC (*)
LC1	Da disegni di carpenteria originali con rilievo visivo a campione; in alternativa rilievo completo ex-novo	Progetto simulato in accordo alle norme dell'epoca e ***indagini limitate*** in situ	Valori usuali per la pratica costruttiva dell'epoca e ***prove limitate*** in situ	Analisi lineare statica o dinamica	1,35
LC2		Elaborati progettuali incompleti con ***indagini limitate*** in situ; in alternativa ***indagini estese*** in situ	Dalle specifiche originali di progetto o dai certificati di prova originali, con ***prove limitate*** in situ; in alternativa da ***prove estese*** in situ	Tutti	1,20
LC3		Elaborati progettuali completi con ***indagini limitate*** in situ; in alternativa ***indagini esaustive*** in situ	Dai certificati di prova originali o dalle specifiche originali di progetto, con ***prove estese*** in situ; in alternativa da ***prove esaustive*** in situ	Tutti	1,00

(*) A meno delle ulteriori precisazioni già fornite nel § C8.5.4.

Table 1 - Definition of knowledge levels – Table extracted from NTC2018

Since the range of documents provided is very broad, it was possible to preliminarily characterize the use of the materials used to build the structure.

In fact, from the carpentry drawings, it was possible to extract information relating to materials such as cement, concrete, and iron.

To calculate the capacity of ductile elements/mechanisms, the properties of existing materials are used, divided by the relevant confidence factors based on the level of knowledge achieved. To calculate the capacity of brittle elements/mechanisms, the strengths of the materials are divided by the corresponding partial coefficients and by the confidence factors relating to the level of knowledge achieved (LC3).

The following table summarizes the mechanical properties considered for the different materials:

Existing concrete R28-300

R_{ck} (characteristic cubic compression strength)	300 daN/cmq
f_{ck}(characteristic cylindrical compression strength)=0.83R_{ck}	250 daN/cmq
f_{cm}(average cylindrical compression strength)=f_{ck}+8	330 daN/cmq
Design strength for ductile fracture mechanisms:	
$f_{cd,duttile}$= f_{cm}/FC=166/1.0	166 daN/cmq
Design strength for fragile fracture mechanisms:	
$f_{cd,fragile}$= f_{cm}/FC/γ=166/1.0/1.5	110 daN/cmq

Concrete upgrading work C32/40

R_{ck} (characteristic cubic compression strength)	400 daN/cmq
f_{ck}(characteristic cylindrical compression strength)=0.83R_{ck}	332 daN/cmq
f_{cm}(average cylindrical compression strength)=f_{ck}+8	412 daN/cmq
Exposure class for internal structures	XC1
Exposure class for internal foundations	XC2
Concrete cover	4 cm

Reinforcing steel for reinforced concrete FEB44K

f_{ym} (average yield strength)	4400 daN/cmq
Design strength for ductile fracture mechanisms:	
$f_{yd,duttile}=f_{ym}/FC$ = 4400/1.0	4400 daN/cmq
Design strength for fragile fracture mechanisms:	
$f_{yd,fragile}= f_{ym}/FC/\gamma$= 4326/1.0/1.15	3826 daN/cmq

Steel for concrete retrofitting B450C

f_{tk} *(characteristic breaking strength)*	450	N/mm²
f_{yk} (characteristic yield strength)	517.5	N/mm²
E_s	210000	N/mm²

Table 2 - Material mechanical properties

4.2 Gravitational actions

The assessment of loads and overloads was carried out in accordance with the provisions of point 3.1 of the NTC 2018. In particular, useful reference was made to Tables 3.1. I and 3.1.II of the NTC 2018, for the specific weights of materials and for the quantification and classification of overloads, respectively. The remaining loads were determined automatically by the software, based on the geometric properties and materials assigned.

In this case, it was also possible to find information on the loads acting on the structure in the project documentation.

Table 3 summarizes the values considered within the model.

Weights of the elements	
Cemento armato	25.000 N/m³
Cemento non armato	24.000 N/m³
Acciaio (per armatura e da carpenteria)	78.500 N/m³
Permanent structural load	
Solaio latero cementizio (16+4)	270 daN/m^2
Permanent non-structural load	
Pacchetto finitura solaio latero cementizio	230 daN/m^2
External tamponade	750 daN/ml
Floor overload	
Load CAT. B2	300 daN/m^2
Stairs	400 daN/m^2
Effect of snow	
Snow load	160 *daN/m²*

Table 3 - Load parameters

For this project, it is important to specify the simplifications adopted for modeling purposes:

- The loads acting on the floors, resulting from the load analysis, are automatically distributed by the calculation program on the elements (beams, columns, walls, floors, foundations, etc.).
- The loads due to the walls, both on the foundation beams and on the floor beams, are modeled as linear loads acting exclusively on the structural elements. It is also possible to apply

additional concentrated and/or distributed actions (variable with linear law and acting along the entire member or on limited sections of it) directly on all structural elements.

4.3 Seismic action parameters

The national normative reference for seismic safety in Italy is represented by the Decree of the President of the Council of Ministers (DPCM) of January 17, 2018, which approves the "New Technical Standards for Construction" (NTC 2018). These standards contain specific provisions for the seismic design of buildings and civil works in Italy, according to which the municipality of Sant'Agapito in the province of Isernia (IS) is classified as seismic zone 1, i.e., an area with medium seismic risk that may be subject to moderate earthquakes.

The structure is assessed for a nominal life of 50 years and a use class of 3.

The geographical coordinates of the site are as follows:

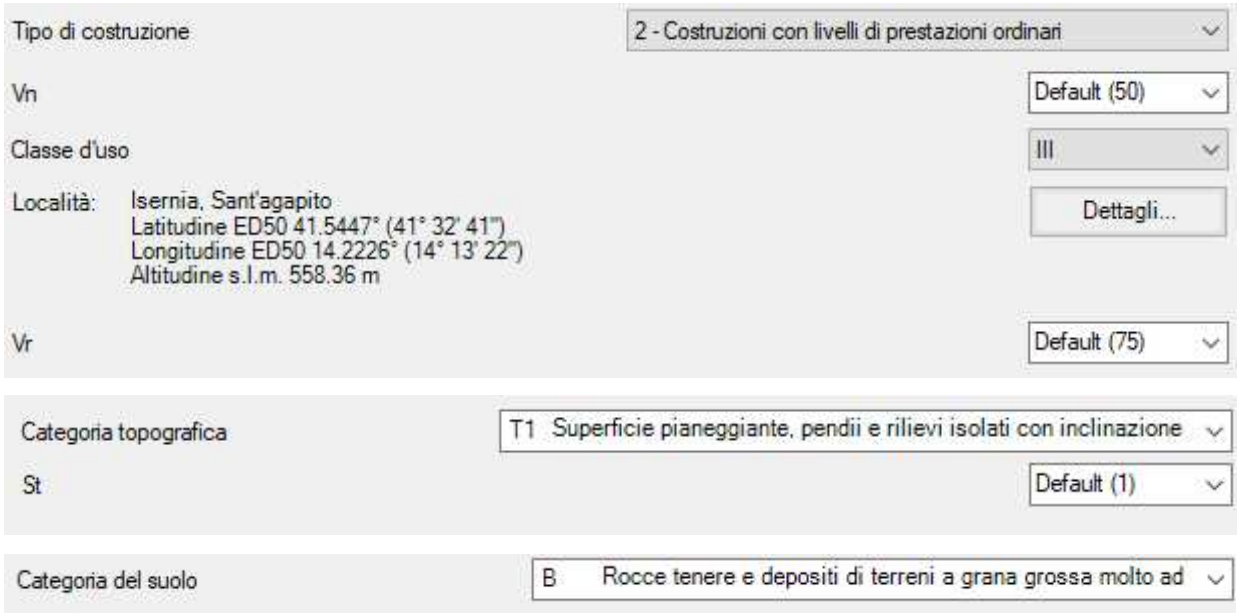

Figure 26 - Parameters for defining seismic hazard

Basing on the parameters indicated previously, the elastic response spectrum required by the standards was generated. This spectrum is the fundamental input for the linear dynamic analysis (modal analysis with response spectrum), as it allows the maximum accelerations expected to be evaluated as a function of the natural period of the structure.

The following figure shows the elastic and design spectra used for the design and verification of the structure.

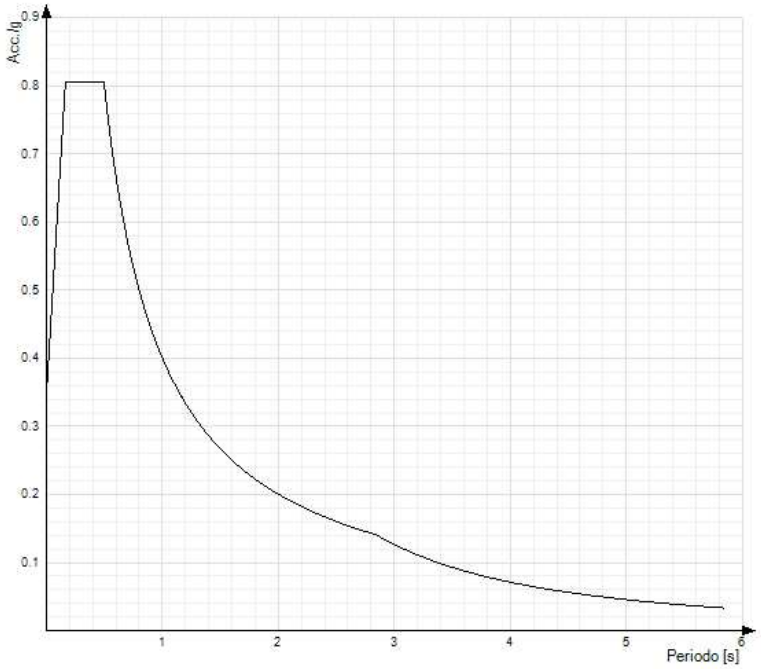

Figure 27 - Elastic and design spectrum SLV- Horizontal component

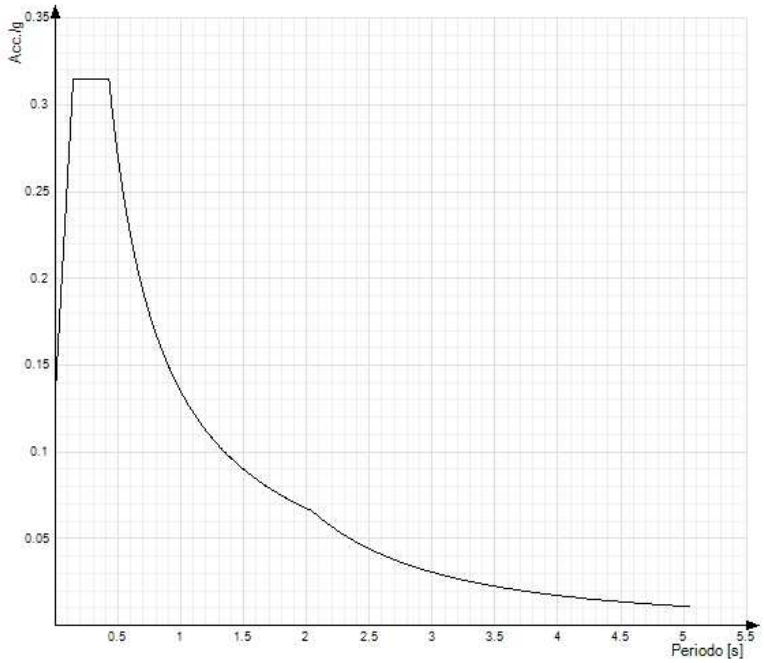

Figure 28 - Elastic and design spectrum – SLD – Horizontal component

LOAD COMBINATION

After defining the individual loads acting on the structure, these must be combined in accordance with the provisions of the 2018 Technical Standards for Construction. The 2018 Technical Standards for Construction require the adoption of the semi-probabilistic method for limit states, which is based on compliance with the following relationship:

$$R_d \geq E_d$$

Therefore, the structural verification will be considered valid if the design capacity is always greater than or equal to the design value of the demand. In accordance with this principle, load combinations allow for the consideration of the concurrence of different actions and the evaluation of the structural response to the various limit states required by the regulations.

With reference to paragraph 2.5.3 of NTC 2018, the combinations considered are as follows:

SLU

$$\gamma_{G1} \cdot G_1 + \gamma_{G2} \cdot G_2 + \gamma_P \cdot P + \gamma_{Q1} \cdot Q_{K1} + \gamma_{Q2} \cdot \psi_{02} \cdot Q_{K2} + \gamma_{Q3} \cdot \psi_{03} \cdot Q_{K3} + \ldots\ldots$$

where:

G_1 → represents the self-weight of all structural elements; self-weight of the soil, where relevant; forces induced by the soil (excluding the effects of variable loads applied to the soil); forces resulting from water pressure (when constant over time);

G_2 → represents the self-weight of all non-structural elements;

P → represents the action of pre-tensioning and/or pre-compression;

Q → actions on the structure or structural element with instantaneous values that may vary significantly over time:

- long-lasting: acts with significant intensity, even if not continuously, for a period of time that is not negligible in relation to the nominal life of the structure;
- short-term: actions that have an effect for a short period of time compared to the nominal life of the structure;

Q_{ki} → represents the characteristic value of the i-th variable action;

γ_g, γ_q, γ_p are the partial coefficients as defined in Table 2.6. I of the 2018 NTC;

ψ_{0i} are the combination coefficients to take into account the reduced probability of concurrence of variable actions with their respective characteristic values.

SLD

The seismic action, obtained from the design spectrum for the Damage Limit State, was combined with the other actions using a relationship completely analogous to the previous one.:

$$G_1+G_2+P+E+\Sigma_i\psi_{2i}\cdot Q_{ki};$$

where:

E → represents the seismic action for the limit state under consideration;

G_1 → represents the self-weight of all structural elements;

G_2 → represents the self-weight of all non-structural elements; P represents the pre-stressing and/or pre-compression action;

ψ_{2i} → variable action combination coefficient Qi;

Q_{ki} → characteristic value of variable action Qi.

The effects of seismic action are assessed taking into account the masses associated with the following gravitational loads:

$$G_K+\Sigma_i(\psi_{2i}\cdot Q_{ki}).$$

The values of the coefficients ψ_{2i} are shown in the table in the SLV.

SLE

For checks on serviceability limit states, depending on the case, reference is made to the following load combinations:

rara	frequente	quasi permanente
$\sum_{j\geq1} G_{kj} + P + Q_{k1} + \sum_{i>1} \psi_{0i} \cdot Q_{ki}$	$\sum_{j\geq1} G_{kj} + P + \psi_{11} \cdot Q_{k1} + \sum_{i>1} \psi_{2i} \cdot Q_{ki}$	$\sum_{j\geq1} G_{kj} + P + \sum_{i>1} \psi_{2i} \cdot Q_{ki}$

where:

G_{kj} → characteristic value of the j-th permanent action;

P_{kh} → characteristic value of the h-th deformation imposed;

Q_{kl} → characteristic value of the variable base action of each combination;

Q_{ki} → characteristic value of the i-th variable action;

ψ_{0i} → coefficient used to define the values of allowable actions that are short-lived but still significant in relation to the possible concurrence with other variable actions;

ψ_{1i} → coefficient used to define the values of actions allowable at the 0.95 fractile of the instantaneous value distributions;

ψ_{2i} → coefficient used to define the almost permanent values of allowable actions at the average values of the distributions of instantaneous values.

The coefficient ψ_{0i}, ψ_{1i}, ψ_{2i} are selected with reference to Table 2.5.1 of the reference standard shown below.

Tab. 2.5.I – *Valori dei coefficienti di combinazione*

Categoria/Azione variabile	Ψ_{0j}	Ψ_{1j}	Ψ_{2j}
Categoria A - Ambienti ad uso residenziale	0,7	0,5	0,3
Categoria B - Uffici	0,7	0,5	0,3
Categoria C - Ambienti suscettibili di affollamento	0,7	0,7	0,6
Categoria D - Ambienti ad uso commerciale	0,7	0,7	0,6
Categoria E – Aree per immagazzinamento, uso commerciale e uso industriale Biblioteche, archivi, magazzini e ambienti ad uso industriale	1,0	0,9	0,8
Categoria F - Rimesse , parcheggi ed aree per il traffico di veicoli (per autoveicoli di peso ≤ 30 kN)	0,7	0,7	0,6
Categoria G – Rimesse, parcheggi ed aree per il traffico di veicoli (per autoveicoli di peso > 30 kN)	0,7	0,5	0,3
Categoria H - Coperture accessibili per sola manutenzione	0,0	0,0	0,0
Categoria I – Coperture praticabili	da valutarsi caso per caso		
Categoria K – Coperture per usi speciali (impianti, eliporti, ...)			
Vento	0,6	0,2	0,0
Neve (a quota ≤ 1000 m s.l.m.)	0,5	0,2	0,0
Neve (a quota > 1000 m s.l.m.)	0,7	0,5	0,2
Variazioni termiche	0,6	0,5	0,0

Table 4 - Combination coefficients from NTC2018 regulations

SEISMIC ACTIONS

The horizontal actions caused by the earthquake on the structure are conventionally determined as acting separately in two predetermined orthogonal directions. In general, however, the horizontal components of the earthquake must be considered as acting simultaneously. To this end, the

combination of the horizontal components of the seismic action has been taken into account as follows:

- The effects of actions due to the combination of horizontal components of seismic action were evaluated using the following combinations:
  - $E_{EdX} \pm 0,30E_{EdY}$
  - $E_{EdY} \pm 0,30E_{EdX}$

wheree:

- E_{EdX} represents the effects of the action due to the application of seismic action along the chosen horizontal X-axis of the structure;
- E_{EdY} represents the effects of the action due to the application of seismic action along the chosen horizontal Y-axis of the structure.

5. Structural modeling

The numerical modeling of an existing building is a crucial step in seismic safety assessment, as it allows the global and local behavior of the building to be simulated in response to the actions required by regulations. The structural model of the building under investigation was developed using SISMICAD calculation software.

The aim is to ensure that the model represents the actual configuration as faithfully as possible, integrating geometric and material data with the necessary load conditions and mechanical properties. The accurate definition of the actions and modeling choices is a prerequisite for subsequent static and dynamic analyses.

As already mentioned, the calculation software used is SISMICAD, a structural calculation program dedicated to the design and verification of reinforced concrete, steel, masonry, and wood elements in civil engineering works. The solution model on which the program is grounded is based on finite element analysis (FEM), a numerical-engineering approach that allows the calculation domain to be disaggregated, facilitating the overall solution through the resolution of discretized elements.

The geometric configuration of the building has been faithfully reconstructed from the available documentation and the BIM model, including the planimetric and altimetric layout of the main frames, partitions, floors, and foundations.

The main elements modeled within the structure are as follows:

- Beam elements for modeling beams and columns;
- Shell elements for representing load-bearing and cantilever slabs;
- Rigid nodes at the connection points between the different elements, in order to ensure the correct transmission of stresses.

As specified in paragraph 2 of this document, the beams all have the same dimensions of 40x40 cm, while the beams have variable sections. In the model, they have been represented faithfully to the design documents and the BIM model. The same reasoning applies to the reinforcing bars.

Furthermore, the foundations are represented graphically but are considered as joints.

After entering all the geometric, mechanical, and load parameters described above into the software, it was possible to obtain the finite element model of the building. This model forms the basis for subsequent structural analyses and allows the overall behavior of the construction to be reproduced consistently.

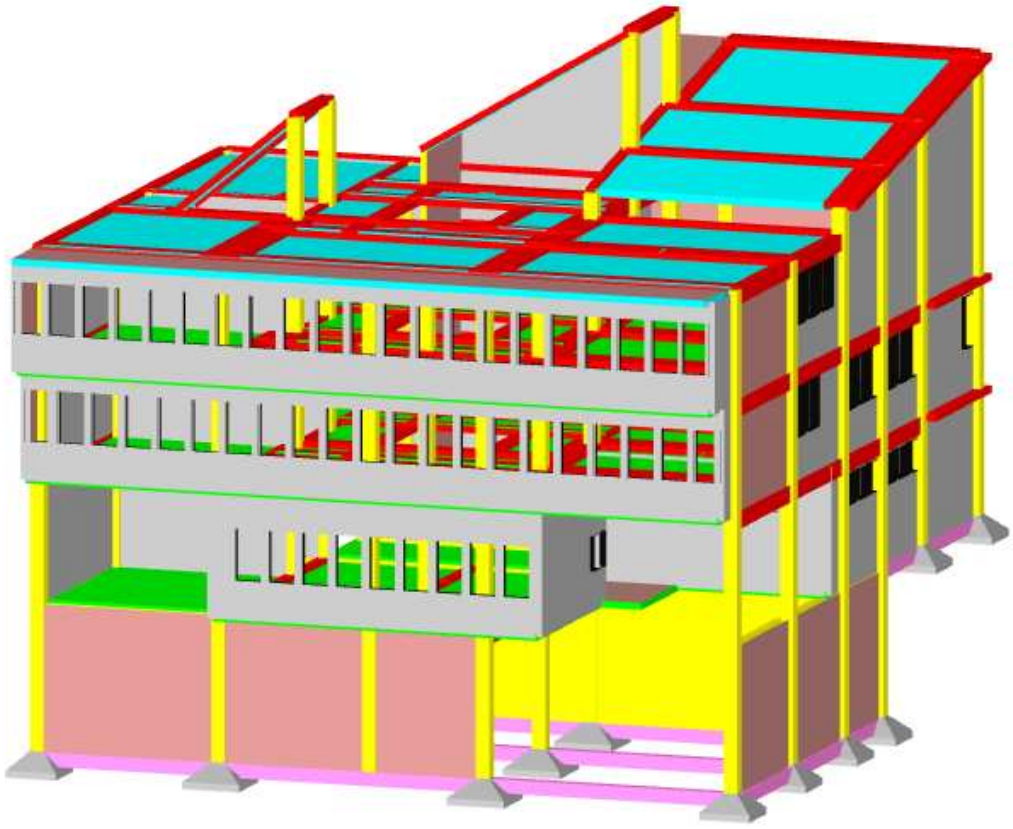

Figure 29 - 3D model of the existing structure

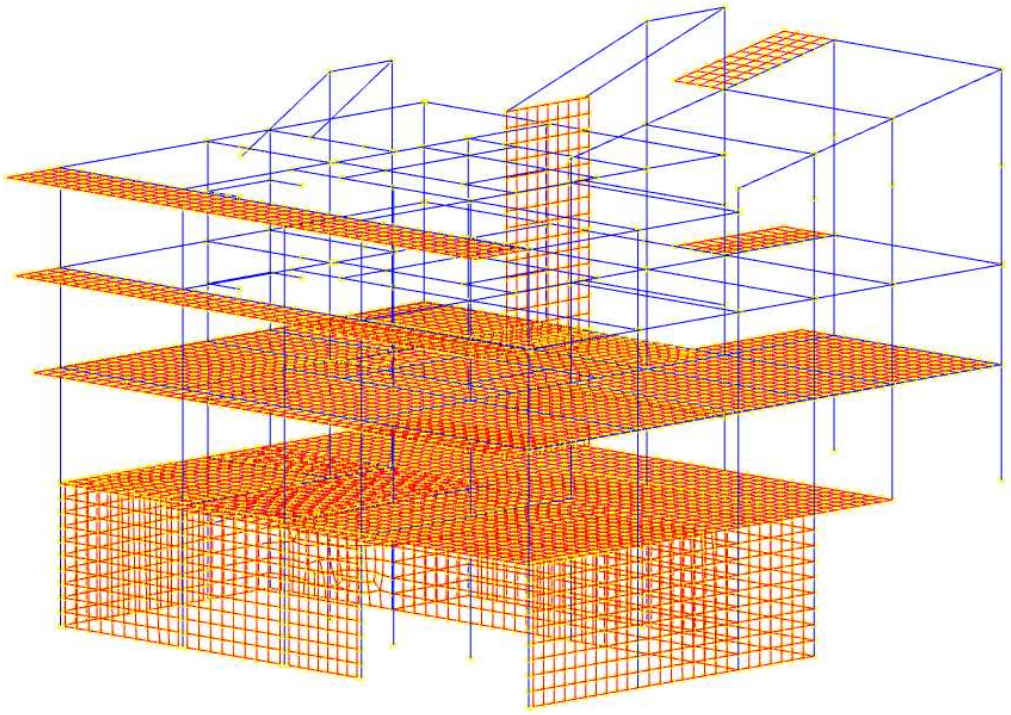

Figure 30 – FEM Model of the existing structure

6. Analysis of the existing structure

Two main types of analysis were carried out on the existing structure: static analysis, aimed at assessing the distribution of stresses under the action of gravitational loads, and dynamic modal analysis, aimed at identifying the natural frequencies and modal deformations of the building. The objective of these analyses is to outline the overall behavior of the building, highlighting any critical issues to be taken into account for possible structural adjustments.

The analyses conducted are to be considered consistent with the level of detail typical of a feasibility study for the intervention: the checks carried out will concern only the reinforced concrete pillars and walls.

6.1 Static analysis

The expected results of this analysis correspond to those obtained: seismic safety has been verified from a static point of view.

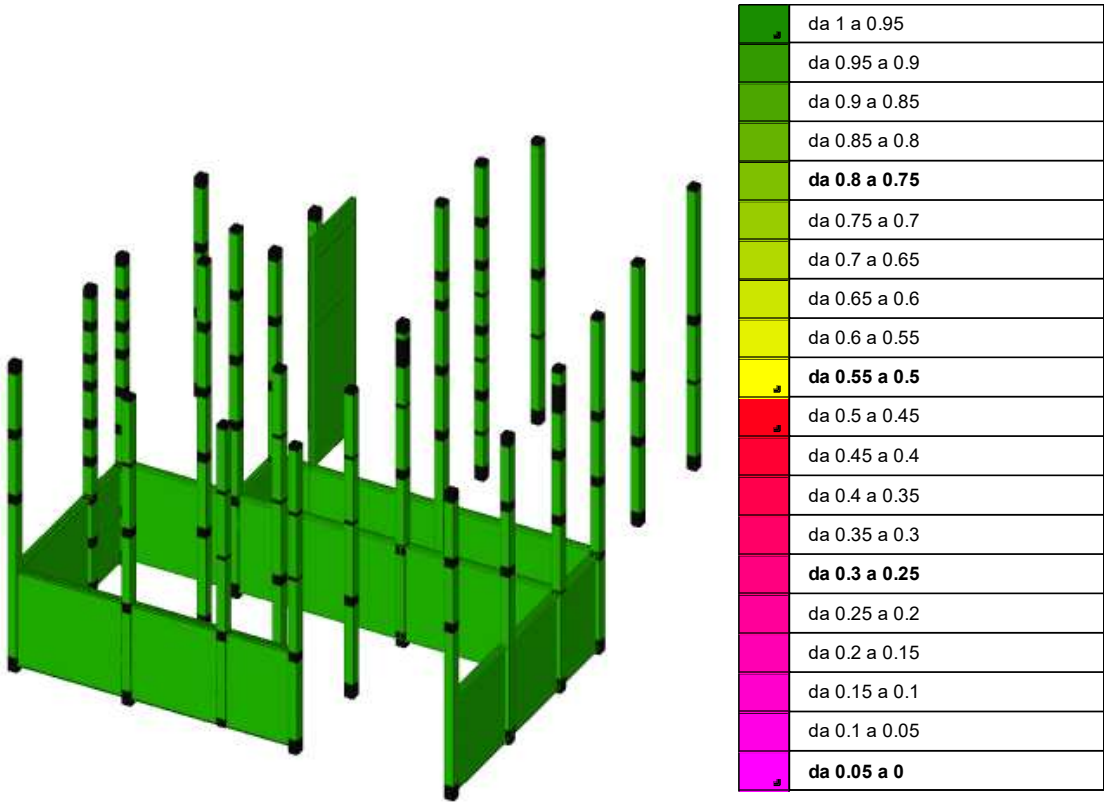

Figure 31 - Minimum security

6.2 Dynamic modal analysis

As already mentioned, modal analysis seeks to identify the modes of vibration of a structure and, for each mode of vibration, calculates its natural period of vibration, i.e., the interval of time that the structure takes to perform a complete oscillation according to a deformed configuration similar to one of its modes of vibration.

The characterization of the input parameters evaluated in accordance with NTC 2018 is illustrated below.

The behavior factor q represents the parameter that permits to account for the dissipative capacity of the structure in the seismic analysis. It is determined according to the following relationship:

$$q = q_0 \cdot K_R$$

Where:

q_0 is the initial behavior factor.

K_R is the reduction coefficient, which in this case is equal to 0.8.

Tab. 7.3.II – *Valori massimi del valore di base q_0 del fattore di comportamento allo SLV per diverse tecniche costruttive ed in funzione della tipologia strutturale e della classe di duttilità CD*

	q_0	
Tipologia strutturale	CD"A"	CD"B"
Costruzioni di calcestruzzo (§ 7.4.3.2)		
Strutture a telaio, a pareti accoppiate, miste (v. § 7.4.3.1)	4,5 α_u/α_1	3,0 α_u/α_1
Strutture a pareti non accoppiate (v. § 7.4.3.1)	4,0 α_u/α_1	3,0
Strutture deformabili torsionalmente (v. § 7.4.3.1)	3,0	2,0
Strutture a pendolo inverso (v. § 7.4.3.1)	2,0	1,5
Strutture a pendolo inverso intelaiate monopiano (v. § 7.4.3.1)	3,5	2,5
Costruzioni con struttura prefabbricata (§ 7.4.5.1)		
Strutture a pannelli	4,0 α_u/α_1	3,0
Strutture monolitiche a cella	3,0	2,0
Strutture con pilastri incastrati e orizzontamenti incernierati	3,5	2,5
Costruzioni d'acciaio (§ 7.5.2.2) e composte di acciaio-calcestruzzo (§ 7.6.2.2)		
Strutture intelaiate Strutture con controventi eccentrici	5,0 α_u/α_1	4,0
Strutture con controventi concentrici a diagonale tesa attiva Strutture con controventi concentrici a V	4,0 2,5	4,0 2,0
Strutture a mensola o a pendolo inverso	2,0 α_u/α_1	2,0
Strutture intelaiate con controventi concentrici	4,0 α_u/α_1	4,0
Strutture intelaiate con tamponature in murature	2,0	2,0
Costruzioni di legno (§ 7.7.3)		
Pannelli di parete a telaio leggero chiodati con diaframmi incollati, collegati mediante chiodi, viti e bulloni Strutture reticolari iperstatiche con giunti chiodati	3,0	2,0
Portali iperstatici con mezzi di unione a gambo cilindrico	4,0	2,5
Pannelli di parete a telaio leggero chiodati con diaframmi chiodati, collegati mediante chiodi, viti e bulloni.	5,0	3,0
Pannelli di tavole incollate a strati incrociati, collegati mediante chiodi, viti, bulloni Strutture reticolari con collegamenti a mezzo di chiodi, viti, bulloni o spinotti		2,5

Table 5 - NTC2018 Table – Behavior factors.

According to the 2018 NTC guidelines, for frame structures, the value of q_0 also depends on the ratio α_u/α_i, which measures the redistribution of resistances in the plastic range. For irregular structures in plan, this ratio is taken as the average between 1 and the value obtained from the normative formula.

a) Strutture a telaio o miste equivalenti a telai
- strutture a telaio di un piano — $\alpha_u/\alpha_1 = 1,1$
- strutture a telaio con più piani ed una sola campata — $\alpha_u/\alpha_1 = 1,2$
- strutture a telaio con più piani e più campate — $\alpha_u/\alpha_1 = 1,3$

Figure 32 - Extract from NTC2018 – Behavioral factors.

Applying these criteria to the case in question, the result is a structure factor in CDB:

$$q=0.8\cdot(1.3+1)/2*3=2.76$$

If reinforced concrete walls are present in the structure, in order to prevent fragile collapse, the q_0 values must be reduced by the k_w factor, with:

$$k_w = \begin{cases} 1,00 & \text{per strutture a telaio e miste equivalenti a telai} \\ 0,5 \le (1+\alpha_0)/3 \le 1 & \text{per strutture a pareti, miste equivalenti a pareti, torsionalmente deformabili} \end{cases}$$

For the structure analyzed, this coefficient is equal to 1, and therefore does not change the calculated value, so:

$$q=2.76*1=2.76$$

For structures with non-dissipative structural behavior, a behavior factor q_{nd} is adopted, reduced with respect to the minimum value relating to the "CDB" according to the expression:

$$1 \le q_{ND} = \frac{2}{3} q_{CD"B"} \le 1,5$$

$$1 \le \frac{2}{3} 2.76 \le 1.5$$

$$1 \le 1.84 \le 1.5$$

which leads to the adoption of a reduced and uniform value in all main directions for the checks.

Therefore, for the purposes of seismic analysis of the existing structure, the assumed behavior factors are as follows:

- X direction: q=1.5q = 1.5q=1.5
- Y direction: q=1.5q = 1.5q=1.5

6.3 Modal response and validation

The number of vibration modes of the structure that were considered is 15. The main modes are the second and third modes, as they have the highest percentage of participating mass for the X and Y directions, respectively.

Total Participating Mass:

X Translation: 0.969778 Y Translation: 0.939287 Z Translation: 0

X Rotation: 0.939287 Y Rotation: 0.995871 Z Rotation: 0.93567

Modo	Periodo	Massa X	Massa Y	Massa Z	Massa rot. X	Massa rot. Y	Massa rot. Z	Massa sX	Massa sY
1	0.673410848	0.029503935	0.103238322	0	0.159337788	0.054503544	0.043668748	0.029503935	0.103238322
2	0.59222779	0.648479628	0.008717966	0	0.012592589	0.895168087	0.000194544	0.648479628	0.008717966
3	0.366947988	0.00055942	0.49025138	0	0.737274398	0.000143896	0.554714235	0.00055942	0.49025138
4	0.272195982	0.012859715	0.019473718	0	0.006619443	0.002901249	0.009481743	0.012859715	0.019473718
5	0.199022913	0.065364055	0.006747786	0	0.002284476	0.005534966	0.003163524	0.065364055	0.006747786
6	0.146653066	0.003003454	0.013091509	0	0.003572228	0.000435603	0.014989457	0.003003454	0.013091509
7	0.120911046	0.005234351	0.003256157	0	0.000710941	0.001223878	0.00199893	0.005234351	0.003256157
8	0.11047437	0.001754029	0.012186757	0	0.003523612	0.000434291	0.012921474	0.001754029	0.012186757
9	0.106155548	0.014977851	0.000000925	0	0.0000069	0.004777314	0.000442695	0.014977851	0.000000925
10	0.09432588	0.004035656	0.059723434	0	0.018171604	0.000699651	0.066846908	0.004035656	0.059723434
11	0.088506162	0.002668535	0.035320094	0	0.011359012	0.000489549	0.037133437	0.002668535	0.035320094
12	0.068055487	0.002962697	0.000687851	0	0.000333334	0.000170444	0.000179672	0.002962697	0.000687851
13	0.060530607	0.00007747	0.018815321	0	0.007784804	0.000020805	0.02230058	0.00007747	0.018815321
14	0.020801578	0.000964931	0.188386935	0	0.030743174	0.000109518	0.183902281	0.000964931	0.188386935
15	0.014865228	0.179481698	0.001490653	0	0.000222679	0.029277794	0.009376495	0.179481698	0.001490653

Table 6 - Modal Response - Natural Vibration Periods and Participating Mass

The behavior of the structure based on the main vibration modes shows a slight torsional contribution, as shown in the images below. Furthermore, when evaluating the seismic response in terms of minimum safety, there are some local critical points at the vertical partition that crosses the entire structure and at some columns near the stairwell.

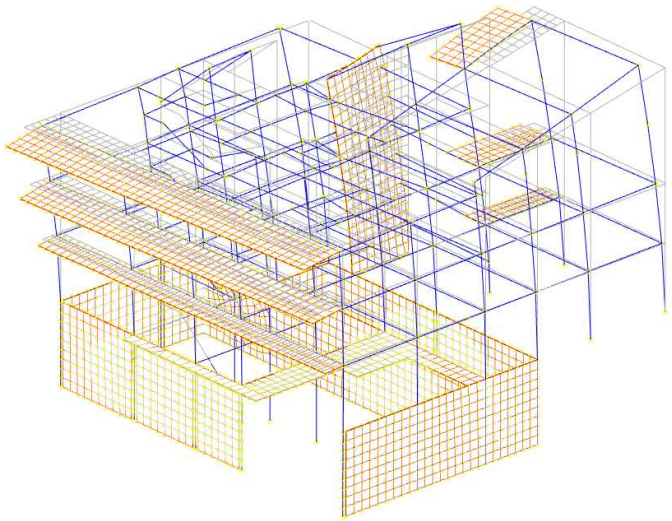

Figure 33 - Displacements in the third vibration mode (T=0.36s).

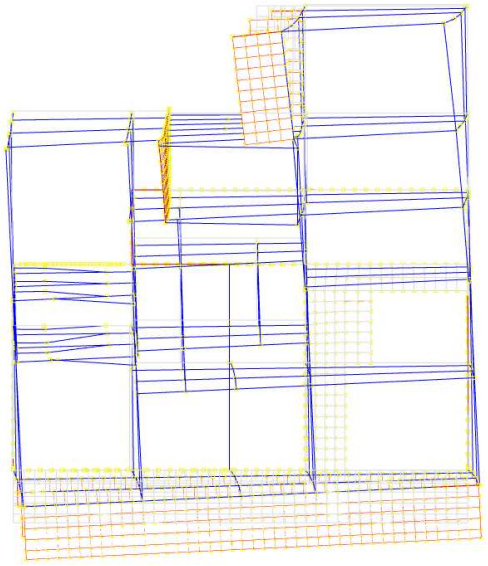

Figure 34 - Displacements in the third vibration mode (T=0.36s).

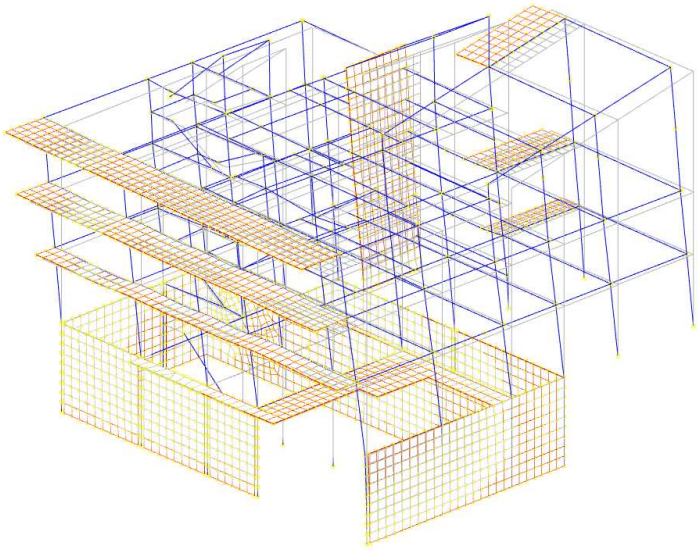

Figure 35 - Displacements in the second vibration mode (T=0.59s)

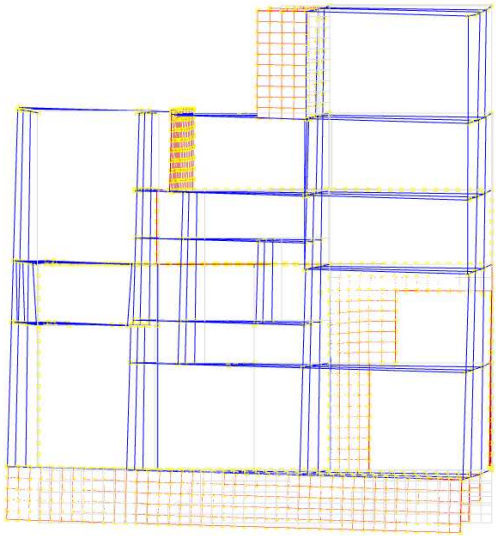

Figure 36 - Displacements in the second vibration mode (T=0.59s)

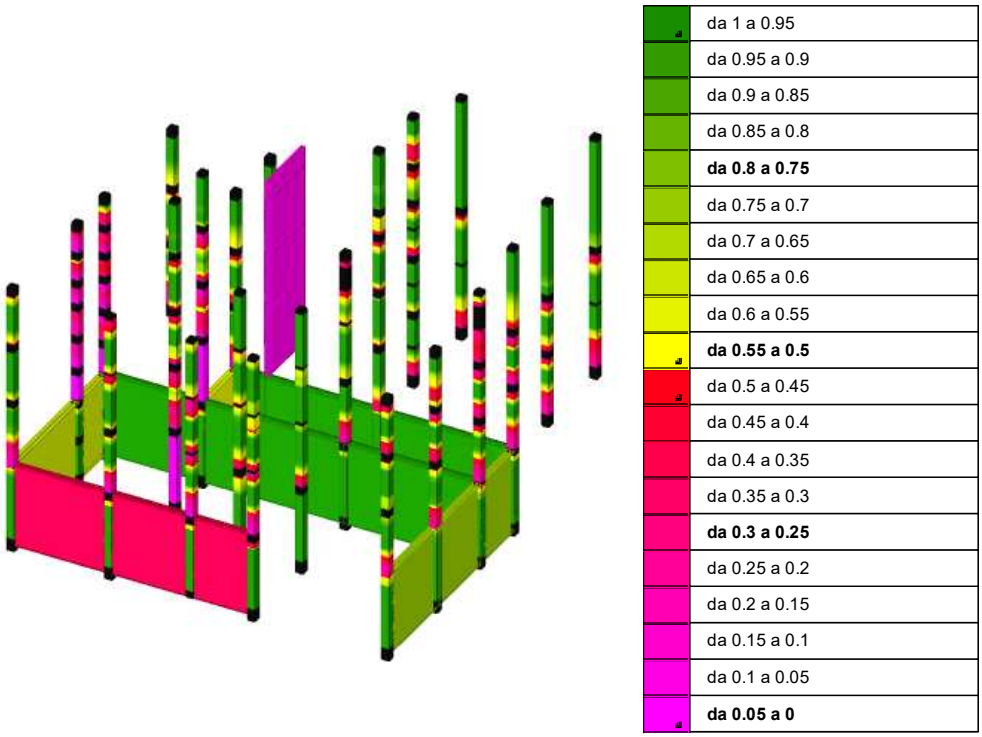

Figure 37 - Minimum security

The following table shows the minimum values of seismic vulnerability indicators referring to the verification of bending and shear of existing columns and walls.

Desc.	Stato limite	Molt.	Comb.	PGA	iPGA (ζE)	TR	(TR/TRrif)^.41	fa	Verifica
Pilastrata 3	Taglio	0.231	SLV 3	0.0962	0.2799	45	0.3223	0.278	No
Pilastrata 2	Flessione	0.088	SLV 1	0.0411	0.1195	8	0.1588	0.118	No
Parete Fondazione - Piano 1_3	Taglio nuclei	0.575	SLV 1	0.2152	0.6258	236	0.6359	0.6255	No
Parete Piano 1 - Falda 2	Pressoflessione nuclei	0.372	SLV 14	0.1467	0.4268	106	0.458	0.4263	No

Table 7 - Minimum indicators – Minimum vulnerability index 0.11

The seismic vulnerability index is a parameter used to summarize the numerical results of a seismic vulnerability assessment. The indicator is given by the ratio between the structural resistance capacity and the resistance or displacement requirements specified by the NTC (Italian Technical Standards for Buildings); therefore, the result of the assessment is favourable if the indicator is greater than or equal to 1, and unfavourable otherwise. In the case of retrofitting work and for use classes equal to III, the minimum value of ζE is 0.8. The value of the index can be used to deduce the vulnerability status of the existing building and understand whether it needs seismic improvement or retrofitting.

$$\zeta_E = \frac{\mathrm{PGA}_C(\mathrm{SLV})}{\mathrm{PGA}_D(\mathrm{SLV})}$$

Figure 38 - Seismic vulnerability index

In this case, the structural response highlights the need for seismic retrofitting. Two different retrofitting methods will be illustrated below: the first using shear walls, the second using seismic isolators.

7 Seismic Retrofit: Shear walls

7.1 Shear walls design

The first seismic retrofitting measure that has been studied exploits the concept of shear walls. Shear walls are structural elements used to resist lateral forces parallel to the plane of the wall. The inclusion of this structural element increases the strength of the structure and limits the lateral deformability of the building: this therefore leads to a drastic decrease in available ductility, a reduction in the natural period of the building, and an increase in the spectral input acceleration.

The walls have been designed and arranged in the plan so as to provide torsional inertia, for example by positioning them along the outer perimeter of the structure. In this way, the center of stiffness is not disturbed.

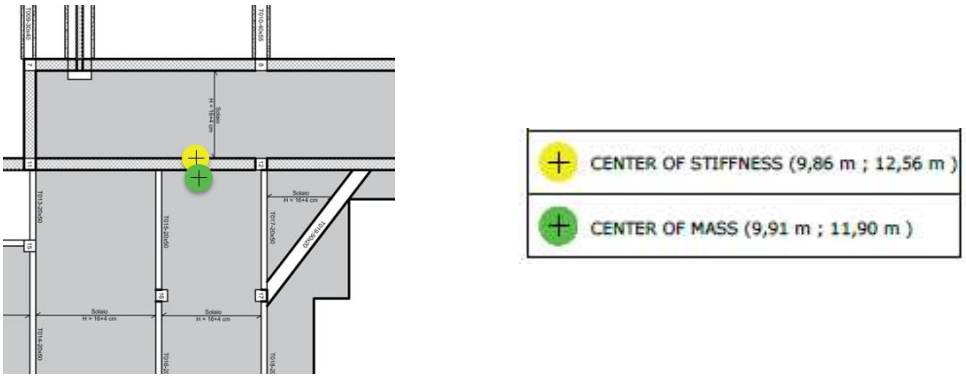

Figure 39 - Mass and stiffness center.

At the same time, the design choice was also guided by other criteria, including:

- maintaining the functionality of the facilities and the current layout of the spaces, avoiding constraints and interference with the use of the facilities;
- compliance with fire safety regulations, ensuring the validity of the escape routes and fire safety strategies currently in place for the structure.
- feasibility of the intervention.

The integration of these criteria has made it possible to identify structural solutions that effectively balance seismic safety, functionality, and feasibility.

In this initial proposal for the retrofitting work, in addition to the insertion of shear walls, the reinforcement of some of the most stressed pillars has also been designed through the insertion of new pillars or through cladding.

In addition, all floors must be reinforced with a new 5 cm layer of electro-welded mesh to create a rigid floor structure. The work extends to all floors of the building.

The insertion and structural reinforcements were carried out in such a way as to bring the center of rigidity and the floor of the building as close as possible.

For a better understanding, the structural adaptation works are listed below.

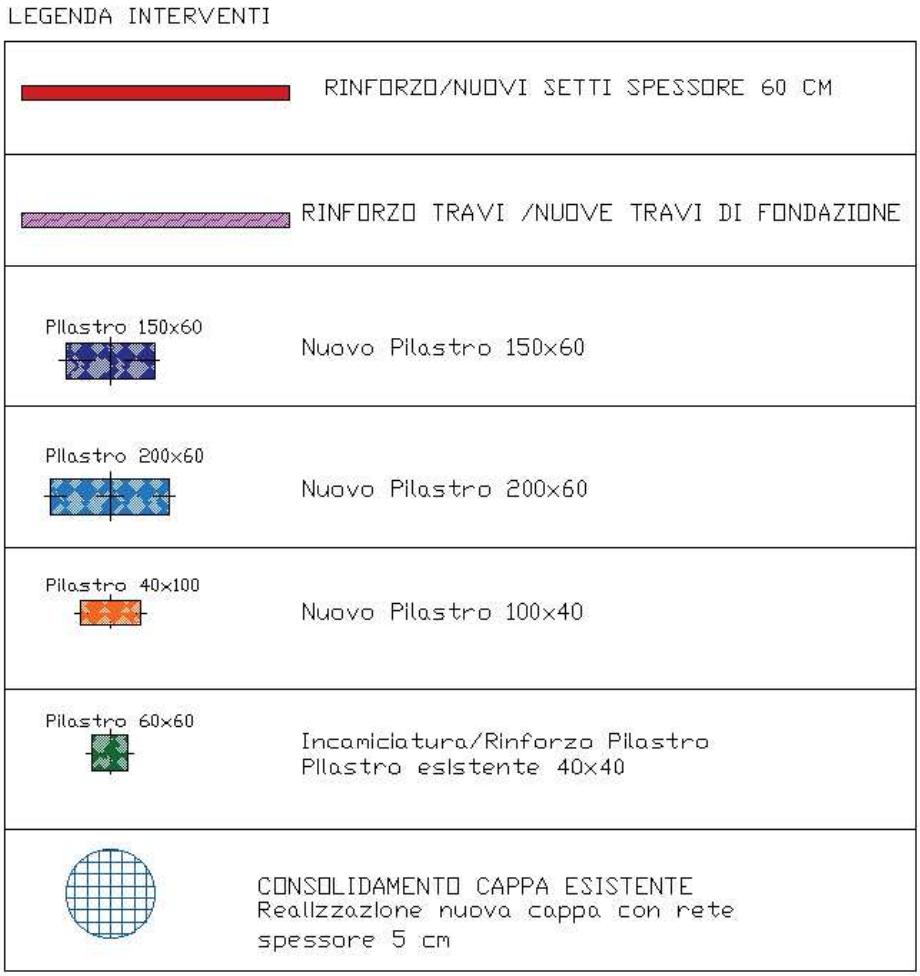

Figure 40 – Seismic retrofitting interventions

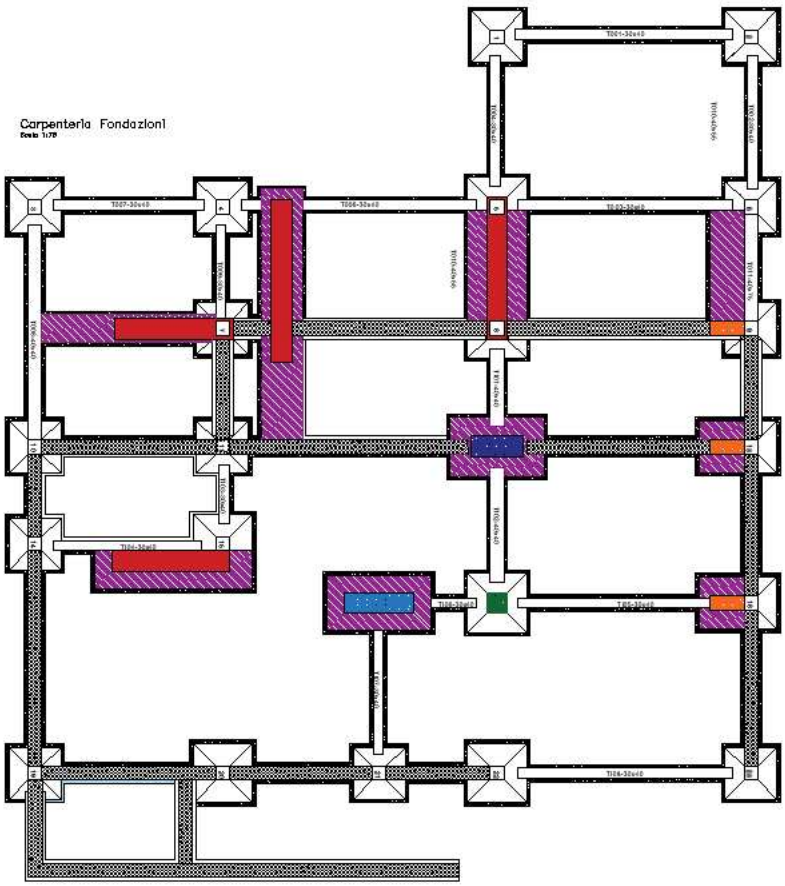

Figure 41 – Carpentry Interventions Foundations

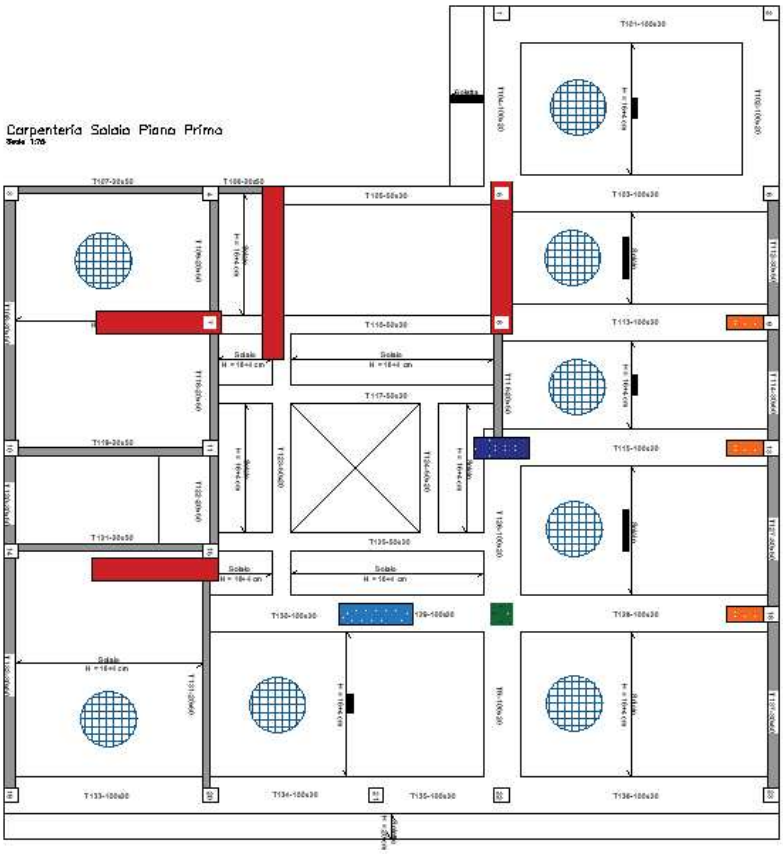

Figure 42 – Typological intervention on the floor

In this case, the behavior factor must be reassessed, this time considering the values relating to the item "Structures with uncoupled walls."

$$q = q_0 \cdot K_R$$

Where:

q_0 is the initial behavior factor.

K_R is the reduction coefficient, which in this case is equal to 0.8.

Tab. 7.3.II – *Valori massimi del valore di base q_0 del fattore di comportamento allo SLV per diverse tecniche costruttive ed in funzione della tipologia strutturale e della classe di duttilità CD*

	q_0	
Tipologia strutturale	CD"A"	CD"B"
Costruzioni di calcestruzzo (§ 7.4.3.2)		
Strutture a telaio, a pareti accoppiate, miste (v. § 7.4.3.1)	4,5 α_u/α_1	3,0 α_u/α_1
Strutture a pareti non accoppiate (v. § 7.4.3.1)	4,0 α_u/α_1	3,0
Strutture deformabili torsionalmente (v. § 7.4.3.1)	3,0	2,0
Strutture a pendolo inverso (v. § 7.4.3.1)	2,0	1,5
Strutture a pendolo inverso intelaiate monopiano (v. § 7.4.3.1)	3,5	2,5
Costruzioni con struttura prefabbricata (§ 7.4.5.1)		
Strutture a pannelli	4,0 α_u/α_1	3,0
Strutture monolitiche a cella	3,0	2,0
Strutture con pilastri incastrati e orizzontamenti incernierati	3,5	2,5
Costruzioni d'acciaio (§ 7.5.2.2) e composte di acciaio-calcestruzzo (§ 7.6.2.2)		
Strutture intelaiate Strutture con controventi eccentrici	5,0 α_u/α_1	4,0
Strutture con controventi concentrici a diagonale tesa attiva Strutture con controventi concentrici a V	4,0 2,5	4,0 2,0
Strutture a mensola o a pendolo inverso	2,0 α_u/α_1	2,0
Strutture intelaiate con controventi concentrici	4,0 α_u/α_1	4,0
Strutture intelaiate con tamponature in murature	2,0	2,0
Costruzioni di legno (§ 7.7.3)		
Pannelli di parete a telaio leggero chiodati con diaframmi incollati, collegati mediante chiodi, viti e bulloni Strutture reticolari iperstatiche con giunti chiodati	3,0	2,0
Portali iperstatici con mezzi di unione a gambo cilindrico	4,0	2,5
Pannelli di parete a telaio leggero chiodati con diaframmi chiodati, collegati mediante chiodi, viti e bulloni.	5,0	3,0
Pannelli di tavole incollate a strati incrociati, collegati mediante chiodi, viti, bulloni Strutture reticolari con collegamenti a mezzo di chiodi, viti, bulloni o spinotti		2,5

Table 8 - Table NTC2018 – Behavior factor.

This results in a structure factor in CDB:

$$q=0.8 \cdot (3) =2.4$$

If reinforced concrete walls are present in the construction, in order to prevent their brittle collapse, the q_0 values must be reduced by the k_w factor, with:

$$k_w = \begin{cases} 1{,}00 & \text{per strutture a telaio e miste equivalenti a telai} \\ 0{,}5 \le (1+\alpha_0)/3 \le 1 & \text{per strutture a pareti, miste equivalenti a pareti, torsionalmente deformabili} \end{cases}$$

Where α_0 is the value mainly assumed by the ratio between the total height (from the foundations or from the rigid box structure referred to in § 7.2.1, up to the top) and the length of the walls; if the α_0 values of the walls do not differ significantly from each other, the value of α_0 for the set of walls can be calculated by taking the sum of the heights of the individual walls as the height and the sum of the lengths as the length

To be defined as a wall, an element must have a rectangular cross-section and the ratio between the longer side and the shorter side must be greater than four. The coefficient α_0 is calculated in both directions.

The project involves 4 walls, each with a plan development of approximately 4 meters and a height of approximately 10 meters. This leads to the following coefficients:

$$\alpha_0 = \frac{\sum wall\ height}{\sum wall\ plan\ development} = \frac{10x4}{4x4} = 2.5$$

$$k_w = \frac{(1+\alpha_0)}{3} = \frac{1+2.5}{3} = 1.16 > 1 \rightarrow k_w = 1$$

From which is obtained q_{DB}:

q=2.4*1=2.4

For structures with non-dissipative structural behavior, a behavior factor q_{ND} is adopted, reduced with respect to the minimum value relating to the "CDB" according to the expression:

$$1 \leq q_{ND} = \frac{2}{3} q_{CD"B"} \leq 1{,}5$$

$$1 \leq \frac{2}{3} 2.4 \leq 1.5$$

$$1 \leq 1.6 \leq 1.5$$

For checks on the existing structure, the behavior factors to be used are as follows:

- X direction: q=1.5q = 1.5q=1.5
- Y direction: q=1.5q = 1.5q=1.5

7.2 Modal response

For the modal analysis, we have considered the first 15 vibration modes of the structure: numerical results of the analysis are shown in table.

Total Participating Mass:

Translation X: 0.999999 Translation Y: 1 Translation Z: 0

Rotation X: 0.999334 Rotation Y: 0.999437 Rotation Z: 1

Modo	Periodo	Massa X	Massa Y	Massa Z	Massa rot. X	Massa rot. Y	Massa rot. Z	Massa sX	Massa sY
1	0.393437631	0.004294187	0.008993225	0	0.018582961	0.013202883	0.00040199	0.004294187	0.008993225
2	0.288394867	0.607132369	0.000424685	0	0.000664762	0.903800062	0.000787212	0.607132369	0.000424685
3	0.224196581	0.00006436	0.5671864	0	0.877967248	0.000030476	0.575761483	0.00006436	0.5671864
4	0.110568256	0.011961678	0.011408405	0	0.006073867	0.006210886	0.003554193	0.011961678	0.011408405
5	0.097590971	0.008497357	0.000047817	0	0.000023314	0.001262422	0.000357809	0.008497357	0.000047817
6	0.079230889	0.000267867	0.001827393	0	0.000426875	0.000004275	0.002115694	0.000267867	0.001827393
7	0.072819465	0.042689928	0.005873355	0	0.002128727	0.009765601	0.001710815	0.042689928	0.005873355
8	0.060327338	0.078710092	0.000281384	0	0.00006828	0.019413999	0.000016134	0.078710092	0.000281384
9	0.057256074	0.001340475	0.110136806	0	0.037300113	0.000422735	0.118671763	0.001340475	0.110136806
10	0.054294991	0.025213765	0.02861064	0	0.00940408	0.007449629	0.028166374	0.025213765	0.02861064
11	0.046228556	0.000746525	0.010515397	0	0.00352061	0.000088552	0.009084725	0.000746525	0.010515397
12	0.034021965	0.026446808	0.003483683	0	0.001155438	0.008619185	0.005687425	0.026446808	0.003483683
13	0.031180611	0.011566323	0.02577424	0	0.007747165	0.004051284	0.020199235	0.011566323	0.02577424
14	0.020046672	0.000016543	0.211623747	0	0.03324989	0.000021527	0.212979815	0.000016543	0.211623747
15	0.017265305	0.153817145	0.000192522	0	0.000066124	0.020586983	0.003879694	0.153817145	0.000192522

Table 9 - Modal response – Periods and participating mass

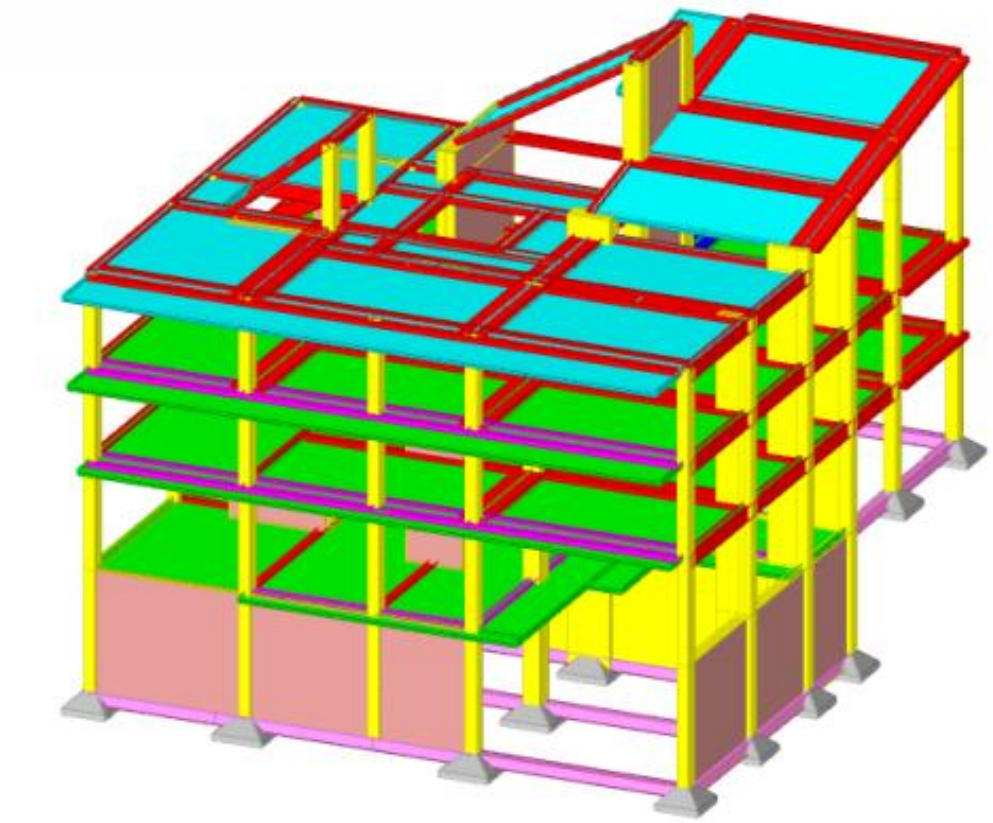

Figure 43 - Model of the intervention with shear walls

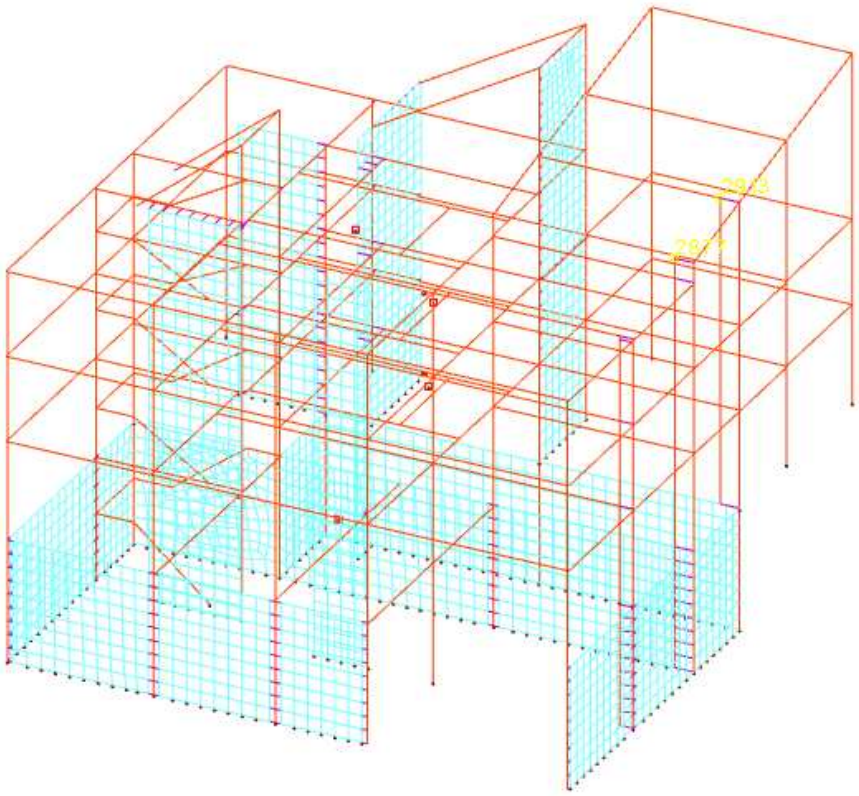

Figure 44 – FEM Model of the intervention with shear walls

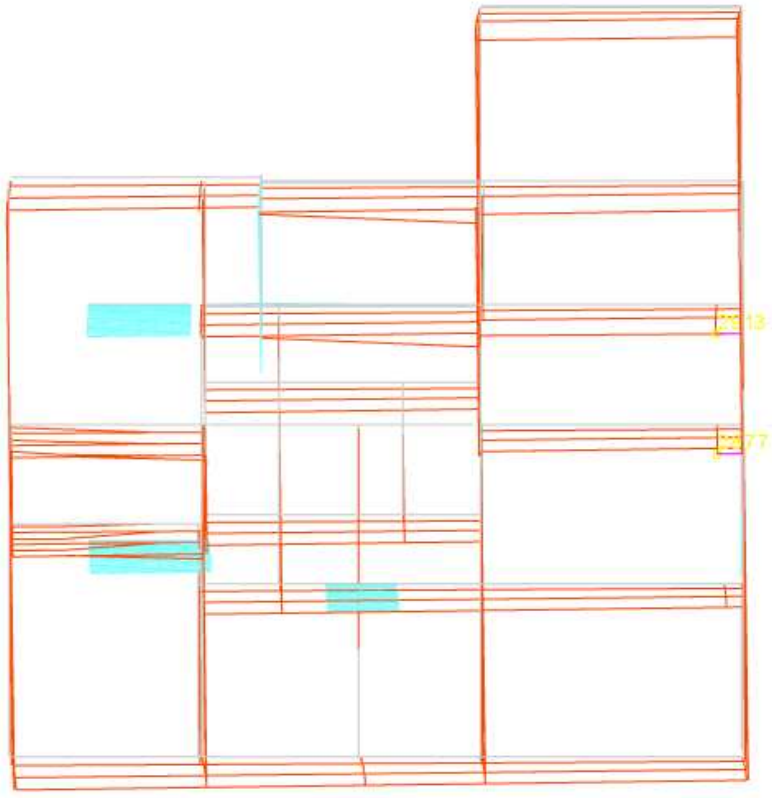

Figure 45 - Displacements in the third vibration mode (T=0.22s)

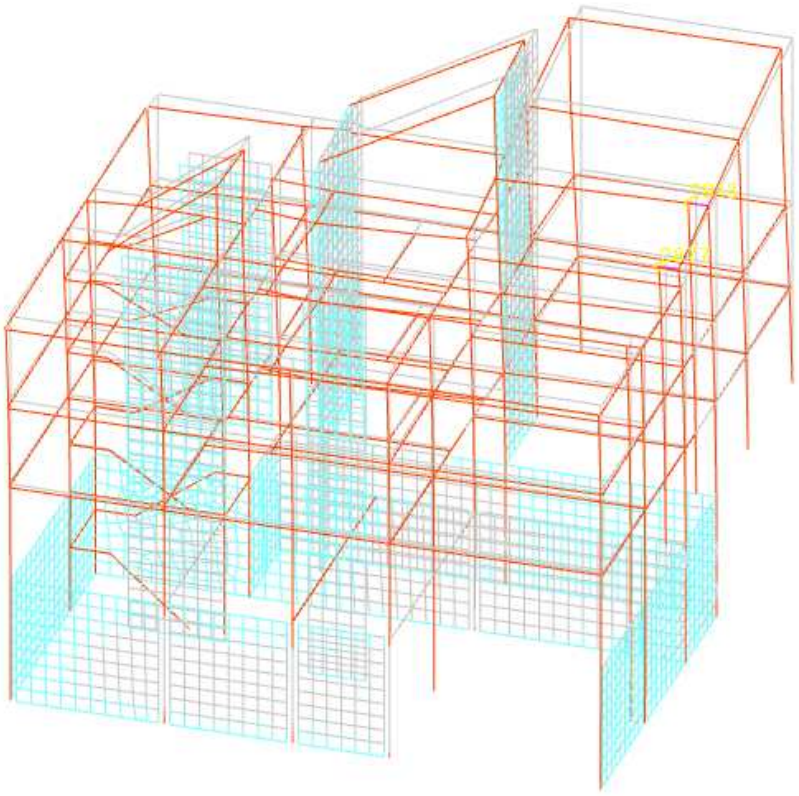

Figure 46 -Displacements in the third vibration mode (T=0.22s)

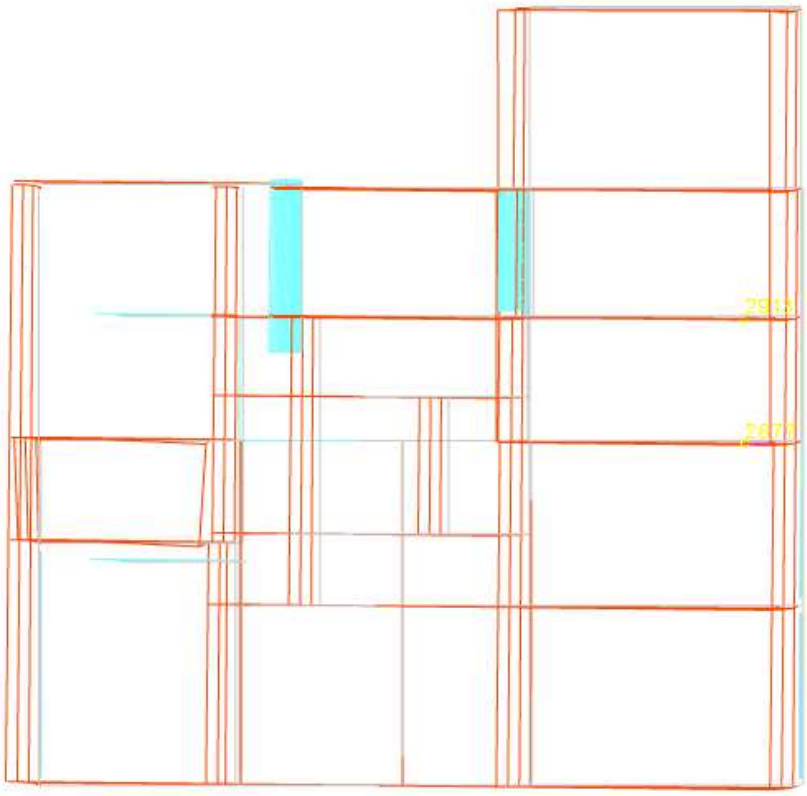

Figure 47 - Displacements in the second vibration mode (T=0.28s)

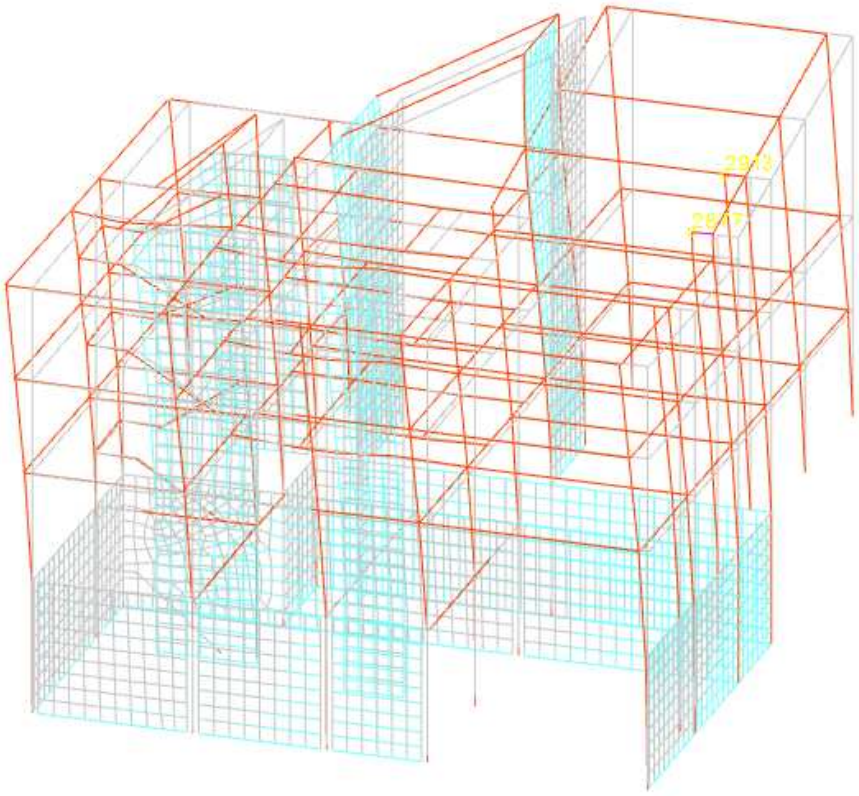

Figure 48 - Displacements in the second vibration mode (T=0.28s)

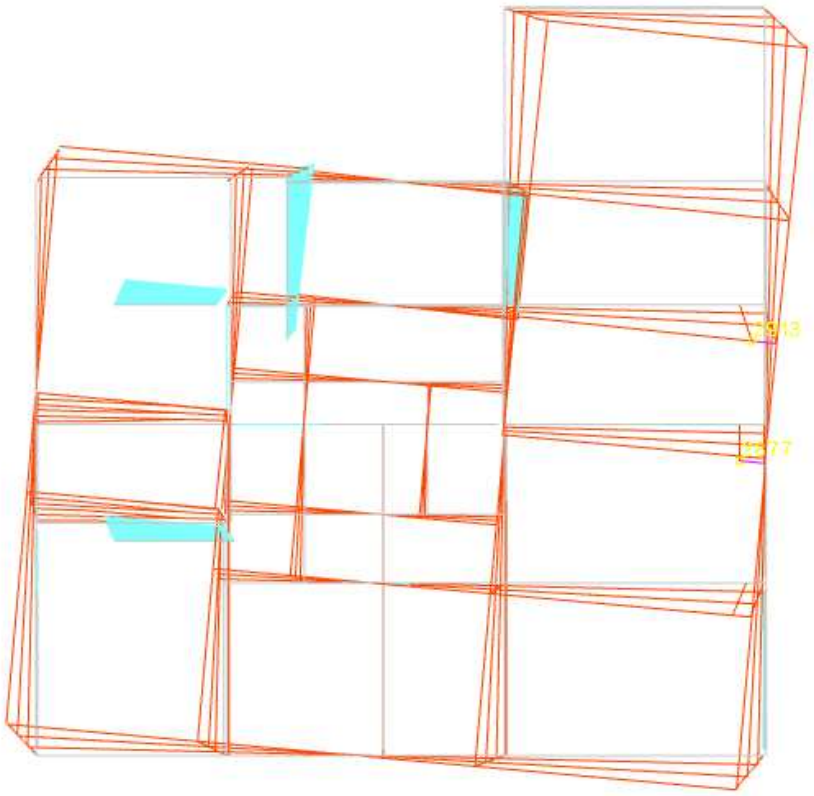

Figure 49 - Displacements in the first vibration mode (T=0.39s)

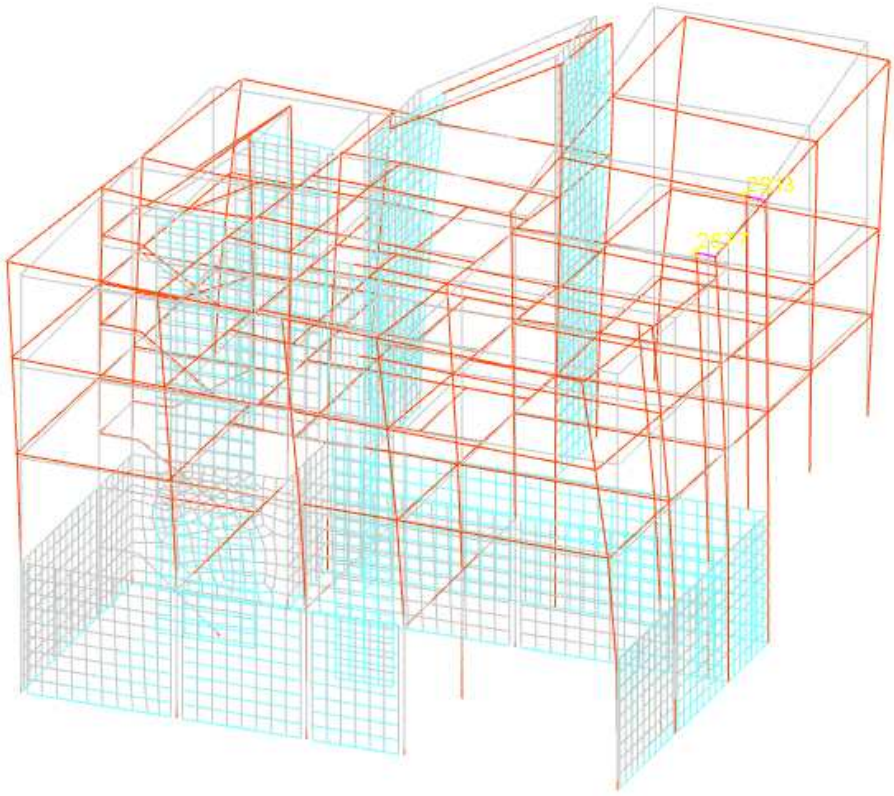

Figure 50 - Displacements in the first vibration mode (T=0.39s)

The main modes of vibration of the structure are predominantly translational, while the third mode is rotational, albeit with reduced eccentricity along the x and y directions.

7.3 Results and verifications

From the point of view of seismic safety, the results obtained show a significant increase in terms of risk index. In particular, the minimum values calculated are higher than 0.8, a threshold commonly assumed in literature and national guidelines as sufficient to guarantee an acceptable level of safety in seismic retrofitting interventions for buildings in use class III.

Desc.	Stato limite	Molt.	Comb.	PGA	iPGA (ζE)	TR	(TR/TRrif)^.41	fa	Verifica
Pilastrata 9	Taglio	0.801	SLV 14	0.2774	0.807	419	0.8046	0.8064	No
	Flessione	0.802	SLV 14	0.278	0.8086	421	0.8062	0.8081	No
Parete Piano 1 - Copertura	Taglio nuclei	0.944	SLV 14	0.3257	0.9472	620	0.9449	0.9469	No
	Pressoflessione nuclei	0.918	SLV 14	0.317	0.9221	579	0.9187	0.9217	No

Table 10 - Minimum indicators of seismic vulnerability

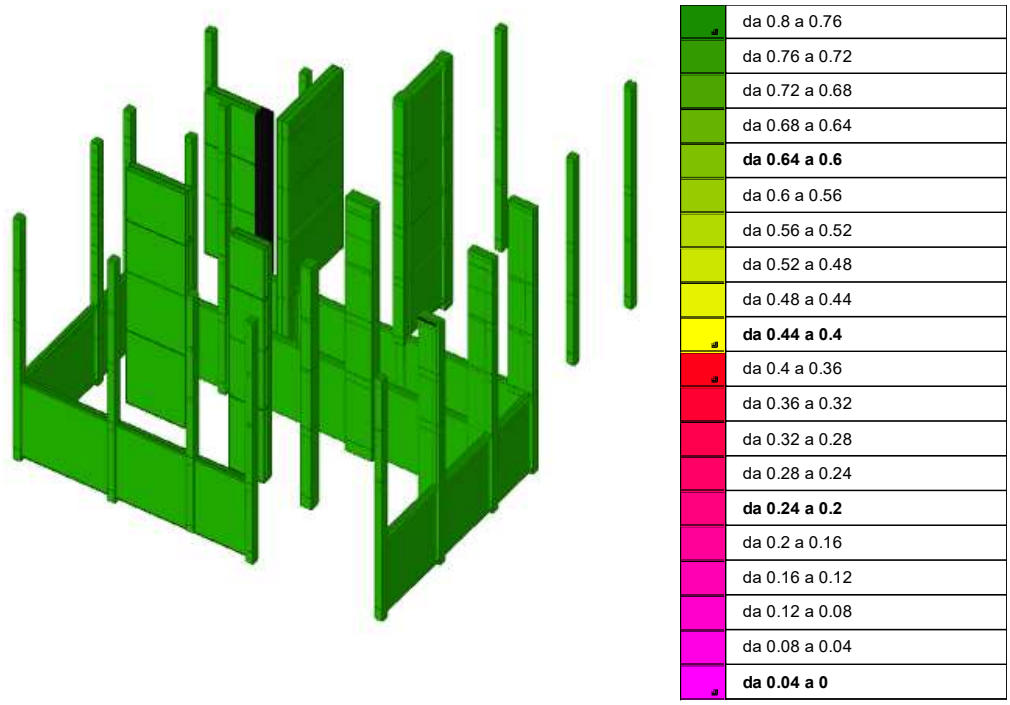

Figure 51 - I.R. Flessione PGA

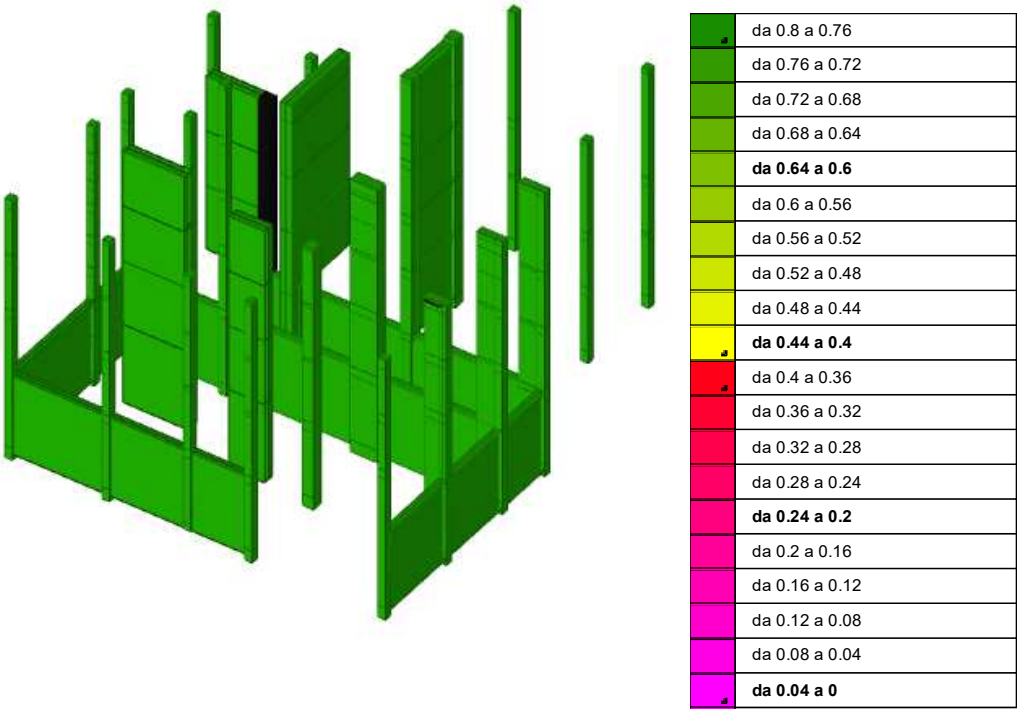

Figure 52 - I.R. Taglio PGA

8 Seismic Retrofit: Base Isolation system

Seismic isolation is a seismic protection strategy based on the principle that a structure is separated from the ground through the insertion of devices designed to decouple their movement. Seismic isolators allow the dissipation of a constant portion of the mechanical energy transmitted to the building, thereby limiting the maximum horizontal force applied to the isolated structure. As a result, when the transmitted forces are reduced, the fundamental period of the structure increases and is consequently shifted into the range of lower response accelerations.

The isolation system is composed of the following elements:

- **Isolation and energy dissipation devices:** these devices support vertical loads and allow horizontal displacements, thanks to their vertical stiffness and low horizontal stiffness.
- **Substructure:** portion of the structure located below the isolation interface. It is characterized by negligible horizontal deformability and it is in direct contact with the forces transmitted from the ground.
- **Superstructure:** upper portion of the structure, i.e., the isolated part.
- **Isolation interface or layer:** surface separating the superstructure from the substructure upon which the isolation system acts.

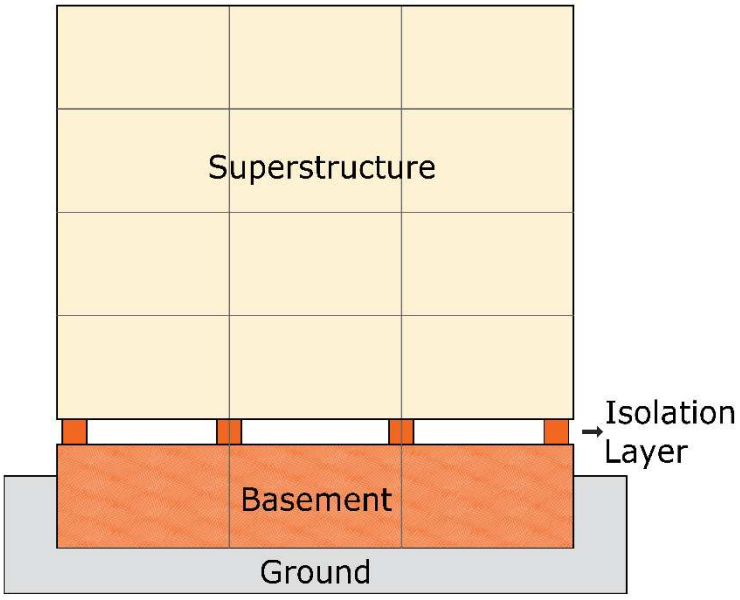

Figure 53 - Superstructure, Substructure and Isolation layer

8.1 Design of the Isolation System

The planimetric configuration and the presence of two-level foundations made the identification of the isolation interface particularly critical. Initially, the possibility of placing the devices on two different levels [6], corresponding to the foundations, was considered. To avoid undesired torsions and non-uniform responses—mainly due to soil behavior—all isolators were ultimately positioned at the same level, aligned with the foundation beams at elevation +4.00 m.

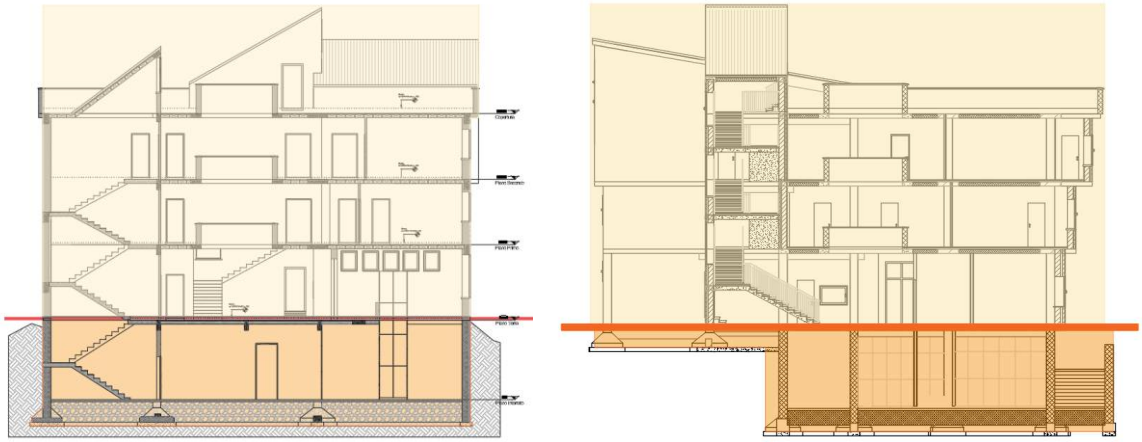

Figure 54 - Isolation layer

This arrangement allowed for the reduction of the effects of elevation differences between foundations and enabled the placement of devices in locations accessible for inspection and potential maintenance. These aspects are fundamental for proper design, as periodic monitoring ensures the correct functioning of the seismic protection system. Moreover, since the structure conforms to the irregular morphology of the terrain, installing isolators at the basement level would have been particularly costly and time-consuming.

The sizing of the devices was then carried out in accordance with the provisions of NTC 2018, paragraph 7.

The seismically active mass was determined by summing the self-weight, permanent loads, and a portion of variable loads, in accordance with the seismic load combinations prescribed by the code. Subsequently, the optimal period of the isolated structure was determined based on the initial response spectrum: the selected period is longer than that of the fixed-base structure in order to fall within a range of the spectrum with lower acceleration.

The equivalent stiffness of the isolation system, K_{esi} , was calculated using the following equation:

$$T_{is} = 2\pi \cdot \sqrt{\frac{M}{K_{esi}}}$$

Where:

T_{is} is the equivalent period of the isolated structure,

M is the seismically active mass,

K_{esi} is the equivalent stiffness of the isolation system.

This stiffness was then distributed among the number of elastomeric devices, yielding the stiffness required for a single isolator.

Furthermore, as indicated in paragraph §7.2.2 of NTC 2018, the vertical component was not considered in the calculation, since the ratio between the vertical stiffness of the isolation system and the equivalent horizontal stiffness is less than 800.

Isolation devices

The selection of isolators was guided by the need to satisfy the building's structural and dynamic performance criteria, with attention to several key aspects:

Horizontal stiffness, to provide the required flexibility under seismic loading;
Vertical load capacity, consistent with the specific weight supported at each location;
Equivalent damping, to dissipate energy and limit vibration transmission;
Displacement capacity, sufficient to accommodate the expected seismic movements.

The parameters adopted are drawn from the manufacturer's catalogue (FIP) and include nominal values together with the corresponding tolerances. These data serve as the reference for the numerical modeling and performance evaluations carried out in the subsequent phases.

Employing standardized, certified isolators not only guarantees a dependable seismic response, but also simplifies future inspection and maintenance activities.

The isolation devices adopted for this structure are reinforced rubber bearing elastomeric isolators. These elements are constructed from alternating layers of steel laminates and hot-vulcanized rubber, and can be produced in either circular or rectangular configurations to suit specific design requirements. The combination of materials allows the isolators to dissipate seismic energy primarily through their low horizontal stiffness. At the same time, the interaction between the elastomeric layers

and the steel reinforcement ensures adequate vertical stiffness and the ability to safely sustain the superstructure loads.

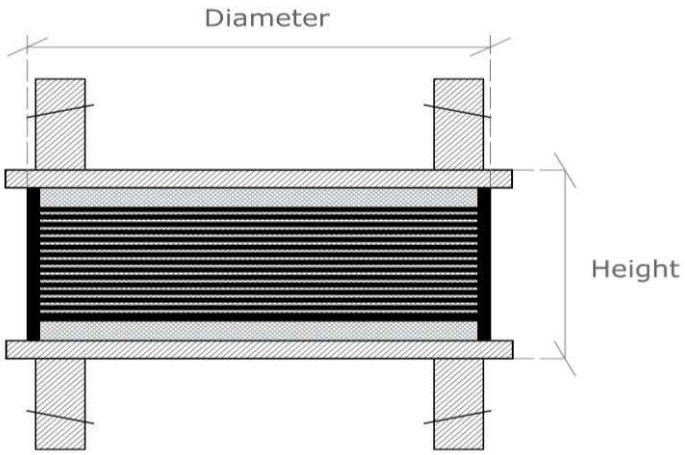

Figure 55 - Elastomeric isolato – SI – N FIP

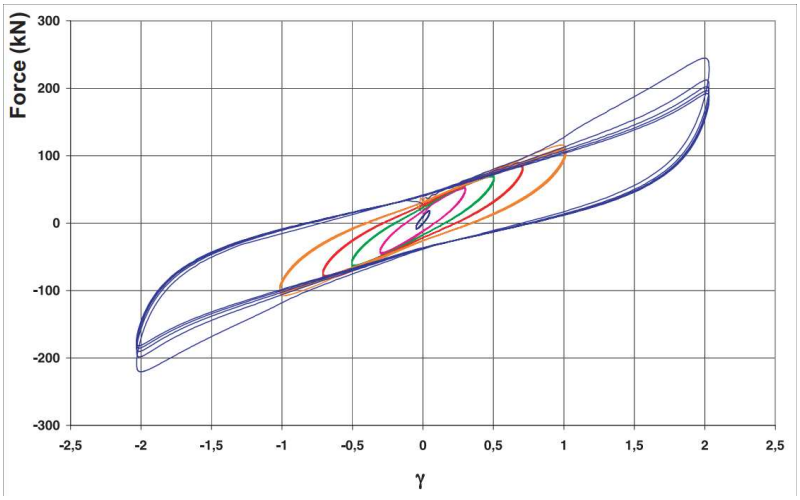

Figure 56 - Typical hysteretic curve of an elastomeric isolator achieved during dynamic tests with increasing shear strain amplitude.

Table 3 - Elastomeric Device SI N

Parameter	Symbol	Value	Unit	Description
Vertical Load Capacity	V	2,800	kN	Maximum vertical load supported
Design Vertical Load	F_{zd}	990	kN	Design vertical load
Effective Horizontal Stiffness	K_e	1.03	kN/mm	Horizontal stiffness under design displacement
Vertical Stiffness	K_v	796	kN/mm	Stiffness in vertical direction
Design Displacement	D_d	350	mm	Maximum horizontal displacement
Total Rubber Thickness	te	75	mm	Sum of elastomeric layers
Rubber Diameter	Z	400	mm	Diameter of the rubber section
Internal Height of Isolator	h	143	mm	Core height excluding cover plates
Total Height Including Plates	H	193	mm	Overall height of the isolator
Unit Weight	W	118	kg	Mass of a single isolator unit

Table 11 - Elastomeric isolator parameters extracted from the FIP-MEC catalogue

For all other columns, sliders were modeled as the isolation devices. Their design was based on the characteristics of the elastomeric isolators, in terms of both the maximum load acting on the device and the allowable maximum displacement.

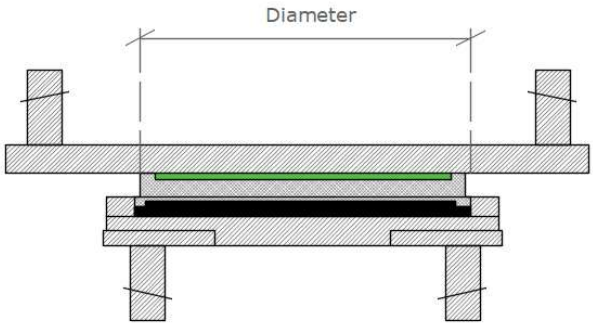

Figure 57 - sliding isolation device

Descrizione	Fonte	Diametro	Altezza	Peso	Ke	Kv	Spostamento max	Carico di progetto SLU	Carico di progetto SLC
D35 SI-N FIP 350/75	Aron	35	19,3	118	1000	796000	20	280000	99000
D35 SLITTA	Aron	35	19,3	100	0,01	1033000	100	351000	159000

Table 12 - Input parameters for the isolation devices

The elastomeric isolators were predominantly positioned along the building's external perimeter, whereas the sliding bearings were located within the interior.

The isolators are arranged as follows:

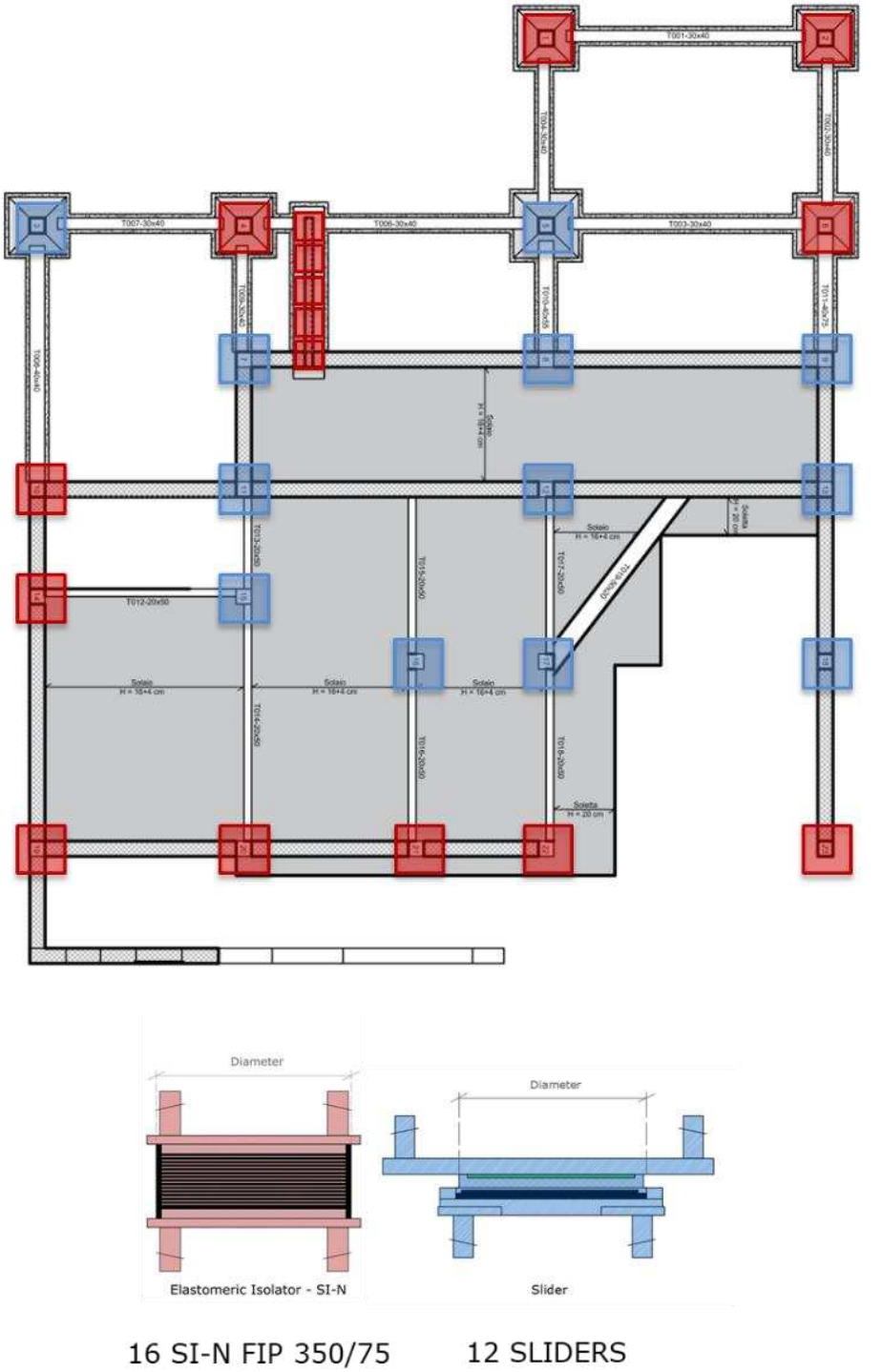

Figure 58 - Layout of the seismic isolation devices. Elastomeric SI-NFIP 350/75 isolators are shown in red, while sliding isolation devices are indicated in blue

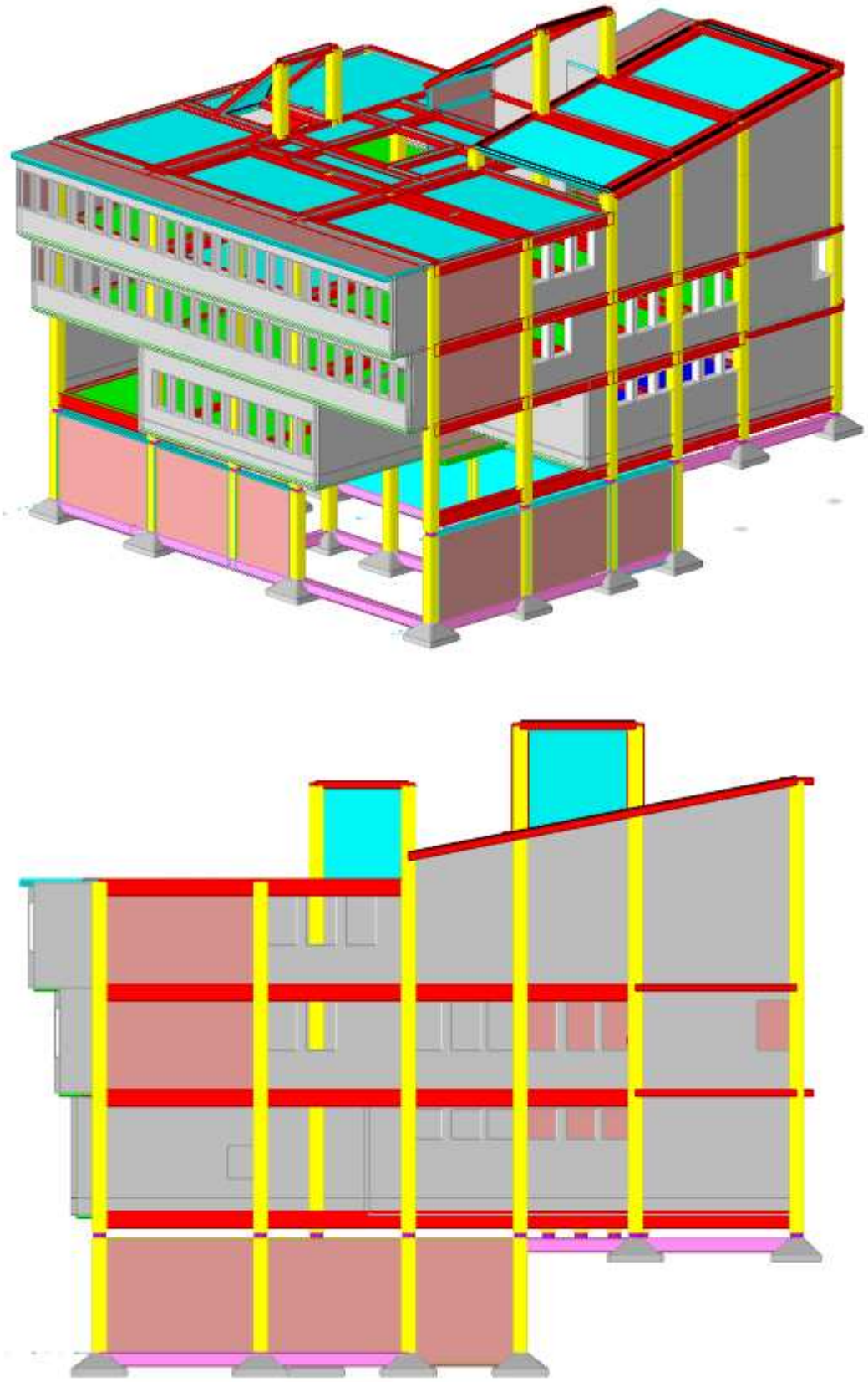

Figure 59 - Axonometric view and side elevation of the model in SISMICAD

8.2 Modal response

For the modal analysis, we have considered the first 15 vibration modes of the structure: numerical results of the analysis are shown in table.

Total Participating Mass:

Translation X: 0.999999 Translation Y: 1 Translation Z: 0

Rotation X: 0.999334 Rotation Y: 0.999437 Rotation Z: 1

Modo	Periodo	Massa X	Massa Y	Massa Z	Massa rot. X	Massa rot. Y	Massa rot. Z	Massa sX	Massa sY
1	2.20923264	0.984803358	0.009230935	0	0.00890827	0.942004639	0.021152691	0.984803358	0.009230935
2	2.150721468	0.013557946	0.744245214	0	0.714290538	0.011137383	0.581084688	0.013557946	0.744245214
3	1.723461695	0.000106126	0.245939354	0	0.223704407	0.000021914	0.39713709	0.000106126	0.245939354
4	0.371944306	0.00043709	0.000032609	0	0.005247542	0.014141857	0.000000078	0.00043709	0.000032609
5	0.30347999	0.000900333	0.000049692	0	0.005628192	0.030773407	0.000007002	0.000900333	0.000049692
6	0.221071175	0.000040273	0.00042883	0	0.037857419	0.00074621	0.000526577	0.000040273	0.00042883
7	0.178693522	0.000050801	0.000047585	0	0.002882825	0.000419608	0.000072635	0.000050801	0.000047585
8	0.158175462	0.00000302	0.000014871	0	0.000301707	0.000005405	0.000012706	0.00000302	0.000014871
9	0.132221336	0.000013132	0.000005314	0	0.000320554	0.000003295	0.000000333	0.000013132	0.000005314
10	0.129394337	0.00007244	0.000001307	0	0.000124077	0.000006712	0.000000001	0.00007244	0.000001307
11	0.096275537	0.000002075	0.000000046	0	0.000028996	0.000070937	0.000000183	0.000002075	0.000000046
12	0.093272441	0.000002251	0.000001786	0	0.000004277	0.000074901	0.000003307	0.000002251	0.000001786
13	0.052978779	0.000000021	0.000002237	0	0.000028423	0.00000246	0.000002452	0.000000021	0.000002237
14	0.031109378	0.000010441	0.000000023	0	0.000000915	0.00002758	0.000000005	0.000010441	0.000000023
15	0.000560297	0	0.000000001	0	0.000005408	0.000000256	0.000000005	0	0.000000001

Table 13 - Modal response – Periods and participating mass

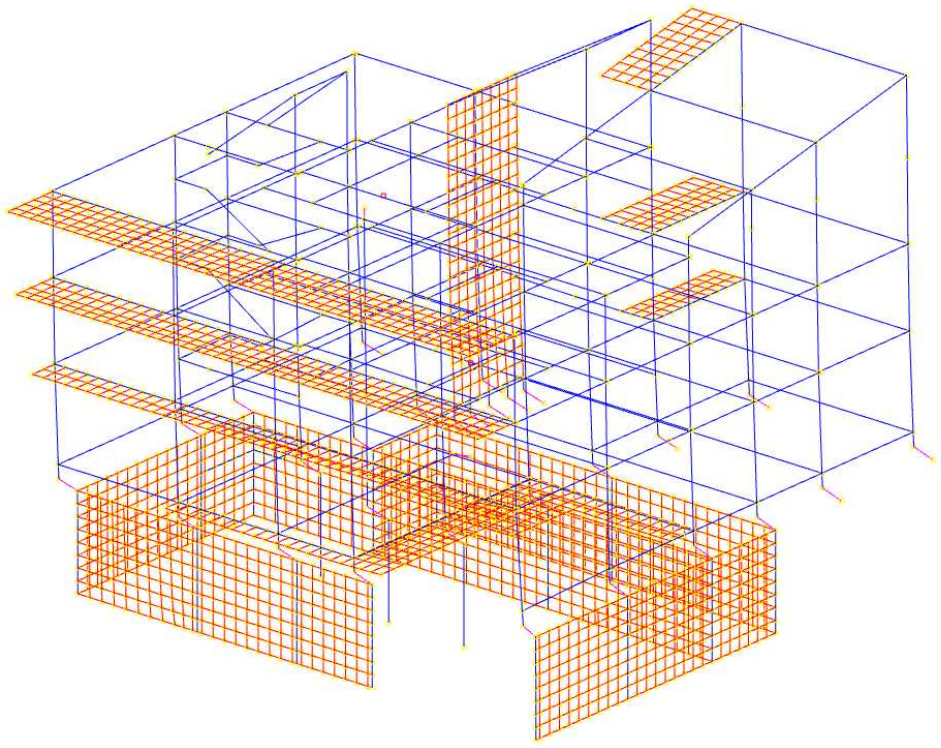

Figure 60 - First mode of vibration – Axonometric view.

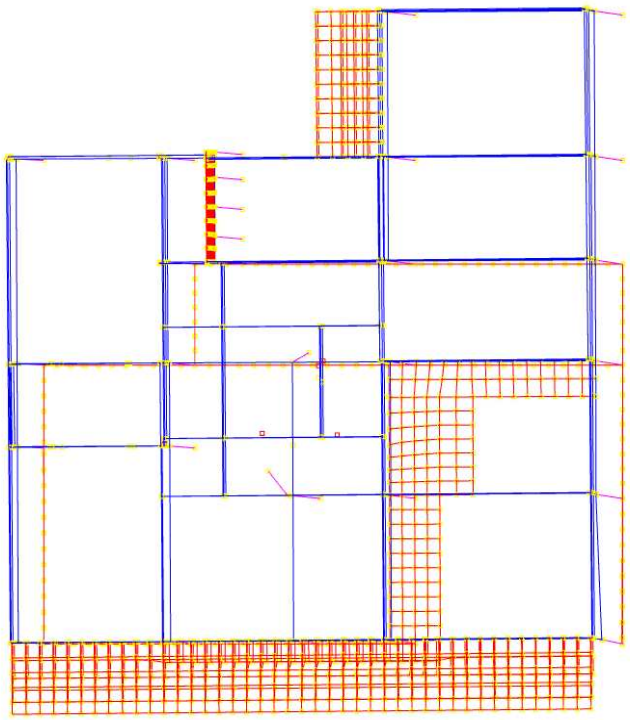

Figure 61 - First mode of vibration – Top view.

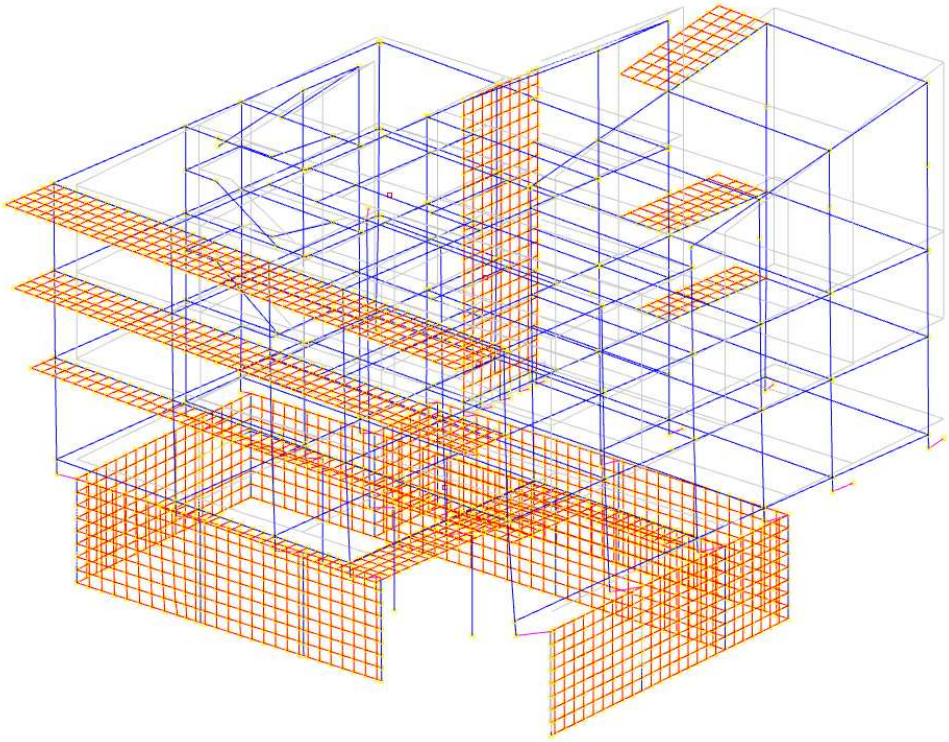

Figure 62 - Second mode of vibration – Axonometric view.

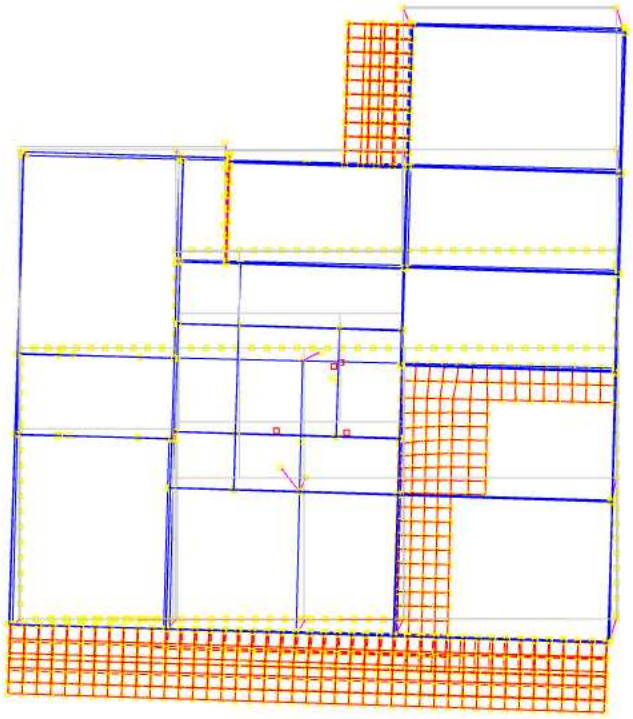

Figure 63 - Second mode of vibration – Top view.

8.3 Results and verifications

MODAL RESPONSE

In this case as well, a regularization of the modal behavior was observed, with a predominance of translational motions. The values of the risk index, as in the previous seismic retrofitting scenario, indicate a significant improvement in the structural response, well above the threshold value of 0.8.

Desc.	Stato limite	Molt.	Comb.	PGA	iPGA (ζE)	TR	(TR/TRrif)^.41	fa	Verifica
Trave a "Copertura" 7-18	Taglio	1.007	SLV 10	0.3117	1.2569	722	1.2599	1.0056	Si
Trave a quota "Rampa_scala2"-"Piano 2" 10-12	Flessione	1.003	SLV 3	0.3107	1.2528	716	1.2556	1.0023	Si
Pilastrata 7	Taglio	1.84	SLV 3	0.4802	1.9361	2403	2.0627	1.549	Si
Parete Piano 1 - Falda 2	Taglio nuclei	1.501	SLV 8	0.4172	1.682	1603	1.7472	1.3457	Si
	Pressoflessione nuclei	1.224	SLV 3	0.3623	1.4607	1068	1.4792	1.1686	Si

Table 14 - Minimum parameters considering only the reinforced concrete material

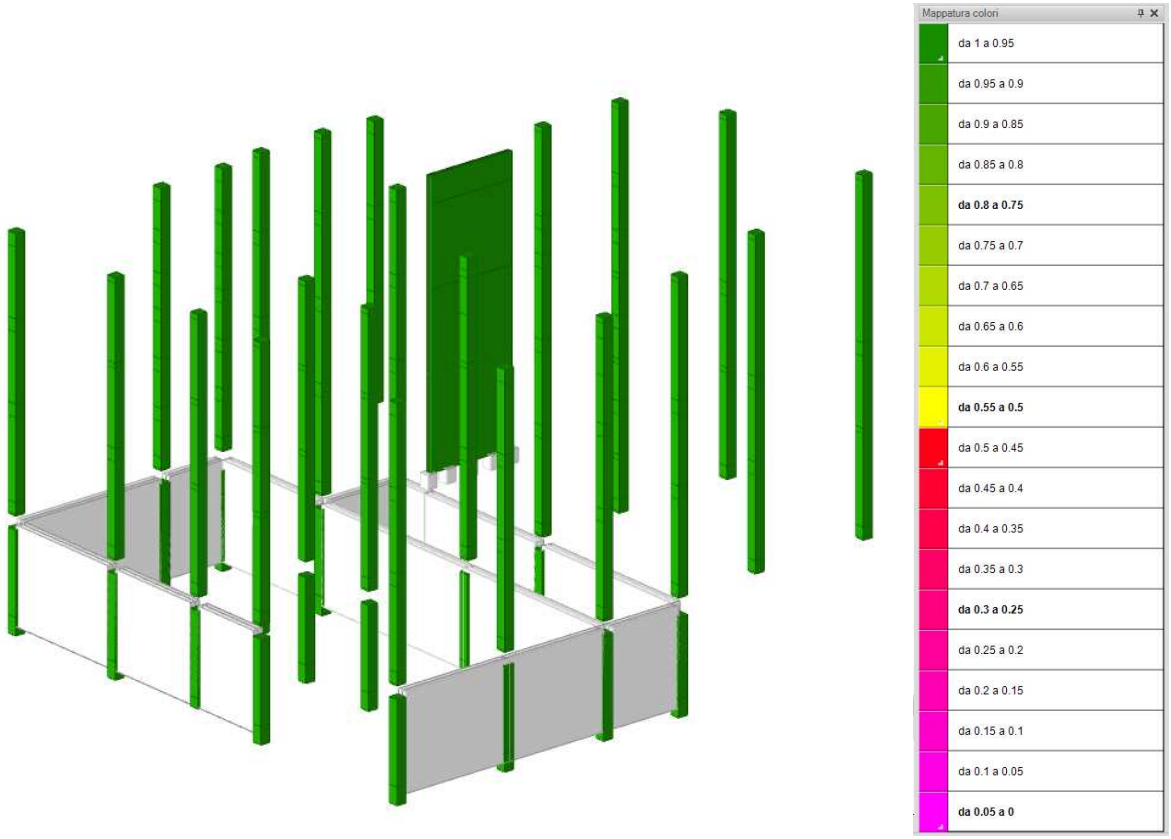

Figure 64 - I.R. Flessione PGA

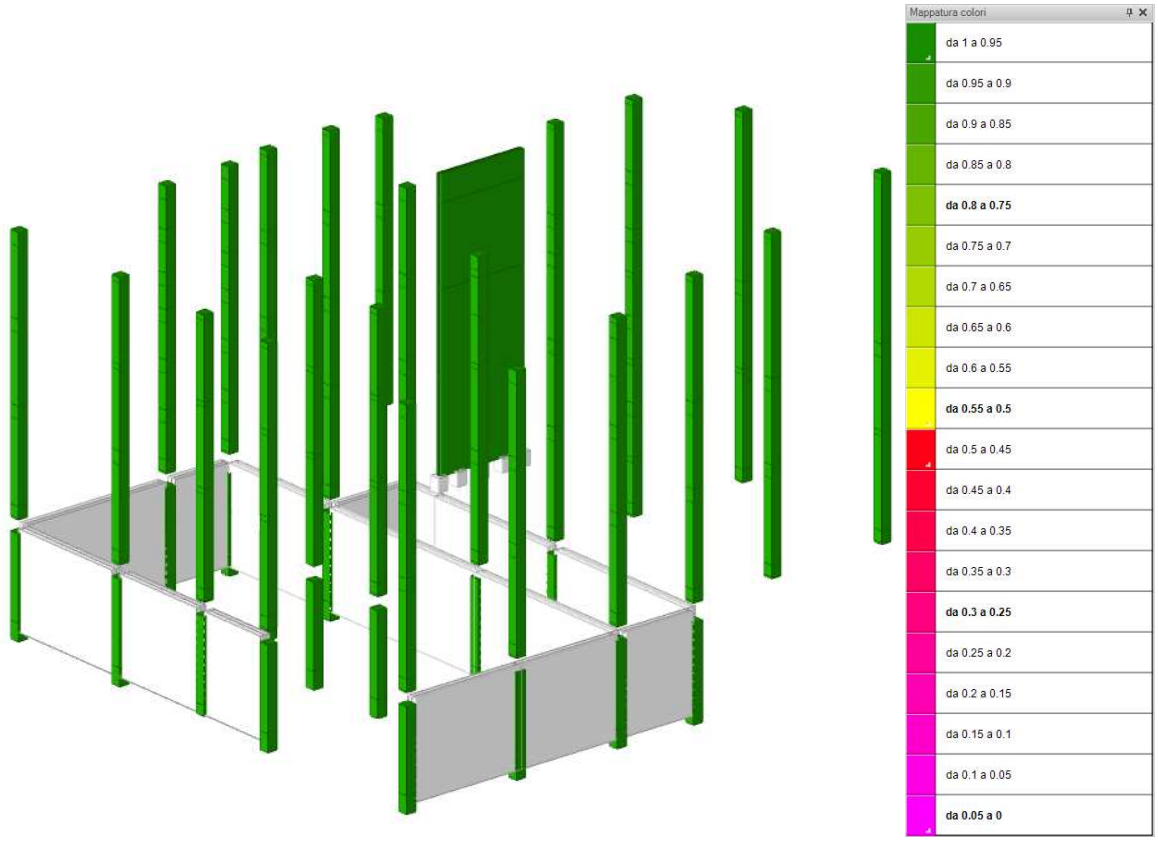

Figure 65 - I.R. Taglio PGA

VERIFICATION OF INTERSTORY DRIFTS AT THE SLD

The structural verification of interstory drifts aims to assess whether the stiffness of a building complies with the limits prescribed by the code. Below is the table from NTC 2018, which specifies, for each use class, the structural elements and the limit states to be considered in performing the stiffness and strength checks.

STATI LIMITE		CU I	CU II			CU III e IV		
		ST	ST	NS	IM	ST	NS	IM(*)
SLE	SLO					RIG		FUN
	SLD	RIG	RIG			RES		
SLU	SLV	RES	RES	STA	STA	RES	STA	STA
	SLC		DUT(**)			DUT(**)		

(*) Per le sole CU III e IV, nella categoria Impianti ricadono anche gli arredi fissi.
(**) Nei casi esplicitamente indicati dalle presenti norme.

Table 15 - Table 7.3.III della NTC2018

In the case under consideration, the structure falls within Use Class III (*buildings intended for occupancy by large crowds*). For the primary structural elements (ST), it is therefore required to perform the stiffness verification at the Damage Limit State (DLS) and the strength verification at the Ultimate Limit State (ULS).

According to the code provisions, the stiffness requirement is deemed satisfied when the resulting deformation of the structural elements does not cause damage to the non-structural components such that the entire building becomes temporarily unfit for use. For civil and industrial buildings, this condition is verified when the interstory drifts obtained from seismic analysis remain below two-thirds of the limits indicated below.

a) per tamponature collegate rigidamente alla struttura, che interferiscono con la deformabilità della stessa:

$qd_r \leq 0{,}0050 \cdot h$ per tamponature fragili [7.3.11a]

$qd_r \leq 0{,}0075 \cdot h$ per tamponature duttili [7.3.11b]

b) per tamponature progettate in modo da non subire danni a seguito di spostamenti d'interpiano d_{rp}, per effetto della loro deformabilità intrinseca oppure dei collegamenti alla struttura:

$qd_r \leq d_{rp} \leq 0{,}0100 \cdot h$ [7.3.12]

c) per costruzioni con struttura portante di muratura ordinaria

$qd_r \leq 0{,}0020 \cdot h$ [7.3.13]

d) per costruzioni con struttura portante di muratura armata

$qd_r \leq 0{,}0030 \cdot h$ [7.3.14]

e) per costruzioni con struttura portante di muratura confinata

$qd_r < 0{,}0025 \cdot h$ [7.3.15]

Figure 65 - Values extracted from NTC 2018

Where:

dr is the interstory drift, i.e., the difference between the displacements of the upper slab and the lower slab, evaluated either through linear analysis or nonlinear analysis on the computational model without accounting for infill walls;

h is the story height.

It follows that the relative displacement limit is equal to:

$$d_{interstory\ limit} = 0{,}0050 * \frac{2}{3} = 0{,}00333$$

Therefore, the verification of the interstory drift will be satisfied only if:

$$d_{interstory} \leq \frac{0{,}0033}{h}$$

In the following example, beam segment number 33 exhibits interstory drift values lower than the limiting value; therefore, the verification is satisfied.

Combination	Displacement lower node		Displacement upper node		δ	δ/h	Validation
	X	Y	X	Y			
1	-2.588347	-0.68466	-2.736555	-0.75719	0.165003	0.000516	Yes
2	-3.25276	-0.761139	-3.437273	-0.836503	0.199311	0.000623	Yes
3	-2.06835	0.811103	-2.186716	0.783418	0.121561	0.00038	Yes
4	-2.732763	0.734623	-2.887435	0.704104	0.157654	0.000493	Yes
5	-1.278542	-2.451419	-1.350335	-2.576722	0.144413	0.000451	Yes
6	-1.924024	-2.525666	-2.031446	-2.653729	0.167152	0.000522	Yes
7	0.454781	2.534456	0.482462	2.558636	0.036754	0.000115	Yes
8	-0.190701	2.460209	-0.19865	2.481629	0.022847	0.000071	Yes
9	0.372258	-2.469064	0.396096	-2.594725	0.127902	0.0004	Yes
10	-0.273224	-2.543311	-0.285016	-2.671732	0.128961	0.000403	Yes
11	2.105581	2.516811	2.228892	2.540633	0.125591	0.000392	Yes
12	1.460099	2.442564	1.54778	2.463626	0.090175	0.000282	Yes
13	2.91432	-0.743478	3.08488	-0.8172	0.185811	0.000581	Yes
14	2.249907	-0.819957	2.384162	-0.896514	0.154549	0.000483	Yes
15	3.434317	0.752285	3.634719	0.723407	0.202472	0.000633	Yes
16	2.769904	0.675805	2.934001	0.644093	0.167133	0.000522	Yes

Table 16 - Interstory drift verification under SLD

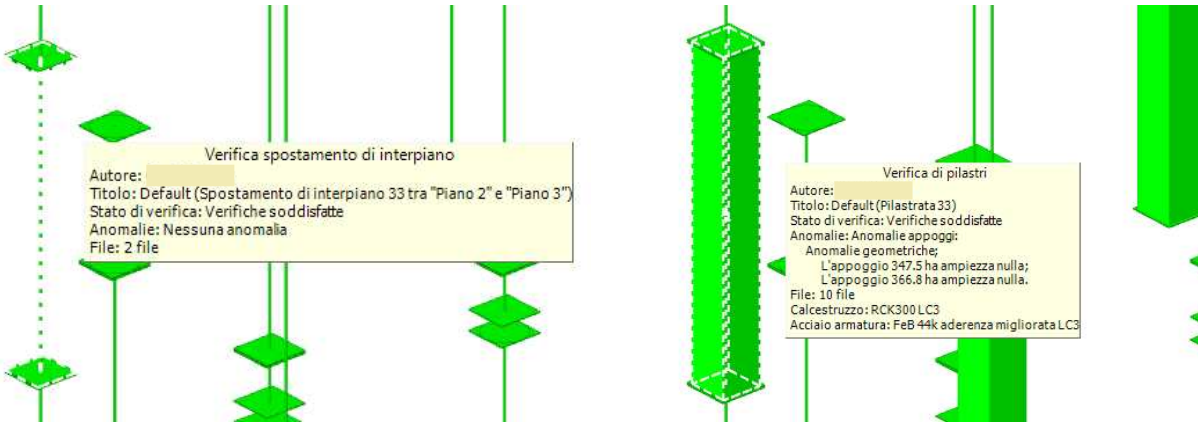

Figure 67 - Interstory drift verification for column number 33

The verification is satisfied for all the remaining columns of the structure.

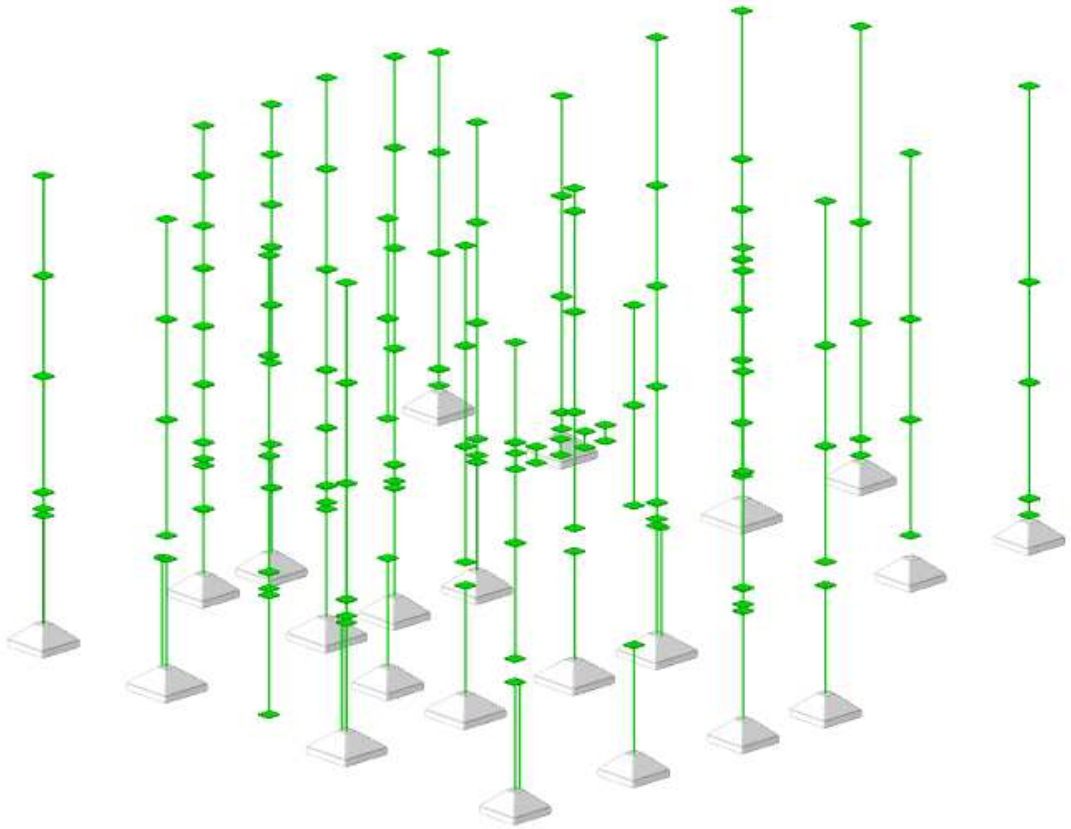

Figure 68 - Interstory drift verification for the entire structure

VERIFICATION OF ELASOMERIC ISOLATION DEVICES

Elastomeric seismic isolation devices require checks for both ultimate and collapse limit states. Specifically, the axial stress developed must remain below the design load for verification under both the SLU (Ultimate Limit State) and SLC (Collapse Limit State). Additionally, for each SLC combination, the device must ensure that the resulting displacements do not exceed the maximum allowed by the device.
The maximum displacement reached by the isolators, in this case, is 16,97 cm under the SLC 7 load combination. According to the FIP-MEC tables, the selected device has a maximum displacement range of ±20 cm; therefore, this verification is satisfied because:

$$16{,}97\ cm\ \leq 20\ cm$$

Similarly, the axial stress values of the isolators are below the maximum allowable loads, which are 2800 kN and 990 kN for the ULS and CLS, respectively.

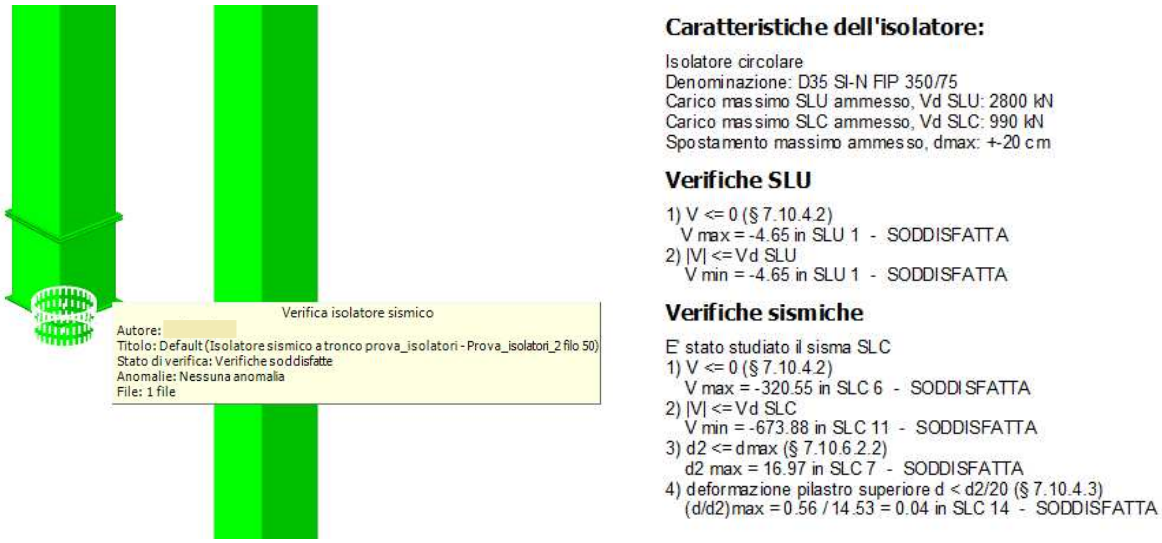

Figure 69 - Verification of Elastomeric Isolators

9 Results analysis

The comparative analysis of the three structural models made it possible to assess the influence of the different seismic retrofitting strategies on the overall behavior of the building. The comparison was initially based on the results of the dynamic modal analysis, which allowed the vibration modes of the structure to be observed; the parameters of lateral displacements and shear forces at the base were then also compared to monitor the response of the model.

Modal analysis of the existing structure highlighted critical aspects of its dynamic behavior. The main vibration modes, in fact, have torsional components, which contribute to an non-uniform distribution of displacements. This behavior is partially predictable, since elements such as the reinforced concrete shear wall that crosses the structure and the central courtyard affect the overall stiffness of the building. In terms of displacement, the overall movements of the structure remain relatively limited; however, the shear forces at the base reach high values, revealing structural vulnerabilities under seismic loading.

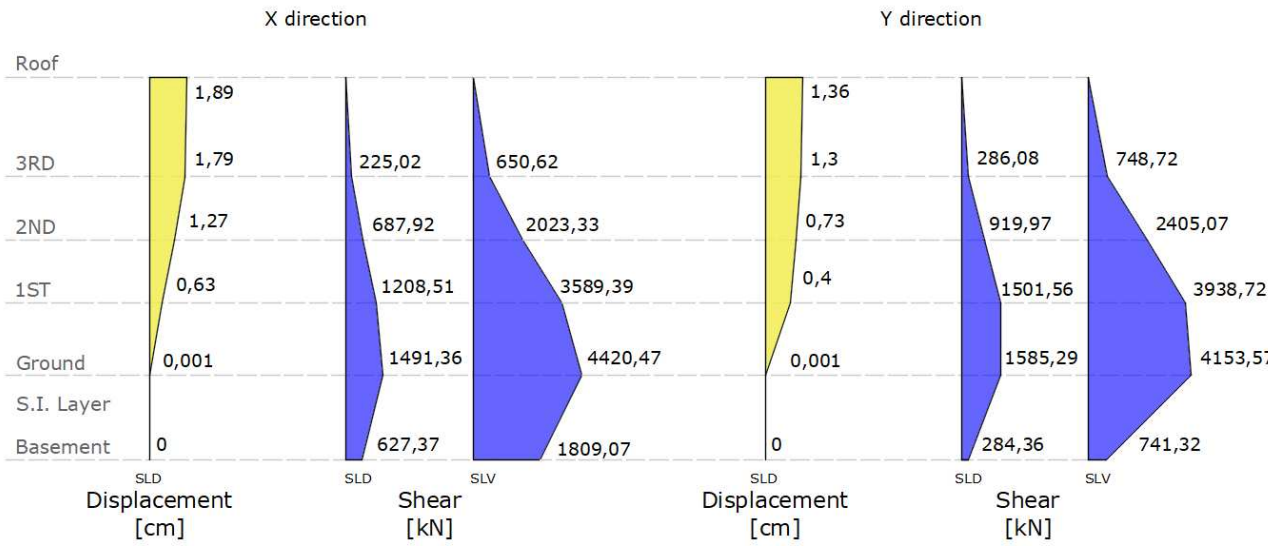

Figure 70 - Displacement and Shear diagramas of the state of art.

The introduction of shear walls, on the other hand, led to a significant increase in the overall rigidity of the structure. As a direct consequence, the main vibration periods were reduced by approximately 50%, causing the dynamic response to shift towards higher frequencies. Lateral displacements were also substantially reduced, by approximately one third compared to the unrenovated structure, while the distribution of shear forces at the base became more uniform and predictable.

The shear walls were carefully positioned to minimize the distance between the center of mass and the center of stiffness. This strategic arrangement helped reduce torsional modes, which are often responsible for irregular floor displacement and localized stress concentrations. Overall, these interventions not only improved the seismic performance of the building, but also increased its structural safety and resilience, providing a more balanced response under seismic action and keeping displacements within acceptable limits.

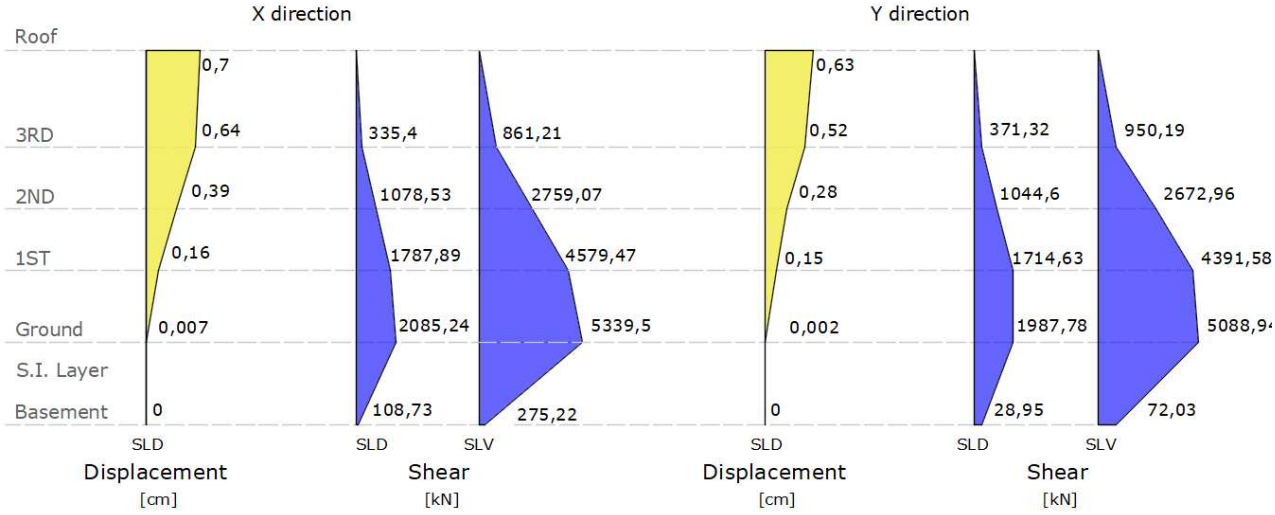

Figure 71 - Displacement and Shear diagramas of the shear walls retrofit.

Finally, the application of seismic isolators at the base significantly transformed the dynamic behavior of the structure, mainly by increasing the fundamental period. This period increase moves the structural response into a lower acceleration range, which in turn leads to a substantial reduction in shear forces at the base and a decrease in seismic stress on the structural elements.

Although overall lateral displacements increase compared to the non-restructured structure, from approximately 1.8 cm at roof level in the original building to approximately 3.9 cm with base isolation, the displacement between floors remains within the permitted limits, at approximately 1.6 cm. This ensures that the inter-story displacement verification is satisfied, even though the overall displacements increase.

In addition, the modal behavior of the building is significantly improved compared to the initial situation. The main vibration modes have become almost purely translational, similar to the response observed after the shear wall retrofit, with significantly reduced torsional components. This leads to a more uniform distribution of lateral displacements along the height of the structure and improves the predictability of its seismic response.

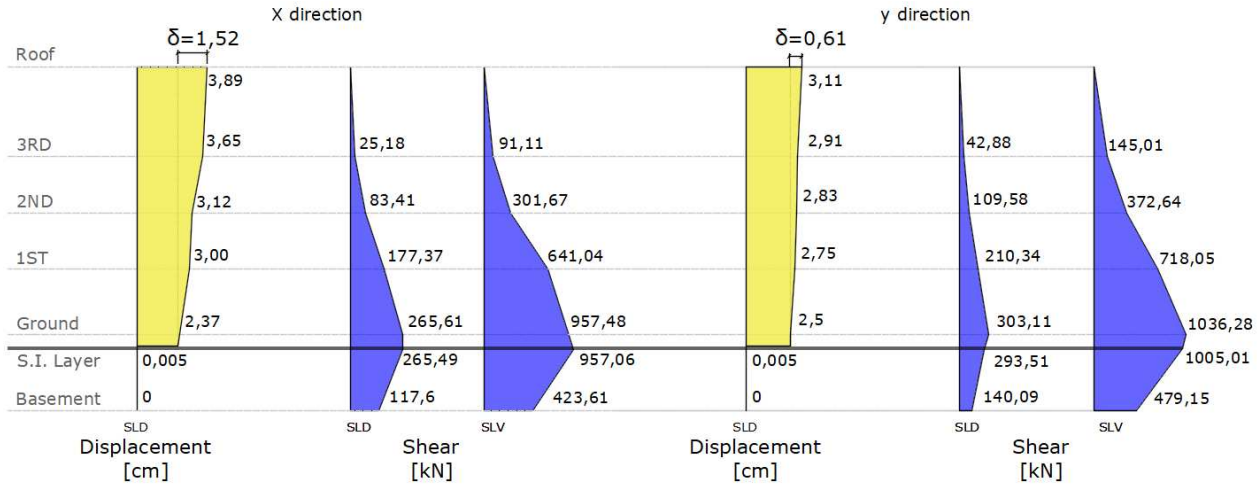

Figure 72 - Displacement and shear diagrams of the retrofit with seismic isolators.

Finally, the application of seismic isolators at the base significantly transformed the dynamic behavior of the structure, mainly by increasing the fundamental period. This period increase moves the structural response into a lower acceleration range, which in turn leads to a substantial reduction in shear forces at the base and a decrease in seismic stress on the structural elements.

Although overall lateral displacements increase compared to the non-restructured structure, from approximately 1.8 cm at roof level in the original building to approximately 3.9 cm with base isolation, the displacement between floors remains within the permitted limits, at approximately 1.6 cm. This ensures that the inter-story displacement verification is satisfied, even though the overall displacements increase.

In addition, the modal behavior of the building is significantly improved compared to the initial situation. The main vibration modes have become almost purely translational, similar to the response observed after the shear wall retrofit, with significantly reduced torsional components. This leads to a more uniform distribution of lateral displacements along the height of the structure and improves the predictability of its seismic response.

Overall, the base isolation system offers a balanced and effective seismic protection strategy: it significantly reduces shear forces at the base, keeps inter-story displacements within safe limits, improves modal behavior, and allows global displacements to increase in a controlled and predictable manner, ensuring both structural safety and improved performance under seismic loading.

In summary, while shear walls are effective in controlling torsional behavior and limiting local displacement, base isolation demonstrates superior performance in reducing seismic forces and ensuring the overall integrity of the building. Both approaches are therefore valid solutions from a

structural point of view, but the decision to adopt one or the other may be further guided by additional considerations, such as economic feasibility and environmental impact, which will be examined in the following chapters.

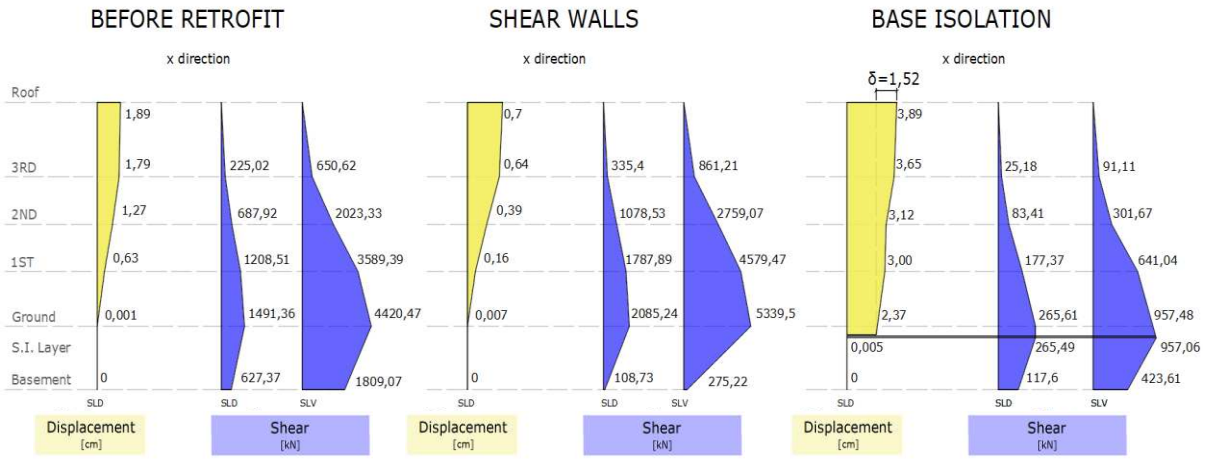

Figure 73 - Comparison of diagrams in the X direction

10 Life Cycle Assessment

10.1 The Methodology

In this study, the two seismic retrofitting strategies were examined not only from a structural and technical perspective, but also in terms of environmental performance. This dual approach reflects the growing awareness that structural safety and sustainability are intrinsically interconnected dimensions in building practice. In line with the objectives set by the European Green Deal and the EU Agenda for a Sustainable Built Environment, the analysis embraces a holistic view of the built environment and encourages the adoption of a life-cycle approach in construction and renovation activities. In this context, rigorous assessment of environmental impacts using scientifically based tools becomes essential to ensure that retrofitting measures are not only effective in reducing seismic vulnerability but also in line with long-term sustainability goals.

The reference methodology used is life cycle assessment (LCA), a quantitative and scientific tool designed to assess the environmental impacts associated with a product, process, or service throughout its entire life cycle. Depending on the boundaries defined, the analysis can follow a "cradle-to-grave" approach, covering all stages from raw material extraction to end-of-life management, or a "cradle-to-gate" approach, limited to processes up to the factory gate. In both cases, the methodology systematically addresses upstream processes (raw material extraction), main processes (production, transport, and use), and downstream processes (end-of-life management).

By adopting this systemic perspective, LCA makes it possible to identify critical points from an environmental point of view, reveal trade-offs between different stages of the life cycle, and highlight opportunities for improvement in terms of resource consumption, pollutant emissions, energy use, and waste production.

At the European level, LCA is governed by international standards ISO 14040 and ISO 14044, which establish a methodological framework structured in four main phases:

- Definition of objectives and scope;
- Life cycle inventory (LCI);
- Life cycle impact assessment (LCIA);
- Interpretation of results.

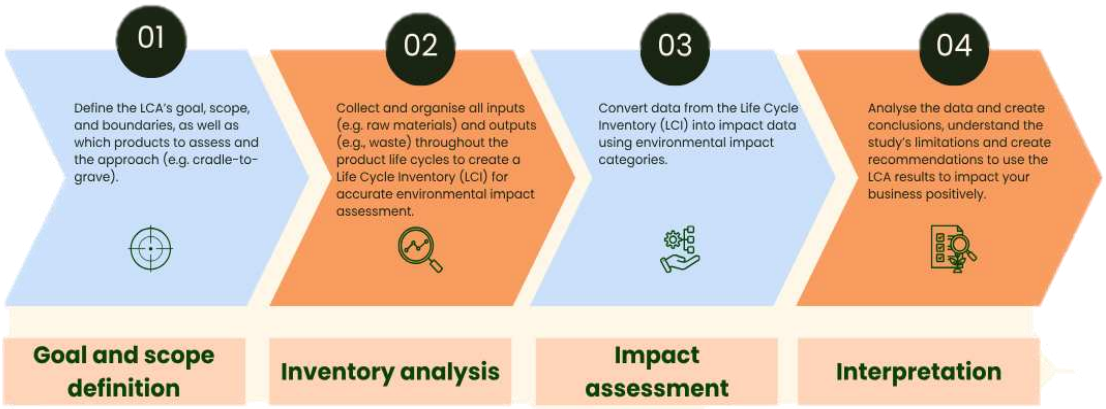

Figure 74 - Methodological steps of LFC analysis

These standards are recognized at European level and form the methodological basis for the Product Environmental Footprint (PEF) and Organizational Environmental Footprint (OEF) initiatives developed by the European Commission to ensure harmonized, transparent, and comparable environmental assessments.

The adoption of advanced technologies, in particular the integration of life cycle assessment (LCA) with Building Information Modeling (BIM), has significantly expanded the applicability of LCA, as demonstrated by numerous recent studies [8] . A growing number of studies have focused on the use of environmental product declarations (EPDs) and emission factor databases to quantify CO_2 emissions associated with building materials. A notable example is provided by the study *"BIM and LCA Integration: A Systematic Literature Review" [11]* , which investigates how environmental databases and EPDs are used to calculate CO_2 emissions, highlighting the evolution of methodological approaches and the integration of environmental data into the design process. This study further emphasizes the growing importance of BIM in life cycle analysis, with increasingly sophisticated synergies between the two approaches.

Similarly, as discussed in "Methods for calculating CO_2 emissions during the construction process for the development of a BIM-based performance evaluation system" [10], the integration of BIM with LCA allows for more accurate emissions calculations through the use of material-specific emission factors. This approach not only facilitates the assessment of life cycle impacts, but also allows for real-time evaluation of the environmental consequences of design choices, thus improving both the efficiency and sustainability of construction processes.

In this study, the objective of the LCA was to quantify the environmental impact associated with the two alternative seismic retrofitting strategies. This was achieved by strictly following the core methodological steps:

1. **Life Cycle Inventory (LCI)** – A detailed quantification of the materials and resources used in each retrofitting scenario was performed. Each material was assigned emission factors (in kg CO_2 eq) derived from recognized LCA databases and Environmental Product Declarations (EPDs), which provide standardized and verified environmental data for the entire life cycle of construction products.
2. **Life Cycle Impact Assessment (LCIA)** – The quantities obtained from the BIM model were translated into environmental impacts, with a focus on global warming potential (GWP), expressed in kilograms of CO_2 equivalent. This indicator allowed for a clear quantitative comparison between the two renovation alternatives in terms of climate performance.
3. **Interpretation** – A critical comparison was made between the two strategies, highlighting the environmental trade-offs. The integration of LCA into the design phase therefore emerges as a key element for evidence-based decision-making in line with sustainability objectives.

EMISSION CALCULATION METHODOLOGY: A PRACTICAL APPROACH

For the analysis of CO_2 emissions, a detailed methodological approach was adopted, inspired by the document “Method for calculating carbon emissions from steel-concrete composite beam bridges based on LCA” [7] , which provides a valuable reference for assessing emissions in engineering projects. As in the bridge case study, the same type of calculations were applied to estimate emissions from materials and construction processes. In that study, the authors used a combination of material-specific emission factors and calculation formulas that take into account different life cycle stages. In addition to emissions related to material production, all other pollution factors were also considered, such as transportation, on-site processing, and landfill disposal. The same logic was applied in this work to ensure consistency in the assessment of the environmental impact of the two seismic retrofit solutions.

The inclusion of these methodological tools, which combine LCA and BIM, not only strengthens the robustness of the environmental assessment but also provides a solid evidence base for informed decision-making, thereby improving the overall sustainability of the retrofit project.

10.2 Environmental Impact Assessment (CO_2 eq)

The growing urgency to mitigate climate change and reduce greenhouse gas emissions, in line with the targets set by the Paris Agreement and the United Nations 2030 Agenda, has brought embodied carbon to the forefront of research in the construction sector.

The built environment is responsible for approximately 42% of annual global CO_2 emissions, of which 27% is attributable to operational emissions and the remaining 15% to embodied carbon. The latter refers to emissions associated with the extraction, production, transportation, installation, maintenance, and end-of-life of building materials. In seismic retrofitting scenarios, embodied carbon becomes particularly relevant, as the materials used, particularly concrete and steel, are highly carbon-intensive.

The emission factors for each material were obtained from a representative set of Environmental Product Declarations (EPDs), in accordance with ISO 14025 and the methodological framework outlined in ISO 14040 and 14044. These data sources ensure transparency, comparability, and standardization in the life cycle inventory.

For this study, the materials considered are concrete, steel, and the elastomeric rubber of the insulators. Transport has been included as a separate item, cal.

Based on the methodology discussed above, the global warming potential associated with the renovation of the shear walls is estimated at 84,582 kg CO_2 eq, while the insulation solution at the base represents 14,663 kg CO_2 eq. The latter represents an 82% reduction in embodied carbon compared to the traditional approach. This significant gap is mainly due to the high quantities of concrete and reinforcing steel required for the installation of the new shear walls. Specifically, the renovation of the shear walls produces over 46 tons of CO_2 eq from concrete alone and more than 21 tons from steel.

In contrast, in the base insulation solution, although the elastomeric supports introduce additional emissions—approximately 5,184 kg of CO_2 eq, mainly due to technical rubber and steel—the overall reduction in traditional structural materials more than compensates for this increase. Emissions related to concrete fall below 5 tons and those related to steel below 7 tons, highlighting the efficiency of this less invasive intervention.

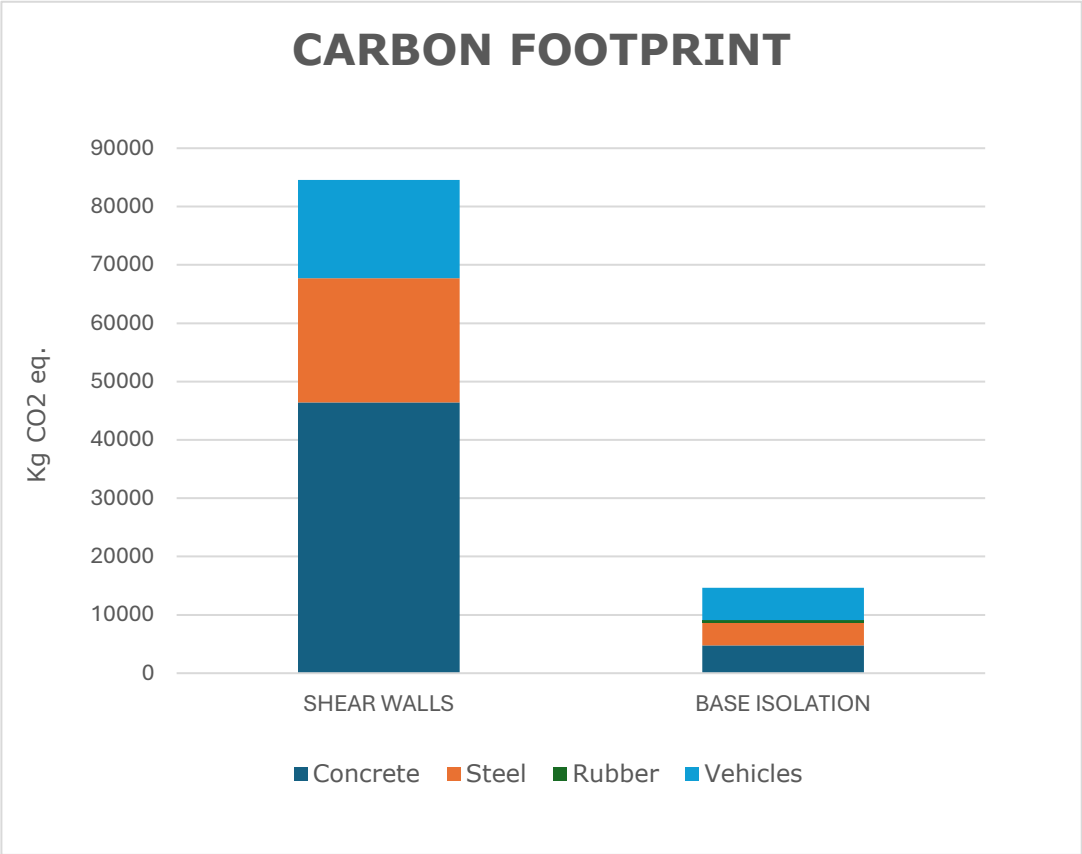

Table 17 - Comparison of the environmental impact of the two interventions.

Emissions due to the transport of materials and the vehicles used for on-site processing were considered separately. For this category, it was possible to find the necessary values in some cases on the EPDs; where this was not possible, an estimate was carried out considering the average emissions of a means of transport and estimating the distance traveled or the time of use of a machine.

Transport and on-site operations, while not negligible, represent a minor share of emissions in both cases: 2,890 kg of CO_2 eq for the shear wall strategy and 942 kg of CO_2 eq for the insulation system, once again reflecting the lower construction intensity and invasiveness of the second intervention.

In conclusion, this analysis demonstrates that base seismic isolation, in addition to offering excellent seismic performance, is also a significantly more sustainable option in terms of embodied carbon. These results underscore the importance of integrating environmental impact assessments into the early stages of structural retrofit design. Future seismic resilience must be aligned with climate resilience, promoting low-carbon solutions as the cornerstone of next-generation building strategies.

11 Economical assessment

A comparative assessment of the two seismic retrofitting strategies cannot overlook the economic dimension, which is one of the main decision-making factors in the planning and implementation of interventions on public buildings. Financial sustainability is, in fact, a decisive factor, particularly in contexts where economic resources are limited and must be allocated according to criteria of priority and urgency. This dynamic is recurrent in the field of public construction, where securing adequate funding is often the most restrictive constraint.

For this study, cost estimates were made using the open source software Blumatica Pitagora, a widely adopted tool for preparing metric computations and analyzing construction costs. Detailed cost estimates were produced for both renovation solutions, based on the quantities of material extracted from the BIM model and the FEM structural model. It should be noted that the figures reported refer exclusively to direct construction costs, thus excluding additional items such as professional fees, VAT, overheads, safety measures, and contingencies, which would normally be included in a complete technical-financial framework.

The price list used was that of the Molise Region Public Works 2025 (the most recent edition available at the time of the analysis). Not all construction items were included in this dataset; therefore, equivalent items were taken from the regional price lists of Abruzzo and Campania, chosen for their consistency from both a technical and economic point of view.

According to this approach, the total cost of the intervention on the shear wall amounted to €541,737.02, while the renovation of the basic insulation had a total cost of €325,110.57, corresponding to a reduction of approximately 40% in favor of the second strategy.

This difference, in addition to being significant in absolute terms, reflects the different operational and construction requirements of the two adaptation solutions. In the case of shear walls, costs are heavily influenced by demolition and architectural restoration activities, which are necessary to insert vertical walls into already defined interior spaces. Specifically, demolition work amounts to €88,386.41, while finishing and restoration work amounts to €263,183.59. These figures contrast with the significantly lower values observed for base isolation—€23,847.18 and €108,344.01, respectively—as this intervention is limited to the foundation level and interferes minimally with the existing superstructure and finishes.

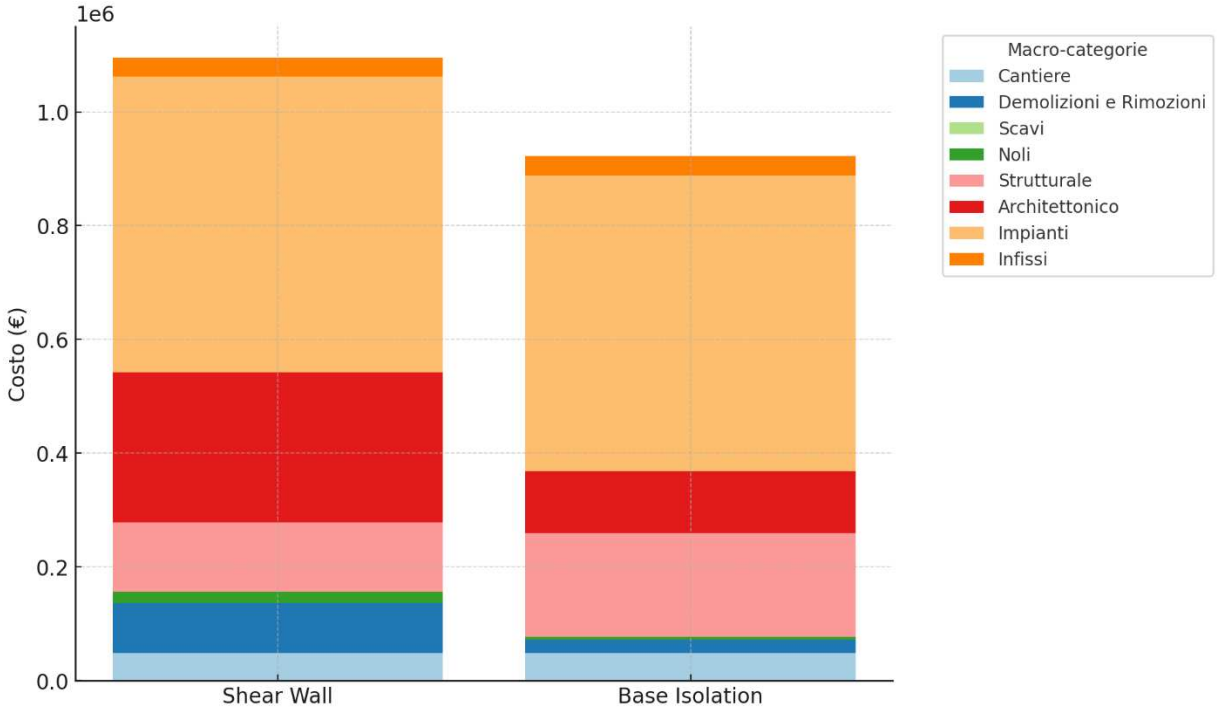

Table 18 - Cost distribution diagrams 1.

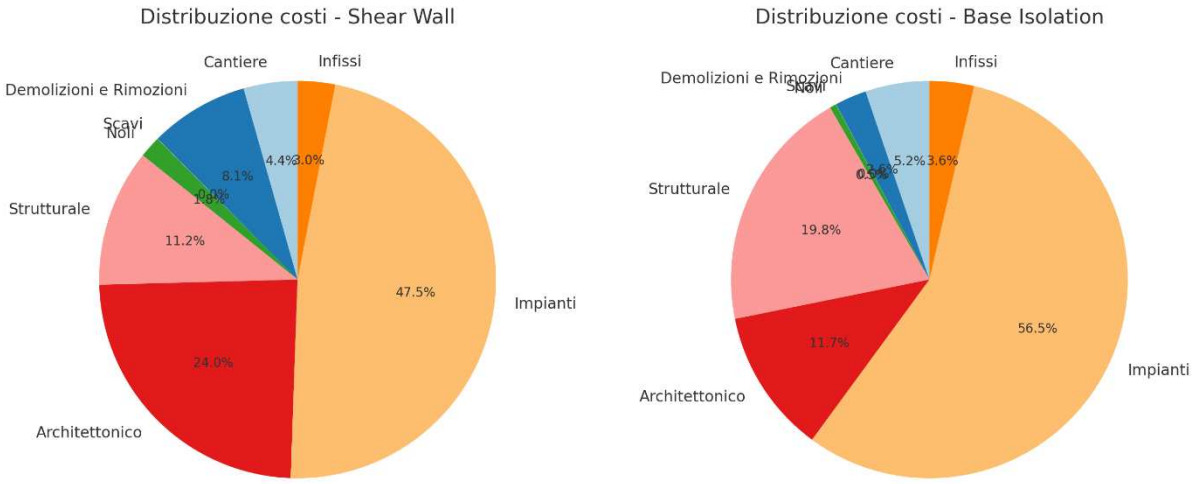

Table 19 - Cost distribution diagrams 2.

Similarly, the costs associated with setting up the construction site and renting equipment are significantly higher for the shear wall solution (€19,375.00) than for base isolation (€4,843.75), further confirming the greater logistical and time complexity of the former intervention.

It is interesting to note, however, that the structural work itself is more expensive in the case of seismic isolation (€182,844.90) than the shear wall system (€122,480.58). This discrepancy is attributable to the higher technical requirements of the isolation solution, which involve the controlled cutting of

columns, installation under temporary support conditions, and the use of specialized labor. However, the substantial reduction in other categories of expenditure more than compensates for the higher structural costs.

In summary, the base insulation intervention proves to be more cost-effective than the shear wall solution, thanks to its lower invasiveness, simplified on-site operations, and reduced need for architectural restoration. Combined with its favorable seismic and environmental performance, this strategy emerges as a more balanced and sustainable option for the renovation of public buildings.

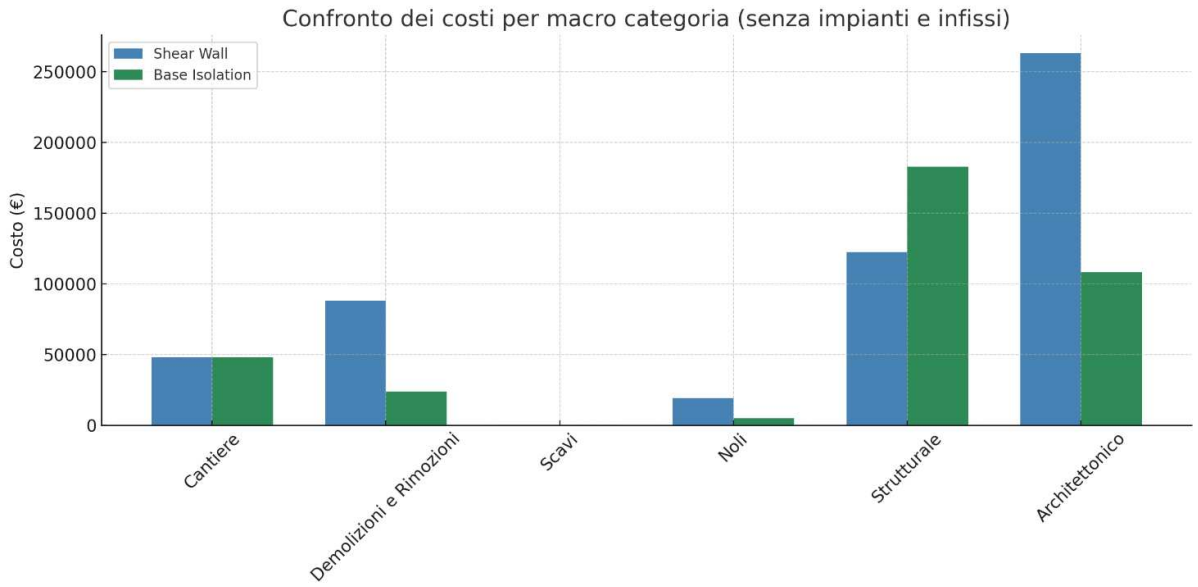

Table 20 - Cost comparison by macro category

12 Conclusions

This study compared two seismic retrofitting strategies for reinforced concrete buildings: the insertion of shear walls and the adoption of a base isolation system. The objective of this thesis is not only to improve the seismic safety of the building, but also to evaluate how design choices can influence the environmental impact and economic sustainability of the intervention. Structural analysis has shown that both strategies significantly improve seismic response, although in different ways.

Shear walls increase overall stiffness and limit local torsion and displacement, ensuring predictable structural behavior. Base isolation, on the other hand, reduces the forces transmitted to the upper structures and promotes a uniform distribution of displacements, keeping the relative deformations between floors within acceptable limits. This approach leads to an increase in overall displacements but ensures effective protection of structural integrity.

At the same time, the integration of an environmental assessment using LCA has made it possible to compare the impact of the two interventions on the life cycle of the materials. Today, environmental issues are a central and binding element in building design and regulations, requiring informed choices about materials and construction strategies. Renovation with shear walls, due to the high use of concrete and steel, generates significantly higher emissions than the base insulation system, which, while requiring specific technological devices, drastically reduces the amount of traditional materials and therefore overall CO_2 emissions.

Economic analysis confirms this trend: the direct costs of renovation with shear walls are higher, mainly due to demolition, architectural restoration, and site management activities, while base insulation, although involving higher costs for the specialized structural component, reduces overall costs thanks to its less invasive nature and the simplification of site operations. From this point of view, economic and environmental considerations become key decision-making tools, especially in cases where the two solutions guarantee equivalent seismic performance.

Finally, a practical and decisive aspect concerns the execution of the works and the time required for their accomplishment. The insertion of shear walls requires invasive work on several floors, with significant impacts on finishes, internal paths, and site logistics. Base isolation, on the other hand, focuses on the foundations, reducing interference with the existing building and allowing for faster and more controllable construction. This often underestimated element can prove decisive in the planning of interventions on public buildings, where reduced downtime and less complex execution constitute significant added value.

In summary, the choice of the most appropriate strategy should combine three logical threads: structural performance, environmental and economic sustainability, and execution feasibility. In the context of public buildings or interventions on existing structures, the base insulation system emerges as a balanced solution, capable of ensuring safety, reduced environmental impact, lower overall costs, and shorter construction times. Shear walls remain a valid alternative in contexts where strict control of local deformations is a priority and the spatial and logistical characteristics of the building allow it.

The choice of seismic retrofitting strategy must therefore be based on a balance between structural performance, environmental impact, costs, and feasibility: there is no universal solution valid in all contexts, but rather decisions weighed according to specific objectives and available resources. The integration of seismic analysis, environmental and economic assessments, and operational considerations represents a comprehensive and modern approach that can guide informed and sustainable design decisions consistent with the practical requirements of construction.

The data collected in this study provide a solid foundation for future research aimed at the in-depth analysis of decision-making methodologies concerning multiple seismic retrofitting strategies. In particular, the next phase will involve conducting a multi-objective analysis using a Pareto front to explore the domain of optimal solutions with respect to the seismic resilience of the structure. As extensively documented in the literature, this approach can be particularly effective during the evaluation phase of an intervention, as it enables the weighting of parameters such as building functionality and seismic resilience—factors that are becoming increasingly critical in contemporary building design practices.

13 References

[1] Marzio Cuni, Andrea Sangalli, “Italia e rischio sismico: strategie per la tutela del patrimonio edilizio”, Ingenio, 2025.

[2] Gülçin Büyüközkan, Öykü Ilıcak, Orhan Feyzioğlu, “A review of urban resilience literature”, Sustainable Cities and Society, Volume 77, 2022,103579.

[3] Paulo Jorge Gomes Ribeiro, Luís António Pena Jardim Gonçalves, “Urban resilience: A conceptual framework” , Sustainable Cities and Society, Volume 50, 2019, 101625.

[4] 2011, Jack Ahern, *From fail-safe to safe-to-fail: Sustainability and resilience in the new urban world*, Landscape and Urban Planning, Volume 100, Issue 4.

[5] 2016, Sara Meerow, Joshua P. Newell, Melissa Stults, *Defining urban resilience: A review, Landscape and Urban Planning*, Volume 147.

[6] 05 October 2022, Lin Liu, Dewen Liu, Lanfang Zhang et al., *Response comparison of different staggered story isolated structures under long-term earthquake*, PREPRINT (Version 1) available at Research Square;

[7] 2024, Xu, Ruofei & Yin, Yang & Miao, Yumo & Yang, Wangyiling & Sun, Jiazhuo & Li, Haoqi. *Carbon emission calculation method of steel-concrete composite girder Bridge based on LCA: A case study of Yanchong Expressway (Hebei Section)*. E3S Web of Conferences. 561. 02015. 10.1051/e3sconf/202456102015.

[8] 2020, Kotula, Bartlomiej & Kamari, Aliakbar. *Development of a BIM-based LCA Tool to Support Sustainable Building Design during the Early Design Stage*.

[9] 2020, Potrc Obrecht, Tajda & Röck, Martin & Hoxha, Endrit & Passer, Alexander., *BIM and LCA Integration: A Systematic Literature Review*. Sustainability. 12. 10.3390

[10] 2020, Sun H, Park Y., *CO_2 Emission Calculation Method during Construction Process for Developing BIM-Based Performance Evaluation System*. *Applied Sciences*. 2020; 10(16):5587.

[11] (a) https://www.incide.it/en/the-10-advantages-of-bim/